The Thesis Committee for Yu Ye
Certifies that this is the approved version of the following thesis:

Depositional Systems and Sequence Stratigraphy of the M1 Sandstone in Tarapoa, Ecuador

APPROVED BY
SUPERVISING COMMITTEE:

Supervisor:

Ronald J. Steel, Supervisor

Cornel Olariu, Co-Supervisor

William L. Fisher

Depositional Systems and Sequence Stratigraphy of the M1 Sandstone in Tarapoa, Ecuador

by

Yu Ye, B.S.; B.S.

Thesis

Presented to the Faculty of the Graduate School of

The University of Texas at Austin

in Partial Fulfillment

of the Requirements

for the Degree of

Master of Science in Geological Sciences

The University of Texas at Austin

December 2014

Acknowledgements

I owe many thanks to my supervisor Dr. Ronald J. Steel and co-supervisor Cornel Olariu. This thesis could not have been done with their guidance and patience. I would also like to thank my committee member Dr. William L. Fisher for his review and advices. In addition, I want to thank everyone in the Dynamic Stratigraphy Research Gourp, visiting scholars Dr. Shengli Li and Shunli Li from China University of Geosciences (Beijing), and all my friends in Jackson School of Geosciences for giving me advices and sharing their ideas during the course of my studies. Finally, I thank the Andes Petroleum Ecuador LTD for their generous sponsorship in my research project.

Abstract

Depositional Systems and Sequence Stratigraphy of the M1 Sandstone in Tarapoa, Ecuador

Yu Ye, MSGeoSci

The University of Texas at Austin, 2014

Supervisors: Ronald J. Steel and Cornel Olariu

Campanian M1 Sandstone is one of the major prospective sandstone units in the Tarapoa field in Oriente Basin, Ecuador. The M1 Sandstone is always markedly sharp based, averages 25 m in thickness, shows upward increasing marine bioturbation and generally fines upward from coarse to very fine grained sandstone. In cores, the sandstones at base are amalgamated coarse to fine grained with prominent cross stratification (dm thick), sometimes clearly bi-directional and contains mud drapes. These suggest strong tidal or fluvial-tidal currents in estuary channels or delta distributary channels. The finer grained intervals in the middle are brackish-water intensely bioturbated and dominated by mud drapes, wavy and flaser bedding suggestive of intertidal flats. Associated overlying coals and coaly shales suggest supratidal conditions. The sandstones at top are cross stratified and contain mud drapes. These again suggest strong tidal or fluvial-tidal currents in estuary channels or delta distributary channels. The stacking pattern of facies in M1 Sandstone reveals the evolution of the M1 depositional system, as well as the sequence stratigraphy of M1 sandstone. The evolution includes four stages of deposition which

indicates an initial sea level rise, a subsequent sea level fall, and another sea level rise. Lateral sand-mud heterogeneity exists in the study area, forming “shale barriers”, i.e. elongate shale-rich zones that are lateral barriers to hydrocarbon migration. They are interpreted to be abandoned tidal channels filled with muddy tidal flat deposits during the sea level fall. An alternative hypothesis was established to explain the stacking pattern of facies in M1 Sandstone. A tide-dominated delta with poor fluvial input experienced intense tidal erosion and produced a sharp base at the base of M1 Sandstone. Then subtidal sand bars, intertidal flats, and supratidal sediments were deposited in sequence during a continuous regression.

The core and well logs in an extension of the study area in the northwest is interpreted as more distal open shelf deposits, beyond the mouth of the Tarapoa estuary system, where transgressive tidal shelf ridges were coeval with the Tarapoa estuary system. This interpretation allows us to predict the environment between the two areas as a transition zone between tide-dominated estuary and open shelf.

Table of Contents

List of Figures

Chapter 1: Introduction

1.1 Study Location

The Oriente Basin, one of three basins within the Putomayu-Oriente- Marañon province, is located east of the Andes Mountains in Ecuador, South America. These basins are bounded by the national borders of Ecuador, Colombia, and Peru (Higley, 2001). The Oriente Basin extends northwards into the Putumayo Basin and southward into the Marañon Basin. Lying between the Andean foothills on the west and the Guyana shield on the east, the Oriente Basin lies on the Andean foreland and covers an area of more than 100,000 km^2 (Higgs, 2001).

1.2 The objectives and significance of the study

The Oriente Basin is a petroleum producing foreland basin in Ecuador, South America. The M1 sandstone, one of the sandstone units in the Cretaceous Napo Formation in this basin, is a major hydrocarbon producing sandstone unit in the Tarapoa oil field (Figure 1.1). The operator of the Tarapoa oil field is evaluating the hydrocarbon potential of M1 sandstone in a new prospective area to the northwest of the original oil field. Since the M1 sandstone has been proved to be productive in the Tarapoa oil field, the operator looks forward to predict the performance of M1 sandstone in the new barely drilled area. Meanwhile, poorly understood muddy intervals and architectures, also known as "shale barriers", have caused unexpected sand-mud heterogeneity that has resulted in problematic low production in some wells of the current field program.

The objective of this present study is to develop a predictive geological model for the M1 sandstone that can be applied to the new prospective area northwest of the Tarapoa oil field, Oriente Basin, as well as to investigate the origin of the occasional muddy architectures in M1 sandstone which are hampering the productivity of some wells. A

predictive geological model will help the operator with better understanding on thickness, distribution, and sand-mud heterogeneity of M1 sandstone in the new area; this will contribute to the resource evaluation in the new area and ultimately will influence the decision about purchase of this new area. On the second objective any improved understanding of the shale barriers will allow a more accurate prediction on its distribution, associated sand-mud heterogeneity, and sandstone thickness changes; this will result in better well positioning and avoidance of low production associated with shale barriers.

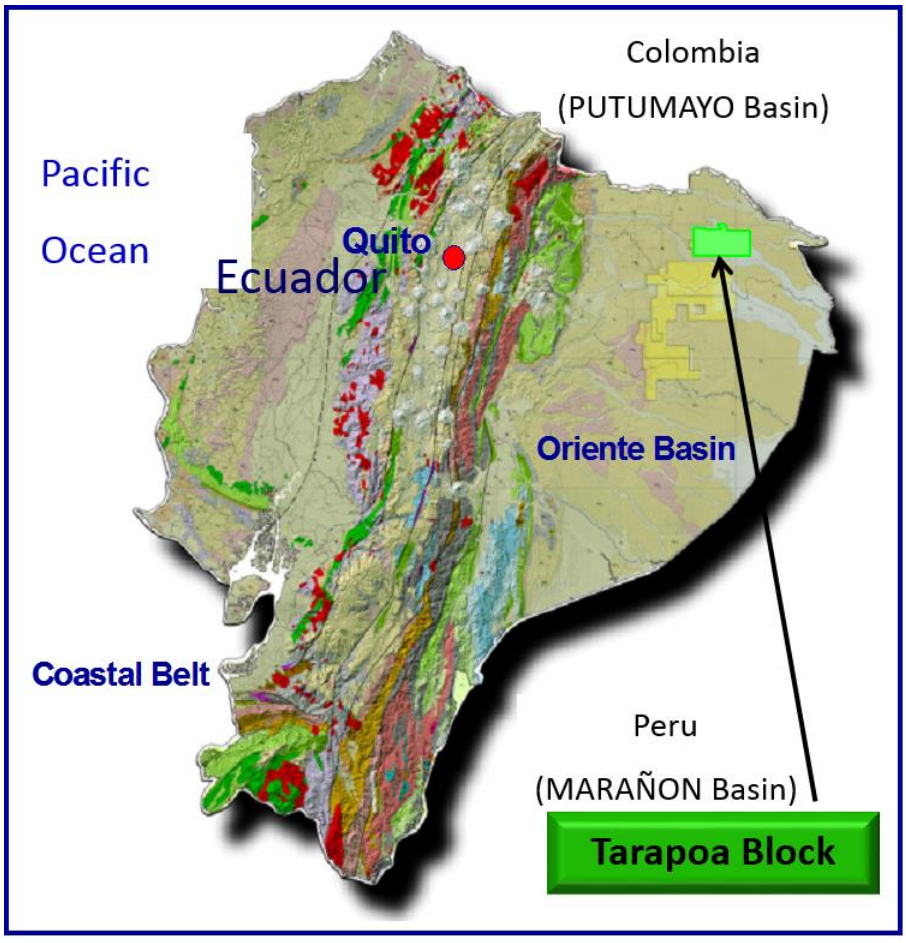

Figure 1.1 Geographic location of study area (revised from Andes petroleum LTD report, 2013)

1.3 TECTONIC AND STRATIGRAPHIC EVOLUTION OF THE ORIENTE BASIN

The modern-day Oriente Basin is a foreland basin; for this reason, it is highly asymmetric. Its sedimentary strata near the Andes Mountains are thicker, more folded and faulted, whereas sedimentary strata towards the east are thinner, less faulted and they onlap the Guyana craton (Marcelo et al, 1991). The basin axis is oriented from north to south and dips towards a depocenter in northernmost Peru (Dashwood and Abbotts, 1990).

Figure 1.2 is the stratigraphic column of the Oriente Basin. The sediment infill of the Oriente Basin can be divided into four successions, each believed to have been deposited during a particular phase of tectonic development of this region. They are, from oldest to youngest: a pre-rift sedimentary succession (Silurian – Permian), **a** syn-rift succession (Triassic – Jurassic), a post-rift succession (Cretaceous), and an Andean foreland basin succession (Tertiary – present).

1.3.1 Pre-rift sedimentary succession (Silurian – Permian)

The pre-rift succession consists of two formations.

The oldest formation that drilling has reached is the Pimbuiza Formation, which is Upper Silurian to Lower Ordovician in age. It consists of deformed and slightly metamorphosed limestones, slates, slatey shales, and sandstone (Dashwood and Abbotts, 1990).

The thinly bedded carbonates and shales of the Macuma Formation overlie the Pimbuiza Formation. The Macuma Formation strata were deposited on a shallow marine carbonate shelf between the Pennsylvanian and the very early Permian. After the Permian, a stratal hiatus with no deposits represented. It was possibly caused by regional (pre-rift) uplift and erosion during a Mid-Jurassic tectonic event (Dashwood and Abbotts, 1990).

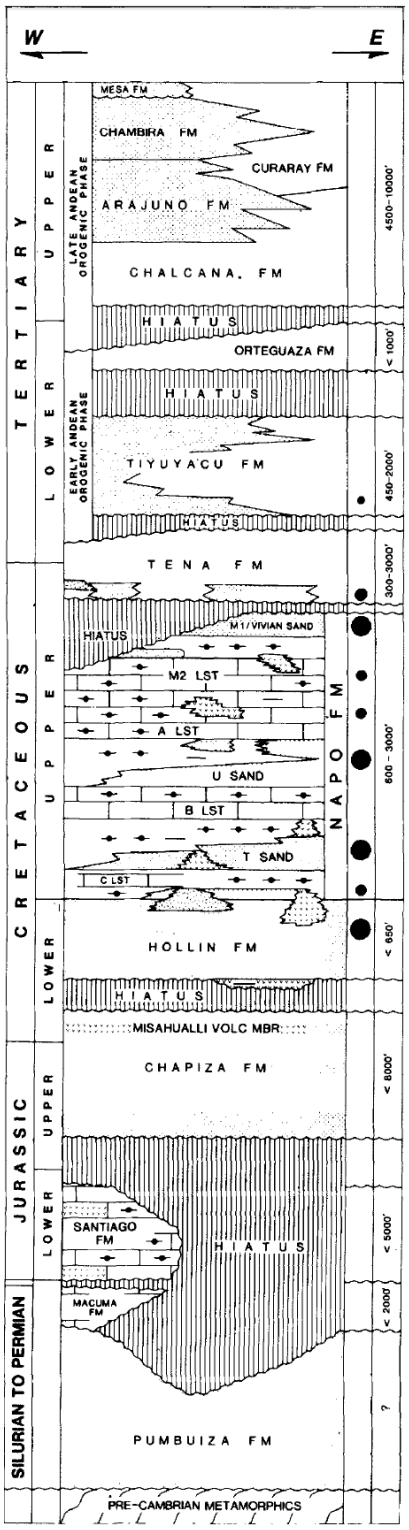

Figure 1.2 Stratigraphic column of the Oriente Basin (Dashwood and Abbotts, 1990)

1.3.2 Syn-rift sedimentary succession (Triassic – Jurassic)

The syn-rift sedimentary succession consists of two formations.

Above the Macuma Formation, the Santiago Formation of Triassic – Lower Jurassic age is found only in the Santiago river area in the Cutucu Uplift of the Andean Foothill Belt (Dashwood and Abbotts, 1990). The marine to continental-rift deposits of the Santiago Formation consist of transgressive marine, thinly bedded carbonates and black bituminous shales; these are overlain by a transgressive sandstone – siltstone sequence (Baby et al, 2013). The Early Jurassic syn-rift deposition of the Santiago Formation may be related to the break-up of Pangea.

The Upper Jurassic Chapiza Formation was deposited during Middle – Late Jurassic back-arc extension produced by subduction of the Farallon Plate under South America (Baby et al, 2013). The Chapiza Formation consists of thick and areally extensive continental clastic deposits; it reaches a thickness of 1500 feet in the rift basin. The graben fill is composed of conglomerates, sandstones, and shales interbedded with minor evaporites (Dashwood and Abbotts, 1990).

1.3.3 Post-rift sedimentary succession (Cretaceous)

The post-rift succession consists of three formations.

The basal Cretaceous formation in this area is the Hollin Formation (Aptian – Albian), which overlies the Chapiza Formation with an angular unconformity. This unconformity was associated with intensive erosion which removed part, if not all the underlying Mesozoic grabens and half-grabens (Baby et al, 2013). Hollin Formation sediments are present throughout the Oriente Basin and extend into western Brazil, southern Colombia, and northeastern Peru. The Hollin Formation thins gradually northeastward from the southwestern Ecuadorian Oriente Basin toward the Guyana Shield. The formation consists of white, thickly bedded to massive quartz sandstone with minor

carbonaceous claystone and coal interbeds. The fluvial and littoral sandstone of the Hollin Formation is extensive because it was deposited during a regressive period that followed a rapid marine transgression. The Hollin Formation was deposited as the Andean retro-arc foreland basin started to develop.

The Napo Formation (Albian – Lower Campanian) overlies the Hollin Formation with conformity. It consists of marine claystones, limestones, and sandstones. The Napo claystones and limestones are the main source rocks in the Oriente Basin; they were deposited during both the transgressive and regressive periods. Napo sandstones (the T, U and M Sandstones) are the important reservoir rocks; these sandstones were deposited during both the regressive and transgressive periods of this interval. The Hollin and Napo Formations of Cretaceous together form a megasequence (from Albian to Campanian) of claystones, limestones, and sandstones (Baby et al., 2013). The sediments were deposited mainly longitudinally along a NW-SE oriented depocenter on a slowly subsiding platform. Global eustasy and Andean orogeny together control the deposition of the sedimentary succession; the main sediment source was the Amazon craton to the east (Baby et al, 2013).

The Tena Formation (Maastrichtian – Palaeocene) is the uppermost portion of the post-rift sediments. This formation overlies the Napo Formation conformably in the east of the basin. However, the contact surface between Tena and Napo Formation becomes increasingly erosive towards the west of the basin. This unconformity marks the beginning of the "Early Andean" compressional episodes which produced regional uplift and led to the formation of Tena Formation (Dashwood and Abbotts, 1990). The Tena Formation consists of predominantly red colored, fluvial claystones, siltstones, and local sandstones at the base; the Tena succession is a typical foreland sedimentary wedge which pinches out towards the east. The Tena sediment emplacement recorded an initial progradation of the Andean orogeny wedge towards east (Baby et al, 2013).

1.3.4 Foreland basin sediment succession (Tertiary – present)

The Post-Cretaceous sediments are 4000-5000 m thick in the most southern part of the basin. The sediments were all sourced from the Andean Cordillera in the west (Dashwood and Abbotts, 1990).

At the bottom, the Tiyuyacu Formation (Eocene) overlies the Tena Formation with angular unconformity. The Lower Member of Tiyuyacu Formation consists of coarse-grained fluvial sediments; the sedimentation rate increased during this time of deposition, suggesting another period of progradation of the Andean orogenic wedge towards east (Baby et al, 2013).

An interval of erosion and missing sedimentary strata occurs above the Lower Member of Tiyuyacu Formation. The associated erosion marks the onset of an isostatic rebound due to the rapid exhumation of the Cordillera Real (Spikings et al, 2000). The subsequent Middle Eocene – Early Oligocene second-order sequence consists of the fluvial Upper Member of the Tiyuyacu Formation, transgressive Orteguaza Formation, and fluvial Chalcana Formation (Christophoul et al, 2002). This second-order sequence is the evidence of ongoing orogenic unloading (Baby et al, 2013).

Above all other sediments, the Neogene sediments were deposited with an increasing sedimentation rate (Baby et al, 2013). The Neogene sediments consist of the non-marine Arajuno and Chambira Formation in the west of the basin, the shallow marine or lacustrine Curaray Formation in the east, and the modern Pastaza alluvial megafan. Deposition was accompanied by a new rapid exhumation of the Cordillera Real; a new orogenic period of loading and eastward progradation of the retro-arc foreland basin system is recorded in this same time period (Baby et al, 2013).

1.4 LITHOLOGY AND SEQUENCE STRATIGRAPHY OF THE STUDY INTERVAL

1.4.1 Napo Formation

The Napo Formation consists of marine claystones, limestones, and sandstones that can be divided into several units. They are, from oldest to youngest: T Sandstone Member, U Sandstone Member, M2 Sandstone and M1 Sandstone (Dashwood and Abbotts, 1990). They can be yet further subdivided into the Lower Napo Shale, T Sandstone, B Limestone, Middle Napo Shale, U Sandstone, A Limestone, M2 Sandstone, M2 Limestone, M1 Limestone, M1 Sandstone and Upper Napo Shale (Ramirez et al, 1997). The claystones and limestones in the Napo Formation are claimed to have been deposited during significant regional transgressions whereas the sandstones were deposited during major regressions (Estupiñan, 2010). This view is probably oversimple, as some of the major sandstones may be transgressive as discussed herein.

The T Sandstone Member consists of sandstones interbedded with siltstones and carbonaceous claystones (Dashwood and Abbotts, 1990). The basal part of this member is believed by some researchers (Dashwood and Abbotts 1990) to have been deposited during a period of sea-level highstand; the sediments comprise coastal-plain deposits, tide influenced shoreline deposits, and offshore marine shoal strata. The basal succession is separated from the overlying T Sandstone by an erosive surface, possibly a sequence boundary. Above the sequence boundary, the T Sandstone was deposited during a subsequent regression and transgression. Relative sea level fall during the (forced) regression apparently resulted in a network of incised valleys; these valleys were filled by T Sandstones during the subsequent sea level rise. The T Sandstone was initially deposited in shoreline and fluvial environments; this passed to tidal shoal, deltaic and tidal channel sandstones, then ultimately lagoonal facies and marine facies. The B Limestone overlies T Sandstone; it was deposited during a period of rising relative sea level (Estupiñan, 2010).

The U Sandstone Member is separated from the underlying T Sandstone Member by a sequence boundary linked to incised valleys; the valleys were transformed into estuaries during the subsequent transgression. The U Sandstone comprises cross-bedded sandstones and wavy-bedded sandy siltstones that were deposited in tidally influenced estuaries during the sea level rise. The top of the U Sandstone Member consists of sandstones interbedded with mudstones; these sediments represent the last stages of transgression (Estupiñan, 2010).

The M2 sandstone only exists in the eastern part of the basin. It was deposited during a less significant regressive episode (Dashwood and Abbotts, 1990).

The M1 sandstone is a medium to coarse-grained, thickly bedded tidal sandstone body which can be locally subdivided into main sand and thinner upper sand. It reaches 120 feet in thickness in the east of the basin but is progressively eroded and thins towards west (Dashwood and Abbotts, 1990).

1.4.2 The M1 Sandstone

This thesis examines the M1 sandstone and other associated stratigraphic units. They are, from base to top: upper part of the Napo shale, M1 sandstone, and Basal Tena sandstone.

The upper part of the Napo Formation (below the base of M1 sandstone), according to a study by Jaillard et al. (2005), was deposited from the Late Santonian to Early Campanian. Near the top of this shale, deltaic deposits are evidenced by the upward coarsening of grain size.

The contact between the Napo shale and overlying M1 sandstone is erosional. The M1 sandstone is a cross-bedded sandstone succession deposited in a tidal estuarine setting. In the study area, the M1 sandstone can be locally subdivided into a main sandstone unit

and a thinner upper sandstone unit. Sharp based tidal channels filled with mud and fluvial-tidal channels that show fining upward grain size are time-correlated with M1 Sandstone in the study area. Above the M1 sandstone, a thin layer of shale was deposited from the Middle to Early Campanian and represents a maximum flooding event (Jaillard et al, 2005). Fine grained, intensively burrowed sandy layers are commonly found in the shale. These sandy layers are interbedded with mud, displaying typical tidally influenced structures such as flaser bedding, wavy bedding or sand lenses. Coal is found locally in the study area; the thickness of the coal layers ranges from less than one foot to eight feet.

The Basal Tena sandstone unconformably overlies the M1 sandstone. This fluvial sandstone was deposited during the early Maastrichtian; it is characterised by reddish terrestrial mud clasts from the west of the basin, which marks a change of sediment source direction from east to west. The unconformity was caused by the fluvial incision into the older sediment. The Basal Tena sandstone is not evenly distributed in the study area; the thickness ranges from zero to more than 5 feet.

1.5 PROBLEM STATEMENT

1.5.1 Facies, depositional systems, sequence stratigraphy, and origin of "shale barriers" in the Tarapoa oil field

Previous studies proposed various interpretations on facies, depositional systems, and sequence stratigraphy. Although these interpretations are supported by some evidence, negative evidence can always be found to negate some of these interpretations. This study aims to make new interpretations on facies, depositional systems, and sequence stratigraphy which are supported by most of the observations from M1 sandstone.

In addition, there are muddy, elongated, and slightly sinuous depositional architectures known as 'shale barriers' within the M1 succession of the study area, in

Tarapoa oil field. Each of them is more than 15 km long and 20 – 30 meters thick. Although the seismic images reveal the main body of the shale barriers, a significant sand-mud heterogeneity adjacent to the main body is not shown on seismic images due to the limitation of seismic resolution. Therefore, the sand-mud heterogeneity near the main body is unpredictable. This leads to a situation whereby, even if the operator avoided drilling into shale barriers, some wells are still drilled into a muddy or heterolithic interval which was thought to be sand. There has not been a convincing hypothesis which explains the origin of "shale barriers". A better understanding of the origin of shale barriers is now desirable, as well as knowledge of the associated sand-mud heterogeneity near the shale barriers, thereby avoiding wells being drilled into the muddy interval.

1.5.2 Predictive geological model in the Tarapoa northwest area

A second major objective of this work relates to the larger scale sedimentological/geological model of the succession in this area. An area northwest of the Tarapoa oil field is now being evaluated by the operator and the M1 sandstone in this target area has the potential be a major hydrocarbon producing unit. A predictive geological model that shows the lateral sandbody distribution, sandbody thickness, and sand-mud heterogeneity of M1 in this new area would be very helpful in the evaluation of the new acreage.

3-D seismic data have been acquired in the target area, however, only three well logs and no core is available until the end of this study. In this circumstance, the challenge is to make the predictive model from the seismic images and from improved knowledge of tidal estuarine sedimentary systems in the main Tarapoa area and from possible modern analogs.

1.6 DATASET AND METHODOLOGY

This study is based on well logs, cores, and seismic interpretation. Our dataset includes a total number of more than 300 well logs, 13 cores, and three seismic surveys.

Cores are described to interpret facies and depositional environments which are critical to this study. The grain size, sorting, roundness, physical sedimentary structures, biological sedimentary structures, and oil stain are examined in detail. The detailed facies information interpreted from cores is used to calibrate the lithofacies in well logs in the adjacent area.

Well logs can hardly provide facies information. The facies in the well logs are assumed to be the same or closely related with the facies found in the nearest core. Well logs are plentiful and have good vertical resolution, and these clearly show the stacking pattern of sand, mud, and organic-rich sediments. Therefore, they are used to extend the facies information from the cores to the gaps between cores. This allows us to map the thickness of facies across the study area.

1.6.1 M1 Sandstone sub-units and key surfaces in Tarapoa oil field

In Tarapoa oil field, M1 sandstone is divided into four sub-units on well logs. They are main M1 Sandstone, muddy M1, coal beds, and upper M1 Sandstone (Figure 1.3). The division of M1 on well logs is solely dependent on the lithology, without considering other aspects of facies. Therefore, each of the subunits represents one or multiple facies. Main M1 Sandstone is the major hydrocarbon-producing sandstone unit. It is generally the thickest sandstone and shows a blocky or slightly fining-upward gamma ray pattern; it is always found at the bottom of M1 sandstone. The main M1 Sandstone exists in most of the wells; this sub-unit can be missing in particular depositional architectures, as will be discussed later in detail. Muddy M1 includes the mud-rich interval which has high gamma ray readings; it is always found above the main M1 Sandstone. This sub-unit is found in

all of the wells in the study area. Coal beds are usually found inside Muddy M1; this sub-unit is missing in some of the wells. Upper M1 Sandstone is the sandstone which is always found near the top of M1 sandstone; it shows a blocky or slightly fining-upward gamma ray pattern. It may sometimes be confused with Tena Sandstone. The thickness of this sub-unit is highly variable and it is missing in some wells.

Surfaces with geological significance within the Napo/M1/Tena succession were picked on well logs in the study area. Important surfaces include M1 limestone top, base of Napo delta, base of main M1 Sandstone, top of main M1 Sandstone (which is equivalent to the base of muddy M1), top of muddy M1 (which is equivalent to the base of upper M1 sandstone), top of upper M1 Sandstone, base and top of coal beds, and basal Tena unconformity (which is the top of M1 sandstone).

Variations exist among the cores and well logs in the Tarapoa oil field. We interpret these variations to represent different depositional processes occuring at the same time in the same depositional system. The facies found in each core is assumed to represent the facies around it. The cores and their adjacent areas are assigned to different parts of the depositional system according to the depositional processes the cores represent. By doing this, the depositional system of the Tarapoa oil field is further separated into sub-environments, which provides more detailed and precise understanding of the geology in the study area.

The facies and depositional system of M1 sandstone in Tarapoa oil field were interpreted from the cores. Isopach maps of facies and facies association were made using the surfaces picked on well logs. The paleogeography was reconstructed for the facies and facies associations based on the isopach maps. Depositional models are built to show the depositional processes and relative sea level changes associated with the facies and facies

association. Finally, the depositional models are put into genetically-related sequences to show the sequences stratigraphy of M1 Sandstone.

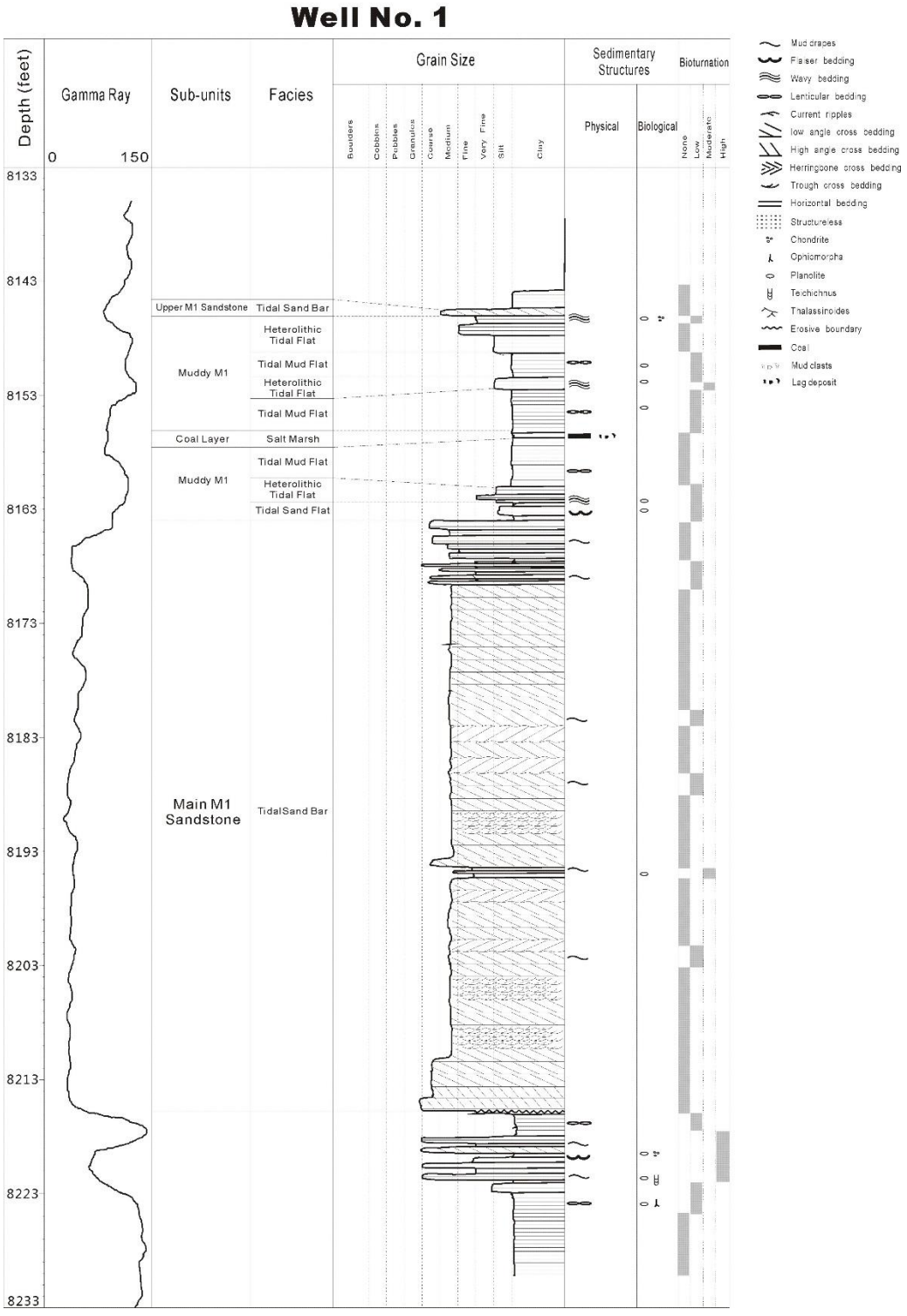

Figure 1.3 Core log of Well No. 1

1.6.2 Predictive geological model in the Tarapoa northwest area

By the end of this study, only three wells will have been drilled in the Tarapoa northwest area. Well logs from three wells are now available but no core was extracted for interpretation. Well data in this area is insufficient to interpret the facies, depositional system, and sand-mud heterogeneity in the Tarapoa northwest area. Although seismic surveys cover this area, the low resolution limits the information that can be extracted from the seismic data. In this study, the solution to the data problem is to project from the data-rich to the data-poor areas and thus interpret the facies, depositional system, and sand-mud heterogeneity further northwest from the study area. We estimate that the Tarapoa northwest area is likely to be the transition zone between the Pichincha-Carabobo area and Tarapoa oil field. Therefore, the character of facies, depositional system, sand bodies, and sand-mud heterogeneity (i.e. "shale barriers") in Tarapoa northwest area should also, to some extent, be transitional between these in the Pichincha-Carabobo area and Tarapoa oil field.

The core of well No. 4 extracted from the Pichincha-Carabobo area is the key for this part of the study. A new interpretation of transgressive shelf sand-ridge facies is now made from the core, predicting that this area was a tidally-influenced open marine environment which is seaward of the tide-dominated estuary in Tarapoa oil field. The Carabobo well logs which occur around the well No. 4 also provide important evidence which support this facies and depositional system interpretation. Geometries of sand bodies and possible "shale barriers" in this area are estimated based on the facies and depositional system. Finally, by comparing the facies, depositional systems, sand bodies and "shale barriers" in Tarapoa oil field and Pichincha-Carabobo area, the facies, depositional systems, sand bodies and "shale barriers" in Tarapoa northwest area are estimated.

Chapter 2: Facies, depositional system, sequence stratigraphy, and origin of "shale barriers"

2.1 FACIES INTERPRETAION

Five lithofacies are interpreted from the cores of M1 sandstone. The lithofacies are interpreted based on: grain size variations; physical sedimentary structures; biological sedimentary structures; oil staining.

1. Cross bedded sandstone with mud drapes and rhythmites

This sandstone is light brown to black colored, fine to coarse grained, cross bedded, oil stained with low abundance of mud drapes. The main and upper M1 sandstones (Figure 1.3) consist of this type of sandstone facies. Below this sandstone, the prodeltaic to delta-front facies of upper Napo shale consists of an upward-coarsening sedimentary package. The main M1 cross-bedded sandstones are bounded below by a sharp and erosive contact (Figure 1.3) which is interpreted to represent a transgressive ravinement surface. Above the cross-bedded sandstones, muddy M1 facies gradually developed as mud-rich muddy M1 sediment.

The dark color of the sandstone is the result of oil stain; light brown and black color indicate low to high degree of oil stain, respectively. The degree of oil stain is generally high, which makes this sandstone dark colored. The sandstone is moderately to poorly sorted and sub-rounded. Unidirectional and bidirectional (herringbone) cross-bedding is common in this sandstone (Figure 2.1A). In rare cases, cross-bedded sets evolve into having a tangential lower contact (Figure 2.1B). Individual bed or set thickness ranges from 0.5 to 3 feet and the amalgamated unit can reach up to 100 feet. Sand layers are difficult to identify and measure because the grain size is uniform and the color of sandstone is dark. Rhythmic thick-thin alternation of sand layers are recognized where the degree of oil stain

is relatively low and sand layers can be distinguished from each other. The bioturbation is low or absent in the sandstone.

Mud drapes are not common in this sandstone. They usually occur in small groups along reactivation surfaces (Figure 2.1C). The reactivation surfaces associate with mud drapes and fine to very fine grained sandstone with low degree or no oil stain. Mud drapes are locally abundant in some intervals. The sandstone is brown colored and less oil stained. In some cases, tangential lower contacts of cross bedding are observed where the mud drapes are relatively abundant and degree of oil stain is relatively low.

We interpret this sandstone unit in terms of tidal sand bar facies. Rhythmic thick-thin alterations of sand layers can be produced by change of tidal current speed in neap and spring tides (Dalrymple, 2012). Heterolithic bedding of sand and mud drapes and low degree of bioturbation caused by high sedimentation rate in brackish-water environment can be a good indication of tidal origin (Dalrymple, 2012). Unidirectional and bidirectional (herringbone) cross bedding are widely used as indicators of tidal deposition (Dalrymple, 2012). In addition, tangential lower contacts of cross bedding are commonly found in tidal bundles which are products of tidal deposition (Terwindt, 1981). The above evidences suggest that this sandstone was deposited as sand-rich bars in a tide-dominated delta or estuary. Because of the sharp erosive base and the lack of any upward coarsening pattern, we prefer the estuary interpretation. The low degree of bioturbation indicates a high sedimentation rate which is unfavorable for the burrowing marine fauna to live (Shanmugam et al, 2000). Coarse grained sediment implies high current speed. In tide-dominated deltas and estuaries, high sedimentation rates, high current speeds, and coarse grained sediments are associated with sub-tidal sand bar conditions.

The generally low abundance of mud drapes could have resulted from the clean-water character of the system and the resultant low suspended-sediment concentration near

tidal sand bars, which limits the amount of mud available for deposition (Dalrymple et al, 2012). The local high abundance of mud drapes may indicates bottomsets of tidal dunes. Mud drapes are more concentrated in the bottomsets than the foresets of tidal dunes. This is because the bottomsets are sheltered by the dune crest so the velocity of tidal currents near the bottomsets is lower than on the foresets of tidal dunes (Dalrymple et al, 2012). The lower current speed near bottomsets allows more mud to be deposited, making mud drapes locally abundant.

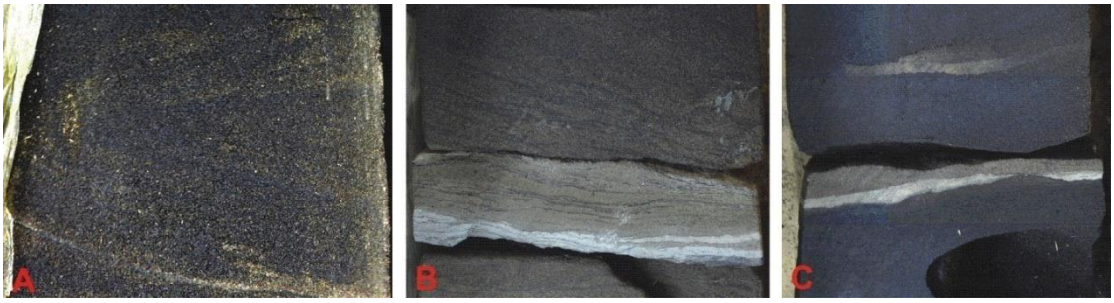

Figure 2.1 Core photos of tidal sand bar facies. (A) Bidirectional (herringbone) cross-bedding. (B) Full-vortex structure. (C) Reactivation surfaces.

2. Heterolithic, flaser-bedded sandstone with rhythmites

This sandstone is white to grey colored, very fine to fine grained, not oil stained, flaser-bedded with abundant mud drapes. It is part of the Muddy M1 sub-unit (Figure 1.3). Below this sandstone, Main M1 sandstone consists of dark colored, cross bedded sandstone. Main M1 Sandstone passes gradually upward to this sandstone. Above this sandstone, the muddier part of Muddy M1 consists of heterolithic sediments which contain approximately only 50% sand. This sandstone passes gradually upwards to the heterolithic deposits above.

The white to grey color of this sandstone is the result of low mud content and the absence of oil stain. The sandstone is well sorted and sub-rounded. Individual bed or set thickness ranges from 0.2 to 1 feet. Mud drapes are ubiquitous. Mud drapes are generally thin, rarely exceeding 1mm. They occur as flasers in the sandstone, and are termed flaser bedding (Figure 2.2A). Rhythmic alternation of sand and mud layers is best pronounced in the transition zone between this facies and muddier facies above (Figure 2.2B). This is because the mud layers in this facies are thin and highly discontinuous. The abundance of bioturbation in this sandstone is low to medium; the bioturbation consist of *Planolites* and *Chondrites*.

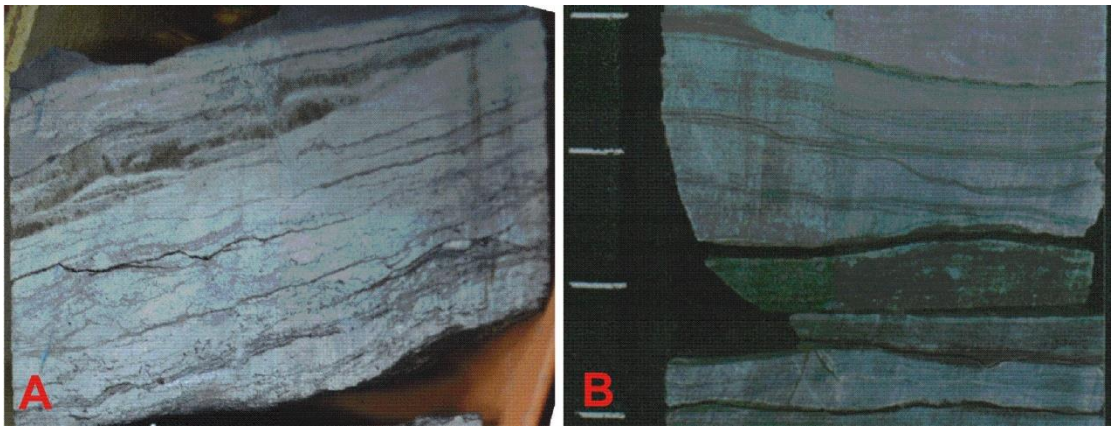

Figure 2.2 Core photos of tidal sand flat facies. (A) Flaser bedding. (B) Rhythmic alternation of sand and mud layers.

We interpret this sandstone as belonging to inter-tidal sand flat facies. Rhythmic alternation of sand and mud forms tidal rhythmites, typically present in the inter-tidal sedimentation zone (between high and low tide levels). Abundance of mud drapes (indicating slack water at either end of a tidal half cycle) is also an evidence of tidal

deposits. Therefore, this facies represents an inter-tidal environment. Low to medium abundance of bioturbation suggests marine environment with relatively low sedimentation rate favorable for the burrowing marine fauna to live (Shanmugam et al, 2000). Very fine to fine grained sand and occurrence of abundant mud drapes together indicate an environment with relatively low energy. A tidal environment with low sedimentation rate and low energy are inter-tidal flats in estuaries, deltas and on some open coasts. Intertidal flats are composed of tidal sand flat, heterolithic tidal flat, and supratidal tidal mud flat are especially common along the margin of tide-dominated estuaries. Tidal flats are bordered by tidal channels at their seaward boundary (Figure 2.3). The velocity of tidal current decreases from tidal channels to supratidal area (Dalrymple, 2012). Because of this, the content of sand also decreases from seaward to landward part of tidal flats. The dominance of sand in this facies indicates it is the most seaward part of tidal flats, which is tidal sand flat. This interpretation is supported by flaser bedding which is a diagnostic feature of tidal sand flat (Reineck and Wunderlich, 1968). This sandstone is not oil stained because the abundant mud drapes may have stopped the oil from entering this sandstone.

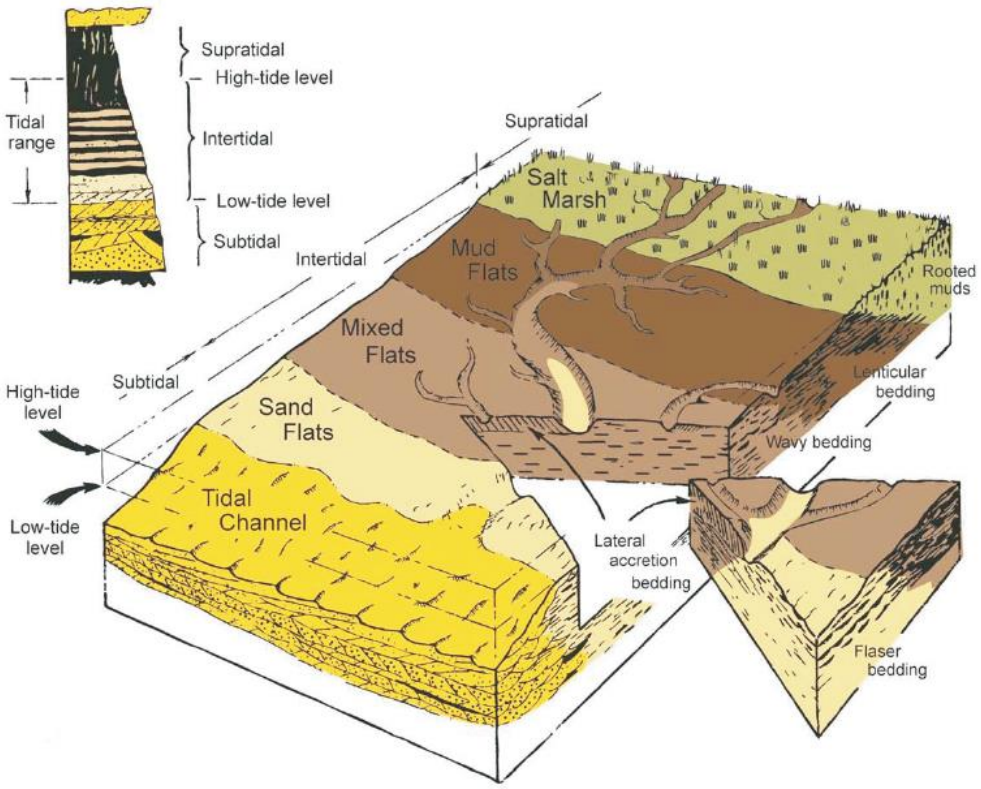

Figure 2.3 Block diagram of a tidal flat associated with tidal channel (from Dalrymple, 2012).

3. Heterolithic deposits with wavy-bedded sandstone, mudstone and rhythmites

These heterolithic deposits consist of interbedded sandstone and mudstone which are grey colored, wavy-bedded, and not oil stained. This facies is part of muddy M1 sub-unit (Figure 1.3). Below this sandstone, tidal sand flat facies consists of grey colored, flaser bedded sandstone. Tidal sand flat facies passes gradually upwards to these heterolithic deposits; the transition between two facies is very gradual (Figure 2.4A). Above these heterolithic deposits, the muddiest part of muddy M1 sub-unit consists of mudstone with

lenticular bedding (isolate sand ripples surrounded by mud). This facies passes gradually upward to the dark colored, lenticular bedded mudstone above.

The grey color of this heterolithic deposits is the result of approximately 50% mud content. Oil stain is absent. The sandstone is well sorted and sub-rounded. Individual bed or set thicknesses ranges from 0.2 to 2 feet. Sand and mud are of approximately equal content. Sand and mud occur in the shape of waves, forming wavy bedding (Figure 2.4B). The abundance of bioturbation in this sandstone is medium to high (Figure 2.4C); the bioturbation is dominated by *Planolites and Chondrites*. Rhythmic alternation of sand and mud layers can be observed where the abundance of bioturbation is relatively low (Figure 2.4B). Physical depositional structures are destroyed in sections which are completely bioturbated.

We interpret these heterolithic deposits as heterolithic tidal flat, somewhat more sheltered or lower energy than the facies described earlier above.. Rhythmic alternation of sand and mud layers is interpreted as tidal rhythmites which are signals of tidally-influenced environment. Medium to high abundance of bioturbation indicates the environment has low sedimentation rate. The abundance of mud suggests low current speed. A tidally influenced environment with low sedimentation rate and low energy can be found in muddy inter-tidal flats. Dominance of wavy bedding implies heterolithic tidal flat. This is because this bedding is most commonly found in heterolithic tidal flats (Reineck and Wunderlich, 1968; Dalrymple, 2012).

Heterolithic tidal flats lie immediately landward or along strike of sandy inter-tidal flats (Figure 2.3). The content of mud increases from tidal sand flat to heterolithic tidal flat as the speed of tidal current decreases from the tidal channels towards supratidal area (Dalrymple, 2012). Because of this, the higher content of mud also supports heterolithic tidal flat interpretation.

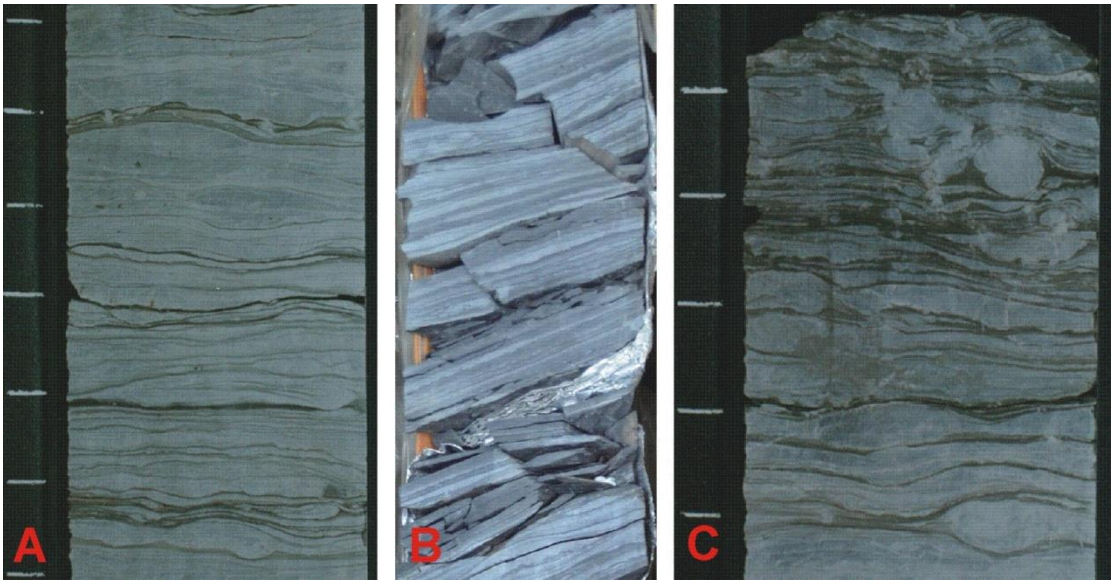

Figure 2.4 Core photos of heterolithic tidal flat facies. (A) Transition zone between heterolithic tidal flat facies and tidal sand flat facies. (B) Wavy bedding and rhythmic alternation of sand and mud layers observed where the abundance of bioturbation is low. (C) Medium to high abundance of bioturbation disrupts physical depositional structures.

4. Heterolithic, lenticular-bedded mudstone with rhythmites

This mudstone is dark grey colored, not oil stained, and lenticular bedded. It is the muddiest part of muddy M1 sub-unit (Figure 1.3). Below this mudstone, heterolithic inter-tidal flat deposits consists of grey colored, wavy bedded sandstone and mudstone. Heterolithic inter-tidal flat facies passes gradually upward to this supratidal mudstone. Above this mudstone, coaly deposits consists of coal, coaly mudstone, and organic-rich mudstone all caused by marsh grasses on the supratidal flats. This mudstone passes gradually upward to the coaly deposits above.

The dark grey color of this mudstone is the result of high mud content. Oil stain is absent. Individual bed thickness ranges from 0.2 to 3 feet. In rare cases it can reach up to 7 feet. Sandstone occurs in lenses which are surrounded by mud, forming lenticular

bedding (Figure 2.5A). Rhythmic alternation of sand and mud layers is best pronounced in the transition zone between this facies and sandier facies below (Figure 2.5B). This is because the sandstone in this facies is thin and highly discontinuous. The abundance of bioturbation in this sandstone is low to medium; the bioturbation is dominated by *Planolites*.

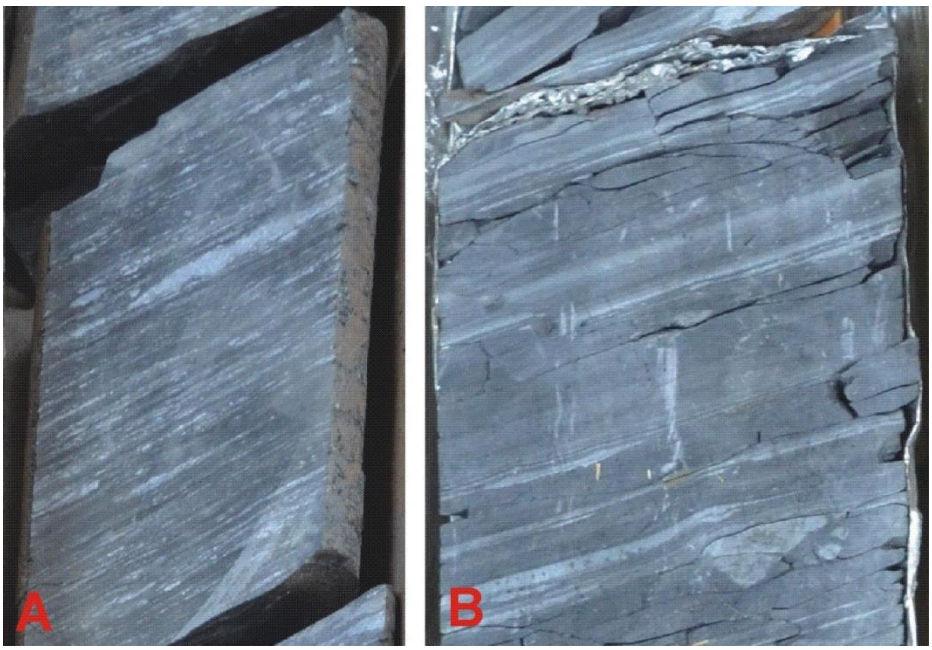

Figure 2.5 Core photos of tidal mud flat facies. (A) lenticular bedding. (B) Rhythmic alternation in transition zone between tidal mud flat facies and heterolithic tidal flat facies.

We interpret this mudstone as belonging to supra-tidal mud flat facies. The rhythmic alternation of sand and mud is interpreted as tidal rhythmites which represent a tidally-influenced environment. The dominance of mud in this facies indicates the environment has very low current speed. This evidence indicates a tidal flat environment.

Tidal mud flats lie immediately landward of heterolithic tidal flats (Figure 2.3), and the content of mud here is higher than in the heterolithic tidal flat deposits. In addition, lenticular bedding and the dominance of mud are the diagnostic features of supratidal mud flats (Reineck and Wunderlich, 1968; Dalrymple, 2012).

Low abundance of bioturbation suggests high sedimentation rates in the previous facies. In this facies, we interpreted that it is the long period of subaerial exposure which leads to low abundance of bioturbation. Because supratidal mud flats are the most landward part of tidal flats, they are subaerial for most of the time and only become subaqueous at highest spring tides. Long periods of subaerial exposure keep most marine faunas away from this environment, and result in low abundance of bioturbation.

5. Coal, coaly mudstone, and organic-rich mudstone

The coaly deposits consists of black colored, planar laminated coal, coaly mudstone, and organic-rich mudstone. Below these coaly deposits, tidal mud flat facies consists of dark grey colored, lenticular bedded mudstone. Tidal mud flat facies passes gradually upward to facies 5. The facies above these coaly deposits are variable between cores. In some of the cores, upper M1 sandstone of tidal sand bar facies lies immediately above this facies. In other cores, tidal flat facies lies between upper M1 sandstone and this coaly deposits. In either cases, sharp contact exists between these coaly deposits and the facies above (Figure 1.3).

The black color of this coaly deposit is the result of high organic and coal content. Oil stain is absent. Individual bed thickness ranges from 0.2 to 2 feet. This facies is dominated by coaly mudstone and organic-rich mudstone. Coal usually occurs as lenses or thin layers (Figure 2.6A). This facies exhibits planar lamination (Figure 2.6B). Bioturbation and rhythmic alternation are not observed. The density of this facies is lower

than other facies in M1 sandstone because of the high content of organic matter and it can be recognized on the density log.

We interpret these coaly deposits as belonging to salt marsh deposits. The gradual transition between this facies and supra-tidal mud flat facies implies that they are laterally connected to each other. Therefore, these coaly deposits were developed on the margins of tide-dominated deltas or estuaries. The absence of rhythmic alternations implies that this environment is not regularly influenced by tides. The absence of sand indicates an environment almost free of water currents. The presence of organic-rich material suggests terrestrial environment. And this is confirmed by the absence of bioturbation. Integrating the above evidence, the terrestrial environment which is connected with tidal mud flat and not influenced by tidal current is salt marsh. Salt marsh is an environment furthest landward of tidal mud flat. Its landward position makes it a terrestrial environment rarely influenced by tide and other currents.

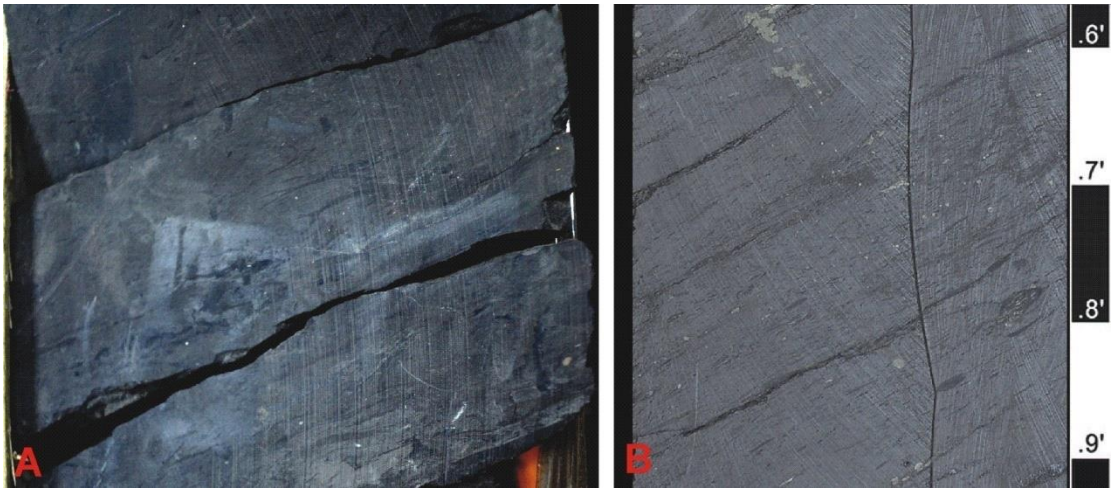

Figure 2.6 Core photos of salt marsh facies. (A) Black colored coal and coaly shale occurs sometimes in the shape of lenses or flasers. Coal is bedded within coaly mudstone and organic-rich mudstone. (B) Planar lamination.

2.2 DEPOSITIONAL SYSTEM

The core study revealed the above five facies in M1 sandstone in Tarapoa oil field. The depositional systems which could explain all the five facies are tide-dominated deltas and tide-dominated estuaries. The difference between tide-dominated deltas and tide-dominated estuaries is that the sediments in tide-dominated deltas coarsen upwards and the delta environment is regressive. Tide-dominated estuaries do not have coarsening upward sediments. Instead, estuaries are transgressive coastlines and transgressive ravinement associated with a rising sea level erodes the underlying deposits and leaves sharp contact between tidal sand bar deposits and the older deposits below it. The gamma ray well logs show that M1 sandstone has a sharp base in most of the wells (Figure 1.3). Although coarsening upward is developed in upper Napo shale in many wells, only in rare cases the upper Napo shale has the appearance of gradually coarsening into M1 sandstone. In most of the wells, sharp contact clearly marks the boundary between M1 sandstone and coarsening upward part of upper Napo shale. Because of the sharp contact at the base of M1 sandstone, a tide-dominated delta interpretation is less likely, and we interpret M1 sandstone in terms of a tide-dominated estuary system.

2.3 DEPOSITIONAL MODELS

Four depositional models are built to show the depositional processes of specific facies and facies associations in M1 sandstone. The depositional processes are associated with relative sea level changes. In this way, we interpreted the relative sea level changes associated with facies and facies associations based on the interpreted depositional processes. Finally, the sequence stratigraphy of M1 sandstone is built from the sequential relative sea level changes.

The depositional models are built based on isopach maps of facies and seismic amplitude map. Making these isopach maps utilizes geological surfaces picked on more

than 300 well logs. To build the models, the first step was to pick the upper and lower boundaries of each facies and facies association on well logs. The facies boundaries are identified using gamma ray, caliber, resistivity, neutron porosity, bulk density, and sonic logs. The second step is to generate isopach maps (i.e. thickness map) of each facies and facies associations with the surfaces picked on well logs. The third step is to reconstruct the paleogeography of Tarapoa oil field during the deposition of each facies and facies associations. The paleogeography is reconstructed based on seismic amplitude map and isopach maps of each facies and facies association. The final step is to create three-dimensional depositional models which show the depositional processes that occurred in Tarapoa oil field during the deposition of each facies and facies association.

2.3.1 Depositional model of Main M1 Sandstone

Main M1 Sandstone is the thickest sub-unit in M1 succession in most of the wells (Figure 1.3). It can be found in almost every well in the study area. Its thickness is usually more than 50% of total thickness of M1 sandstone. Core study interpreted this sandstone as tidal sand bar facies. On well logs, the upper and lower boundaries are identified using gamma ray readings (Figure 2.2). At the bottom of this sandstone, this sandstone and the underlying upper Napo shale are separated by a sharp erosive surface, interpreted as a transgressive ravinement surface. Fine grained sediments of upper Napo shale change to much coarser grained sediments in the main M1 Sandstone across this surface. On well logs, gamma ray reading decreases sharply across this surface; this marks the lower boundary of main M1 sandstone. At the top of this sandstone, it passes gradually to tidal flat deposits (muddy M1 sub-unit). Gamma ray reading increases as content of mud increases. The upper boundary is picked where gamma ray reading increases to 75. The

isopach map of this sandstone reflects the distribution and orientation of tidal sand bars, tidal channels, and swatchways (Figure 2.7). In a tide-dominated estuary, tidal sand bars are usually elongated and oriented approximately parallel to the dominant tidal current (Dalrymple et al, 2012). Tidal channels are the large-scale channels which work as pathways of tidal currents and they are also oriented parallel to the dominant tidal current. Tidal channels are connected by swatchways. Swatchways are smaller-scale, shallower channels which lie at an angle deviated from tidal channels. They connect the tidal channels and cut across the tidal sand bars, splitting large and elongated tidal sand bars into clusters of smaller tidal sand bars (Robinson, 1960).

A seismic amplitude map is also used to build the model for tidal sand bar facies. Three seismic amplitude maps are provided by the oil field operator, each covers a different area in the oil field. They are assembled into one map to that covers both Tarapoa oil field and Tarapoa northwest area (Figure 2.8). The light color in the seismic amplitude map indicates thick sand and dark color indicates thin sand. The resolution of seismic data is limited; it can only reflect the total thickness of sand in M1 sandstone. The limitation of resolution makes it impossible to interpret the thickness of every subunit within M1 sandstone with seismic data. However, seismic data can reflect the thickness of main M1 sandstone because most of the sand in M1 sandstone is in this sub-unit. In areas where the density of wells is low, the accuracy and precision of the isopach map is poor. The seismic amplitude map has uniform lateral resolution across the study area, and this serves as a good compensation in areas with low well density.

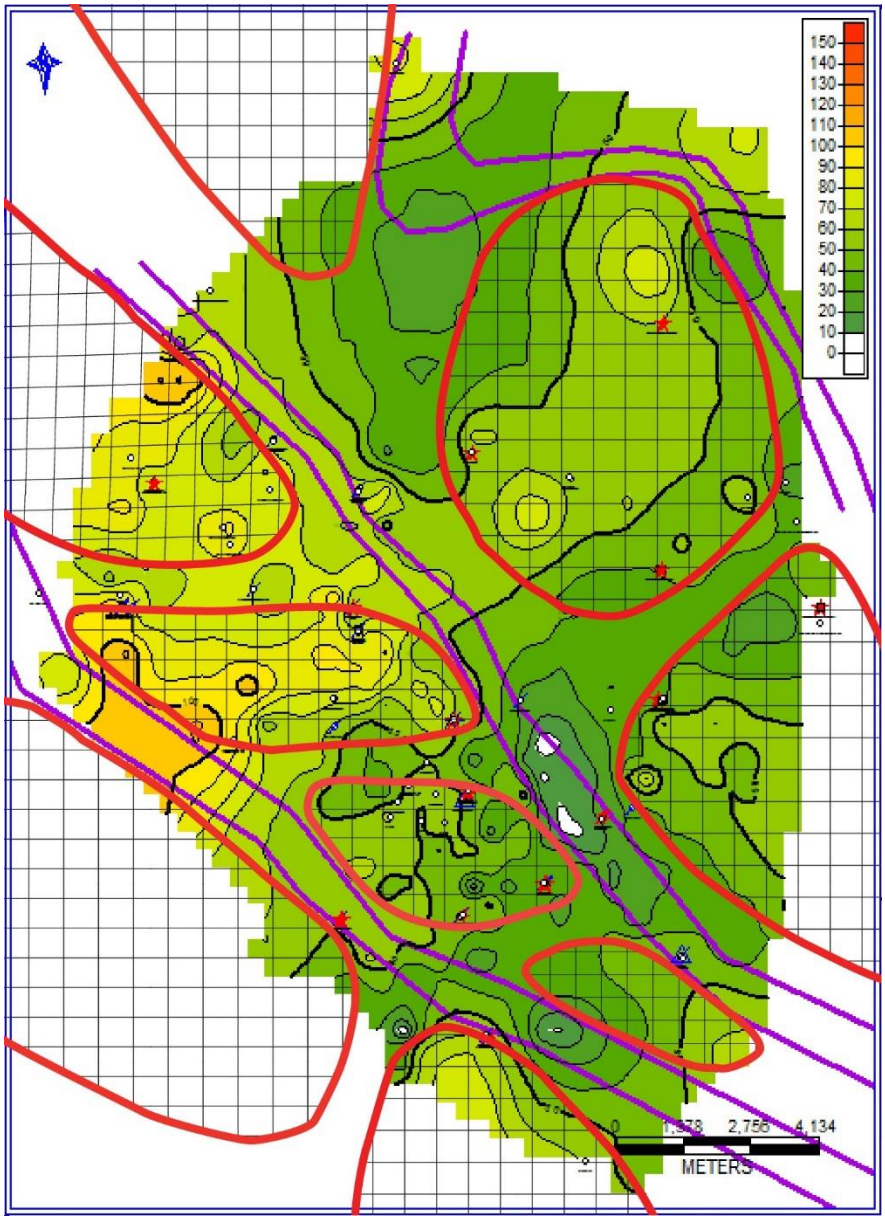

Figure 2.7 Isopach map of Main M1 Sandstone. Tidal sand bars are outlined with red boundaries. Purple double lines mark boundaries of "shale barriers" (i.e. tidal channels). As the bars migrate they generally infill a channel.

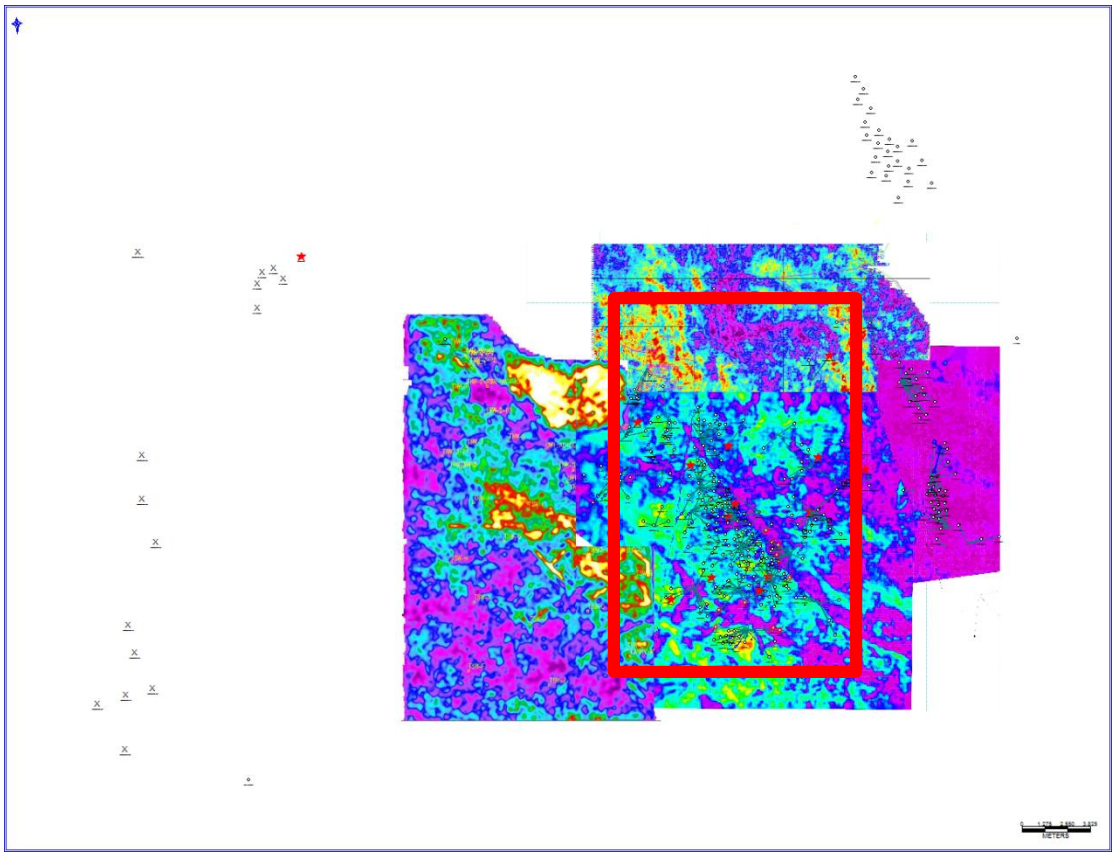

Figure 2.8 Assembled seismic amplitude map of the study area. Figure 2.7 occupies only a part of this map (inside red box).

The distribution and orientation of tidal sand bars and tidal channels are outlined on the isopach map of main M1 Sandstone (Figure 2.7). Although the distribution and orientation of tidal sand bars and tidal channels are not directly mapped on seismic amplitude map, it is useful to interpret thickness of sand and mud in areas with low well density and distribution of sand and mud on large-scale. There are two criteria to locate tidal sand bars on the isopach map: tidal sand bars occur where the tidal sand bar facies thickness is high; tidal sand bars have more or less elongated shape. Two criteria are used to locate tidal channels on the isopach map: tidal channels occur at places where the

thickness of tidal sand bar facies is very low because the currently active channels are water pathways which should not be filled with much sediment; tidal channels are very elongated and slightly sinuous. The tidal sand bars and tidal channels interpreted from the isopach map are oriented in broadly the same direction, which is the direction of dominant tidal current. Three criteria are used to locate swatchways: they occur inside the large-scale elongated tidal bars and separate them into cluster of smaller tidal bars; the tidal sand bar facies thickness of swatchways is greater than tidal channels but less than tidal bars because swatchways are smaller and shallower than tidal channels; they are very elongated, like other channels; they are deviated from the dominant tidal current. The distribution and orientation of tidal sand bars, tidal channels, and swatchways are shown in the paleogeography reconstruction of study area in Figure 2.9.

Three tidal channels are shown in the reconstructed paleogeography. The tidal channel in the northeast only has tidal sand bars on its southwest side. This strongly suggests that during the deposition of this tidal bar facies, tidal flats were positioned on the northeast side of this tidal channel and this tidal channel was the boundary between tidal sand bars in the southwest and tidal flats in the northeast. In other word, this tidal channel marks one of the main boundaries of the ancient Tarapoa tide-dominated estuary. Moreover, part of this tidal channel is more sinuous than other tidal channels. In modern tide-dominated estuaries, the boundaries of tide-dominated estuaries can have similar geometry which makes tidal channels locally more sinuous (Figure 2.10). Other tidal channels in Figure 2.7 have tidal bars at both sides and these channels have low sinuosity. These tidal channels are not likely to be at the boundary of tide-dominated estuary. Because only one tidal channel is interpreted as a boundary of the estuary and the other boundary is missing, it is likely that the study area is just part of a larger tide-dominated estuary.

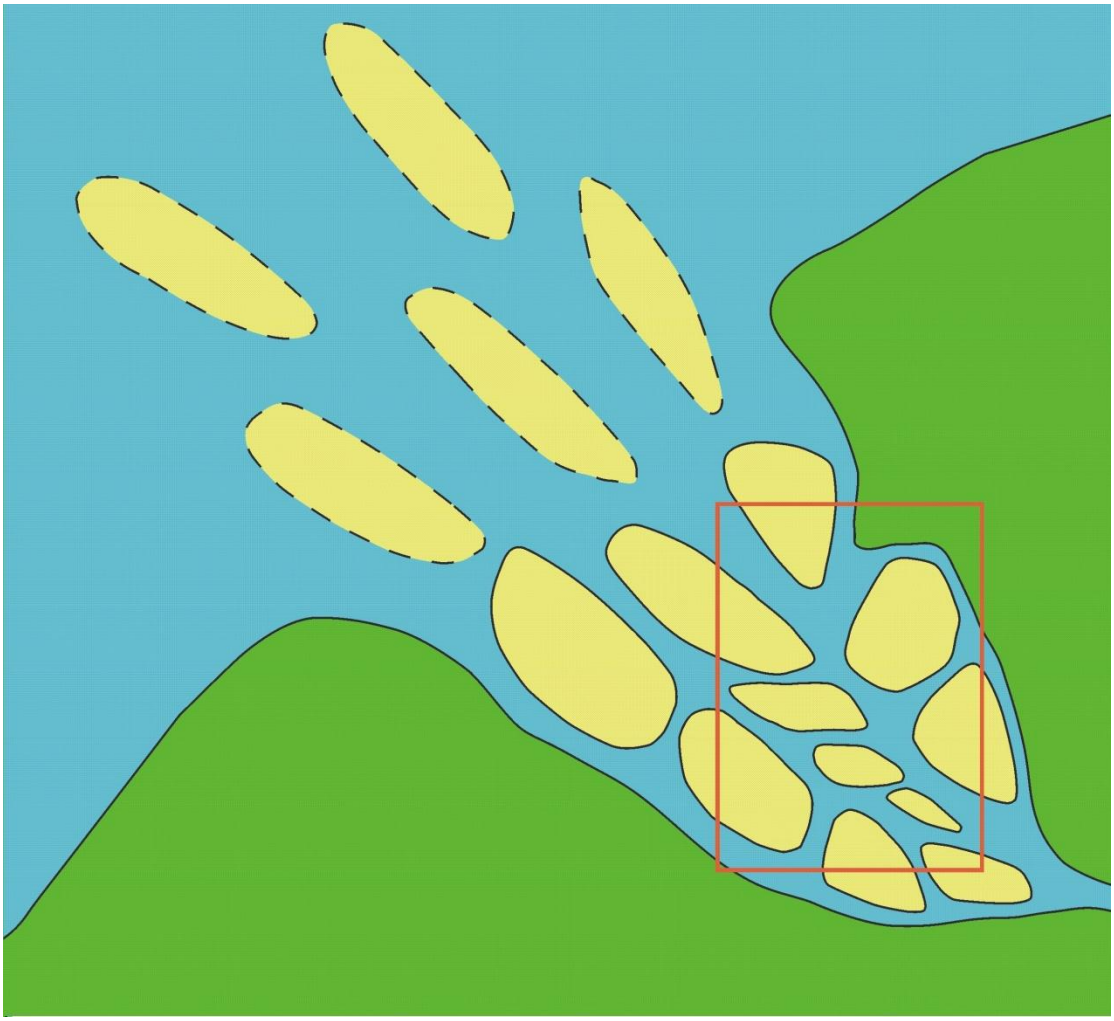

Figure 2.9 Reconstructed paleogeography during the deposition of main M1 Sandstone. The study area (and area of Figure 2.7) is marked by a red rectangle.

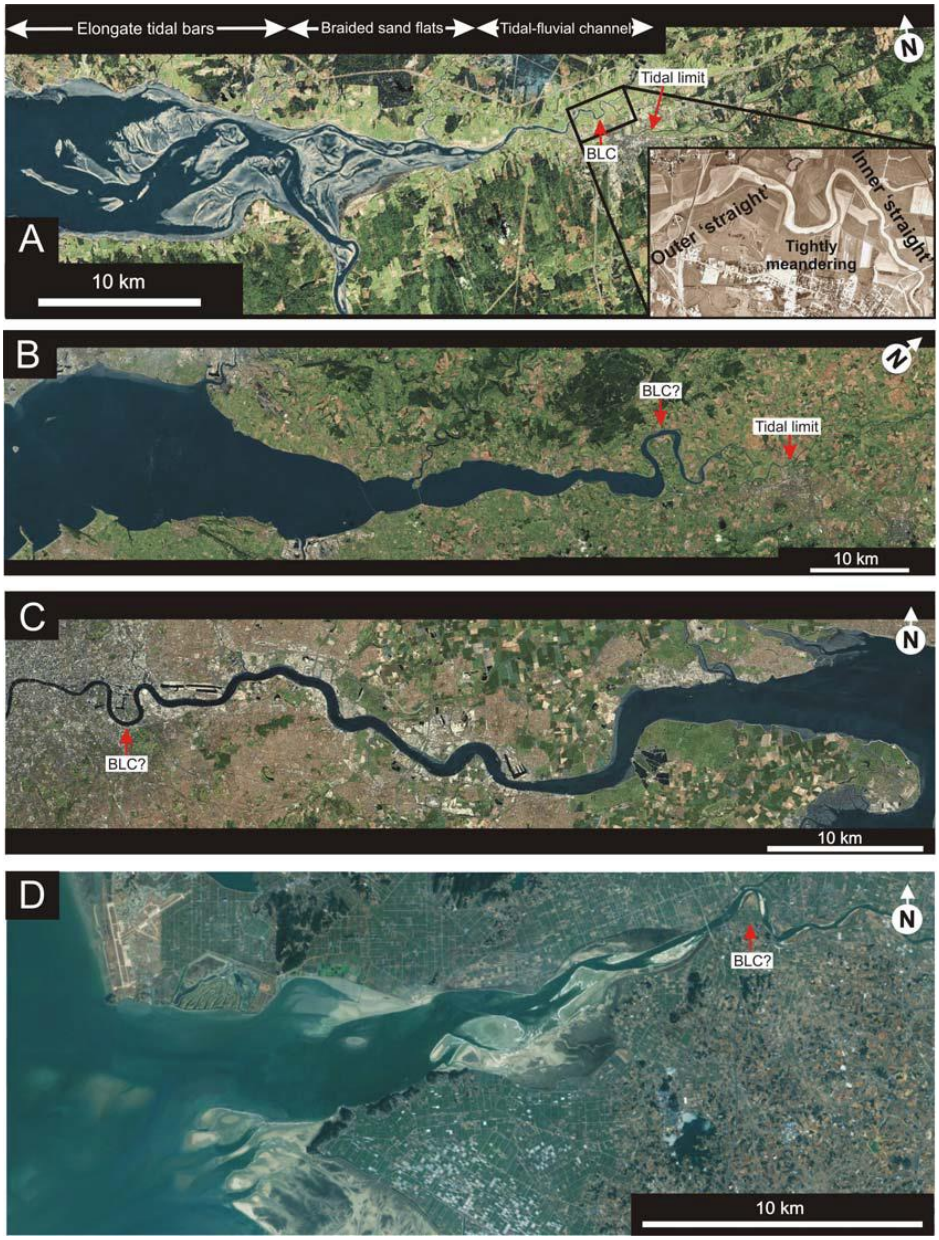

Figure 2.10 Modern tide-dominated estuaries. The tidal channels along the margin of these estuaries show locally enhanced sinuosity. (A) the Cobequid Bay—Salmon River (CB—SR) estuary, Bay of Fundy; (B) the Severn estuary, England; (C) the Thames estuary, England; and (D) the Mangyeong estuary, Korea. (From Dalrymple et al, 2012).

Figure 2.11A shows the three dimensional depositional model of Tarapoa oil field during the time of deposition of the main M1 Sandstone. During the deposition of this sandstone, the relative sea level was rising. Transgressive ravinement truncated the coarsening upward part of underlying upper Napo shale. A tide-dominated estuary was formed over the study area and it deposited tidal sand bar deposits on the ravinement surface. During this period, the tidal channels were active.

An important variation exists between the northeastern area and other areas of the Tarapoa oil field. In the northeastern area, the main M1 Sandstone is generally thinner and less amalgamated than that in other areas (Figure 2.12). Main M1 Sandstone in all other areas is generally thick and amalgamated. It shows blocky or slightly fining upward patterns on the gamma ray curve. In the northeastern area, however, only the lower part of the main M1 Sandstone is amalgamated. The upper part of M1 sandstone is irregular and broken into several thinner sandstone layers, separated by muddy intervals which are one to five feet thick (Figure 2.12). This subdivided aspect of the main M1 Sandstone limits the thickness of reservoirs in the northeastern area, which limits the resource potential of M1 sandstone in this area. The core from well No. 2 provides an example of the evidence of this important lateral variation of main M1 Sandstone (Figure 2.13).

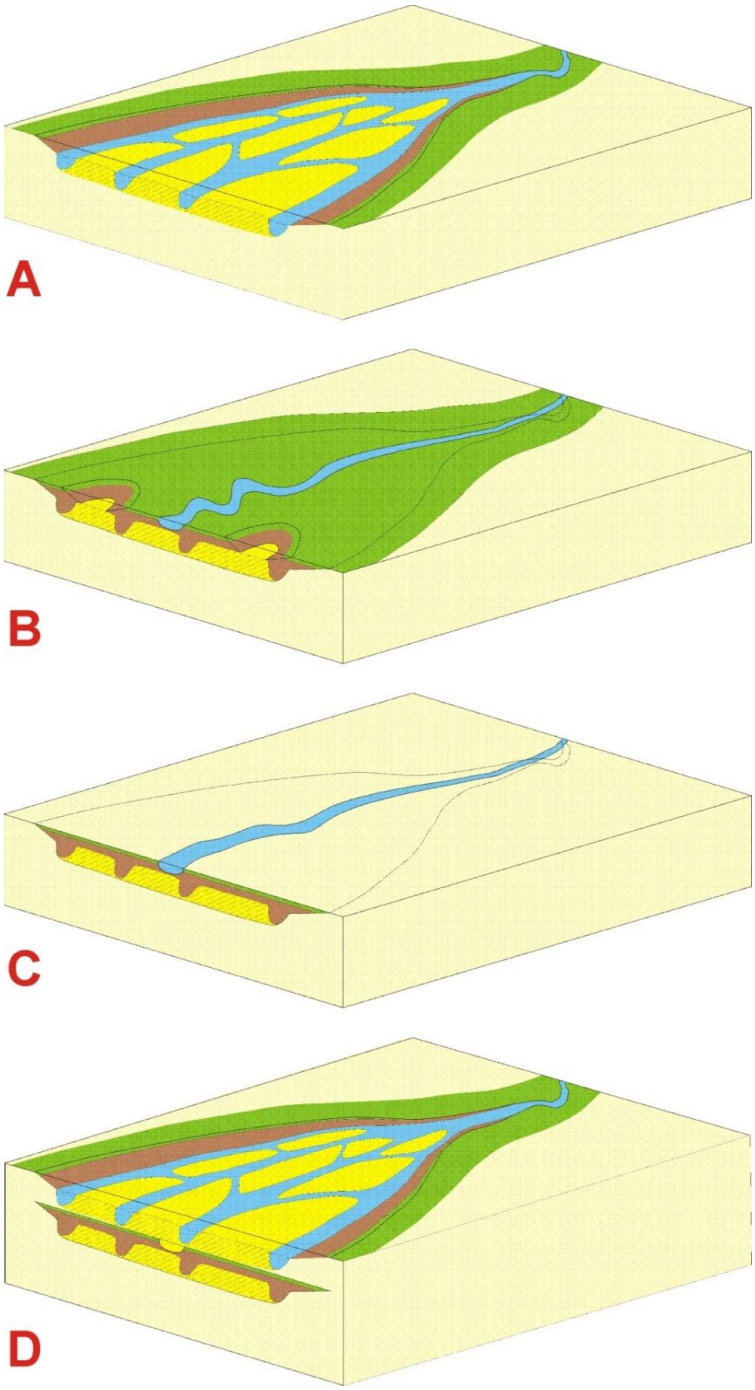

Figure 2.11 Depositional models during the deposition of M1 sandstone. (A) During the deposition of main M1 Sandstone. (B) During the deposition of muddy M1 and coal layer. (C) During the sediment bypass period. (D) During the deposition of upper M1 Sandstone.

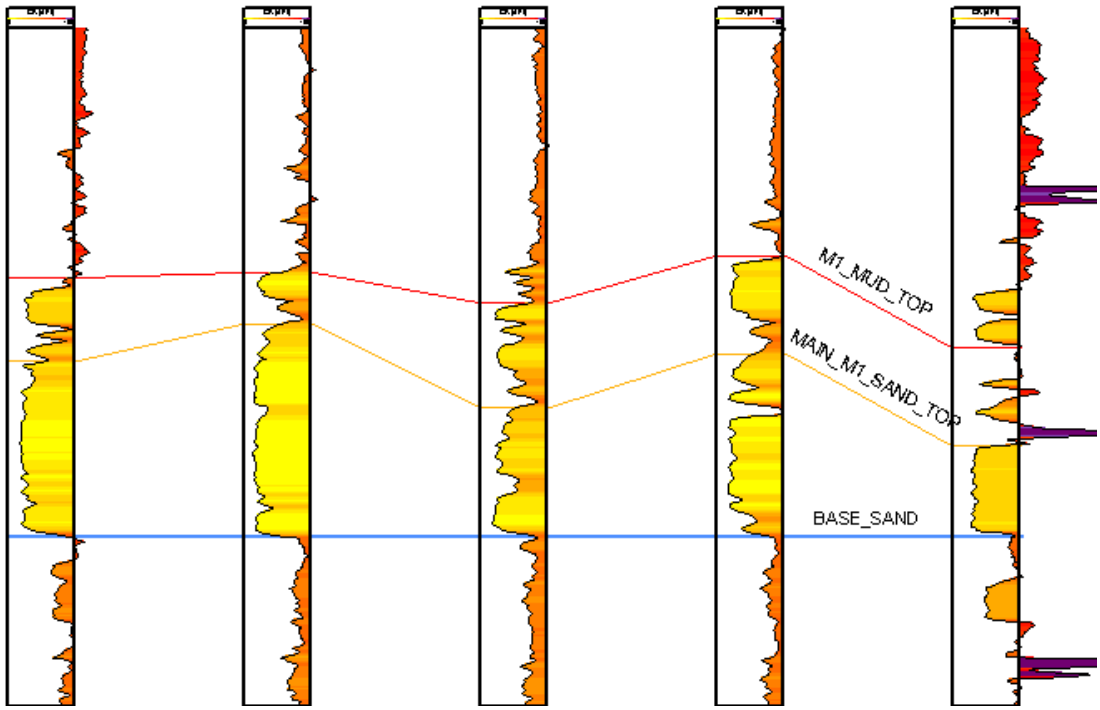

Figure 2.12 Well logs in the northeastern area of Tarapoa oil field. The main M1 Sandstone is not well amalgamated in its upper portion, but is rather broken into thinner sandstones separated by mudstone.

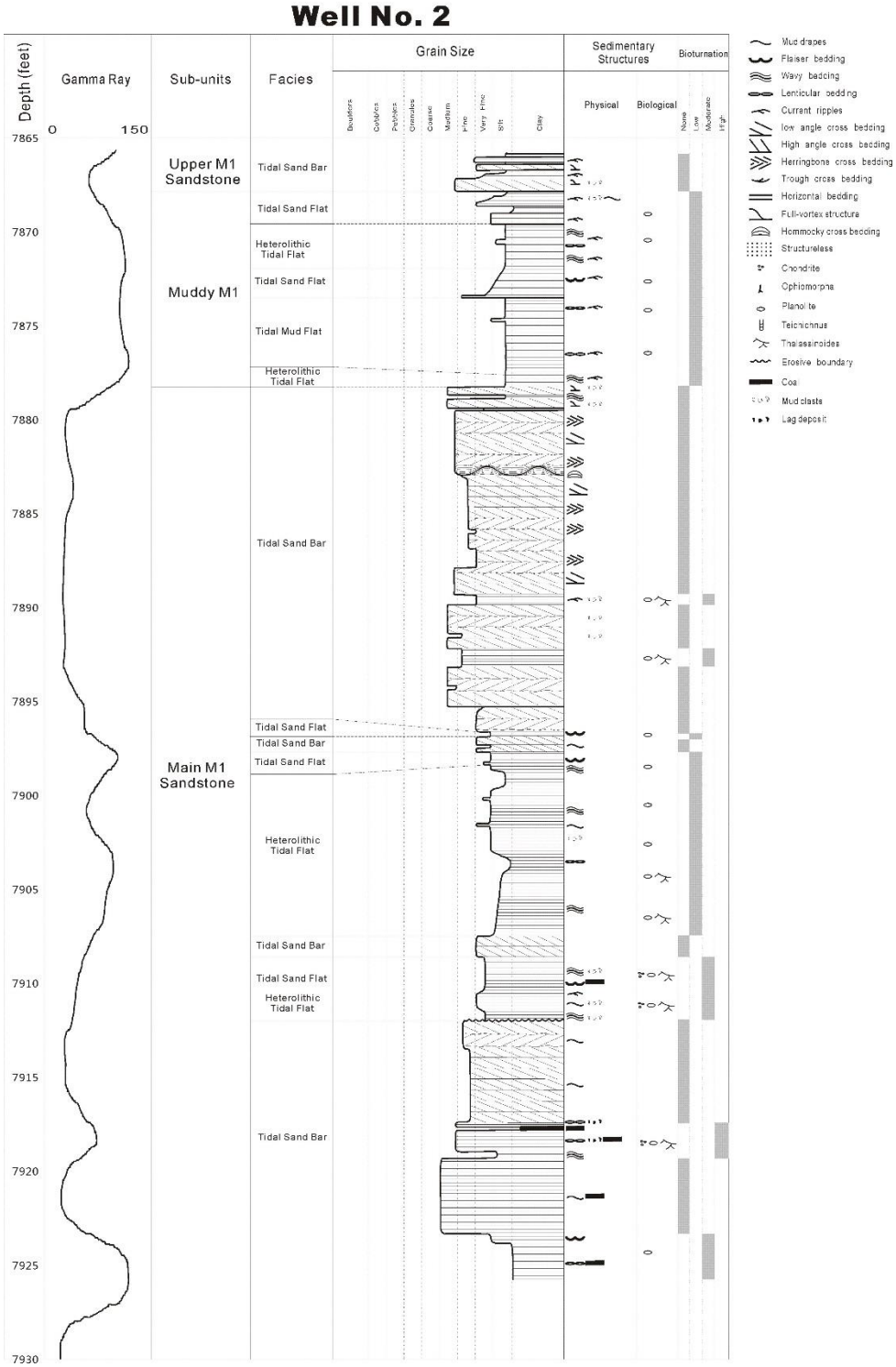

Figure 2.13 Core log from well No. 2.

Very poorly sorted, very coarse grained, yellow colored sandstone with mud, coaly mud, and coal layers and clasts are found near the bottom of the core (Figure 2.14A). This section of core is highly broken. The sandstone mainly consists of very poorly sorted and very coarse grained sand. The grain size ranges from fine grained sand to pebbles and the dominant grain size is very coarse grained. Mud, coaly mud, and coal occur as clasts and layers. Planar lamination is the only physical sedimentary structure in this facies. No bioturbation is observed. The very poorly sorted and very coarse grained sandstone at the base of the core is interpreted as fluvial deposits, remaining in the channel since the time of relative sea level fall, just prior to the subsequent transgression. The gradient of the distributary river system would have increased as the relative sea level fell and the increase of gradient resulted in greater water energy which enabled the river to carry coarser grained materials. It is not uncommon that the very basal part of an estuary system contains thin amounts of older fluvial distributary channel deposits.

Above the very coarse grained sandstone, three facies are interpreted from the core (Figure 2.13). Subtidal sand bar facies consists of yellow to black colored, fine to coarse grained, oil stained, cross-bedded sandstone with a low abundance of mud drapes (Figure 2.14B). The heterolithic, very fine to fine grained sandstone with abundant mud drapes is interpreted as tidal sand flat facies (Figure 2.14C). The heterolithic deposits in which sandstone and mudstone contents are approximately equal are interpreted as heterolithic inter-tidal flat facies (Figure 2.14D).

From the top of the very coarse grained sandstone to the top of the core, tidal sand bar facies, tidal sand flat facies, and heterolithic tidal flat facies occur successively (Figure 2.13). These facies do not have distinctive boundaries between each other, instead, the facies change gradually into each other. For an example, tidal sand bar facies changes into tidal sand flat facies as oil stained, cross-bedded sandstone becomes interbedded with

heterolithic fine grained sandstone. As the content of heterolithic fine grained sandstone increases and ultimately becomes dominant, the facies change is complete. Two large-scale cycles of facies changes can be observed on both core and well log.

The occurrence of such rapid vertical change from subtidal to intertidal facies can be explained as the perfectly normal situation in an estuary whereby the marginal intertidal facies gradually builds out across the deeper subtidal sand bars. There need not be any significant sea-level change at all to accomplish this; the estuary naturally tries to become infilled by lateral progradation of the intertidal to supratidal margins. However, this infilling and lateral accretion of the muddier margins will likely happen more quickly if there is a slight relative fall of sea level. In the core of well No. 2, we interpret that the change of tidal flat facies up into subtidal tidal sand bar facies to represent a rise of relative sea level, whereas the change of subtidal tidal sand bar facies upwards into intertidal tidal flat facies represents fall or still stand of relative sea level. According to the depositional model of main M1 Sandstone, the main M1 Sandstone in well No. 2 (which is not present in the core) represents the stable, long term relative sea level rise. The deposition of very poorly sorted and very coarse grained sandstone previously at bottom of this core represents the termination of stable, long-term relative sea level rise and the initiation of relative sea level fall. After that, the relative sea level was generally stable. The tidal sand bar facies, tidal sand flat facies, and heterolithic tidal flat facies occur successively as a result of autogenic processes and small-scale relative sea level changes.

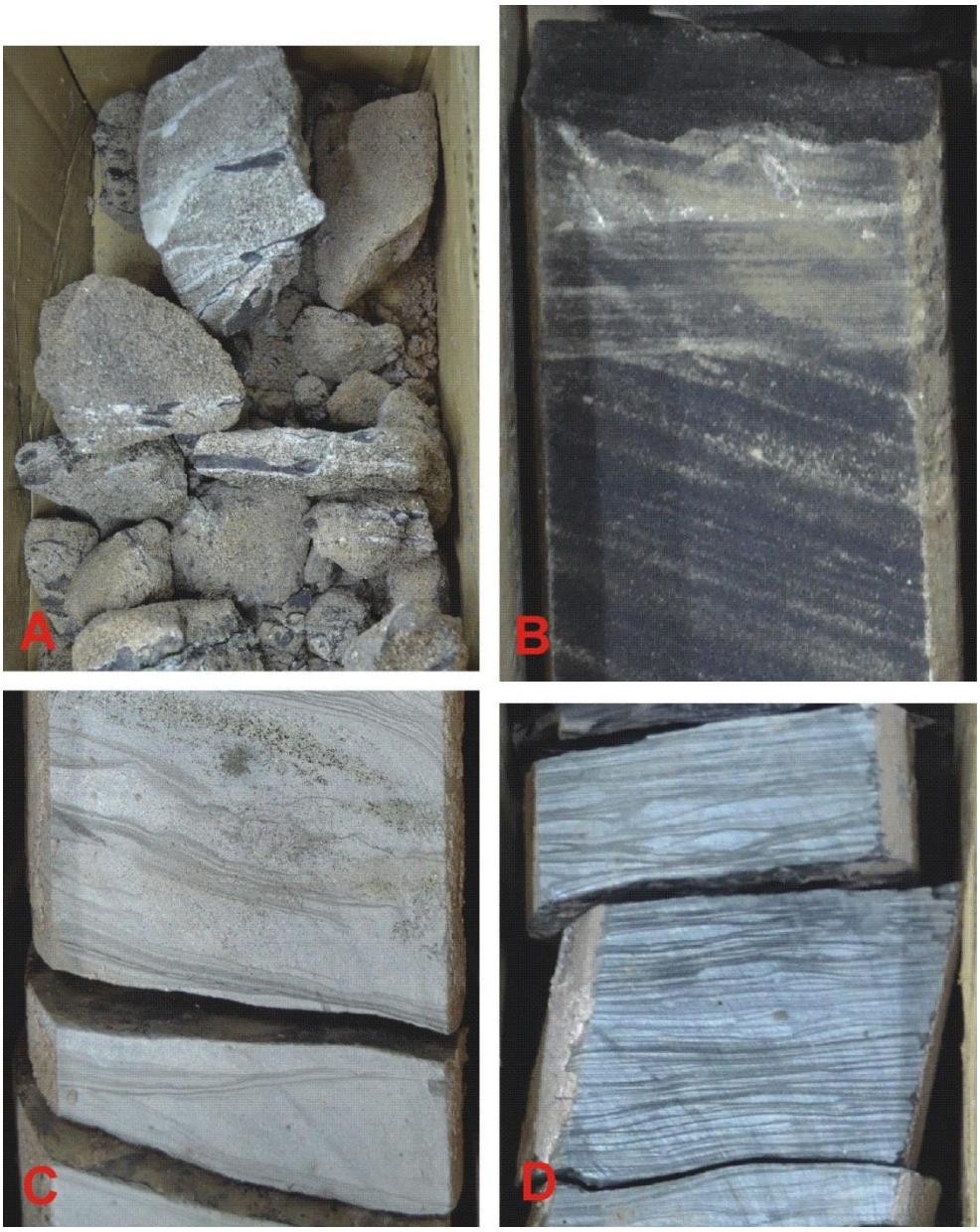

Figure 2.14 Core photos of well No. 2. (A) Very poorly sorted and very coarse grained, sandstone with mud, coaly mud, and coal layers and clasts. (B) Cross-bedded sandstone of tidal sand bar facies. (C) Flaser bedding in tidal sand flat facies. (D) Wavy and rhythmic bedding in heterolithic tidal flat facies.

Because thinner and less amalgamated main M1 Sandstone is dominant in the northeastern part of the study area but not common in other parts of the study area, we interpret that only the northeastern area is affected by the autogenic processes and small-scale relative sea level changes we interpreted from the well No. 2 core. In the depositional model of main M1 Sandstone, the tidal channel in the northeast is interpreted as the boundary of the ancient tide-dominated estuary. Therefore, the tidal sand bars lie beside this tidal channel (i.e. main M1 Sandstone in northeastern area) is near the boundary of the estuary. Tidal flats aggrade towards the center of estuary as a result of autogenic processes or sea level fall. Tidal flat deposits were laid down on the top of the tidal sand bar deposits as tidal flats moved onto previous tidal sand bars. Subsequent relative sea level rise occurred before the tidal flats reach the center of estuary, making tidal flats retreat to the landward and allows tidal sand bars to deposit again. In one cycle of tidal flat movement, the area near the boundary of estuary is first occupied by tidal flats and then taken back by tidal sand bars. Because tidal flats could not reach the areas in the center of estuary in small-scale relative sea level fall, no tidal flat deposits are deposited and only tidal sand bar deposits are laid down in these areas. This process explains why the upper part of main M1 Sandstone is not amalgamated in the northeast area. Figure 2.15 shows the sediment of tide-dominated estuary influenced by small relative sea level change.

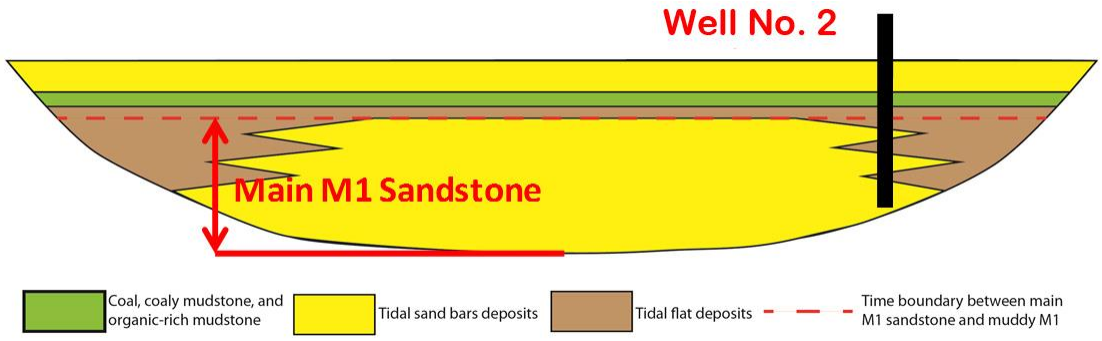

Figure 2.15 The distribution of tidal sand bar deposits and tidal flat deposits in the ancient tide-dominated estuary as a result of autogenic shifting of the inter-tidal growth area and small relative sea level changes.

2.3.2 Depositional model of muddy M1 and coal layer

The tidal sand flat, heterolithic tidal flat, tidal mud flat, and salt marsh facies are found above the main M1 Sandstone (Figure 1.3). Tidal sand flat, heterolithic tidal flat, and tidal mud flat together are named "muddy M1" by the oil field operator because these facies contain relatively high content of mudstone; and salt marsh facies is named "M1 coal" by the oil field operator because it looks like coal on well logs. The thickness of these facies is usually 30% to 50% of total thickness of M1 sandstone. In rare cases these facies compose 90% of total thickness of M1 sandstone.

Tidal sand flat, heterolithic tidal flat, tidal mud flat facies are distinct from tidal sand bar facies on gamma ray curves. Because tidal sand bar facies contains very little mud, it has low gamma ray readings and the gamma ray curve is blocky or slightly fining upward. The tidal flat facies have higher content of mud so they have high gamma ray readings and the gamma ray curve does not show any regular pattern. Tidal sand flat, heterolithic tidal flat, and tidal mud flat all contains relatively high content of mudstone and the transitions between these facies are gradual. As a result, the above three facies have similar reading on gamma ray and other well log curves, making it difficult to distinguish these facies from

each other on well logs. This is the reason why the oil field operator gives only one name – "muddy M1" to three facies. Salt marsh facies contains high content of organic matter and/or coal, which makes it relatively easy to be distinguished from other facies on well logs. Salt marsh facies usually have low density and high resistivity. This is because organic matter and coal have lower density and higher resistivity than sand and mud. However, it is difficult to identify this facies with gamma ray curve. Although coal and organic matter usually have high gamma ray readings, the gamma ray reading of salt marsh facies in this study area is not always high. This may be caused by the high content of mud in this facies. Based on the character of these facies on well logs, tidal sand flat, heterolithic tidal flat, and tidal mud flat facies are picked as one unit and are named "muddy M1". This unit is distinguished from tidal sand bar facies by higher gamma ray readings and distinguished from salt marsh facies by lower density and resistivity readings. Salt marsh facies are distinguished from other facies by higher density and resistivity readings. Salt marsh facies are not contacted with tidal sand bar facies. They are separated by "muddy M1" in all the cases (Figure 1.3).

The models for tidal flat facies and salt marsh facies are built based on the isopach maps of "muddy M1" unit (i.e. tidal flat facies) and salt marsh facies (i.e. coal, coaly mudstone, and organic-rich mudstone). Figure 2.16 is the isopach map of "muddy M1" unit and Figure 2.17 is the isopach map of salt marsh facies. It can be observed that the entire study area is covered by tidal flat facies. The study area is also covered by salt marsh facies except in one sinuous and elongated belt-like area. The reconstruction of paleo geography of the study area is made based on the isopach map of salt marsh facies (Figure 2.18). Figure 2.11B shows the three dimensional depositional model of tidal flat facies and salt marsh facies. Salt marsh facies represents the most landward environment of the tide-dominated estuary so the spread of salt marsh facies across the entire study area indicates

the environment of the study area became supratidal during the deposition of salt marsh facies. In the model of tidal sand bar facies, the study area was part of the active tide-dominated estuary so it was subtidal. The change from subtidal to supratidal can be caused by a natural infilling of all accommodation space in the estuary without sea-level change or alternatively by gradual sea level fall. The latter explanation is preferred here because of the widespread character of the vertical change to supratidal deposits. As sea level falls, what happens in the tide-dominated estuary is that the tidal flat and supratidal salt marsh accrete or prograde laterally from the original marginal position towards the center of the estuary (Dalrymple et al, 1992). As this process continues, the entire estuary will be first covered by tidal flat facies. Then salt marsh facies, which is further landward, will cover tidal flat facies. This process explains: first, the reason why tidal flat facies and salt marsh facies are spread across the entire study area; second, the reason why tidal flat facies are always found on top of tidal sand bar facies; third, the reason why salt marsh facies is always separated from tidal sand bar facies by tidal flat facies. We interpret the sinuous and elongated belt-like area in the isopach map of salt marsh facies to be the fluvial-tidal channel which is still active during the sea level fall.

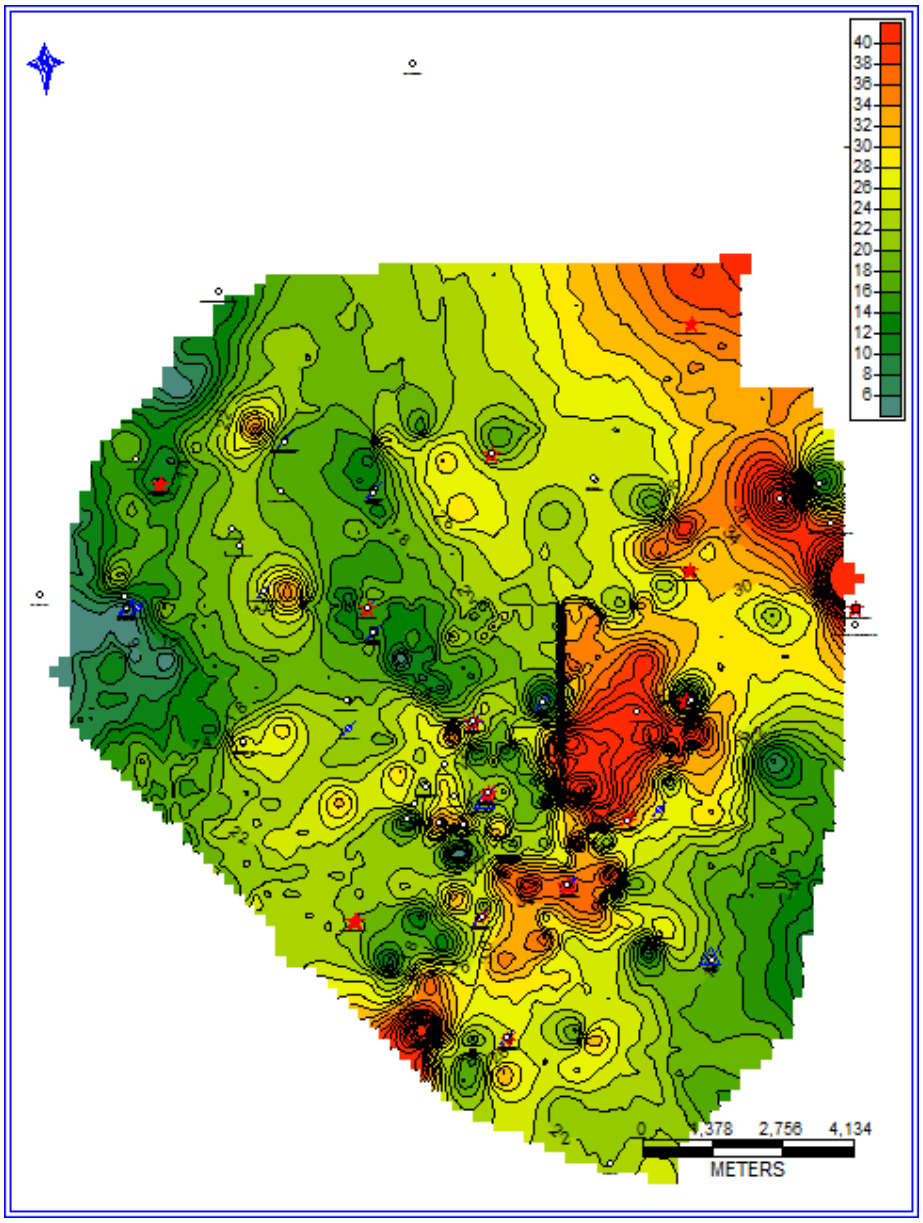

Figure 2.16 Isopach map of muddy M1 sub-unit.

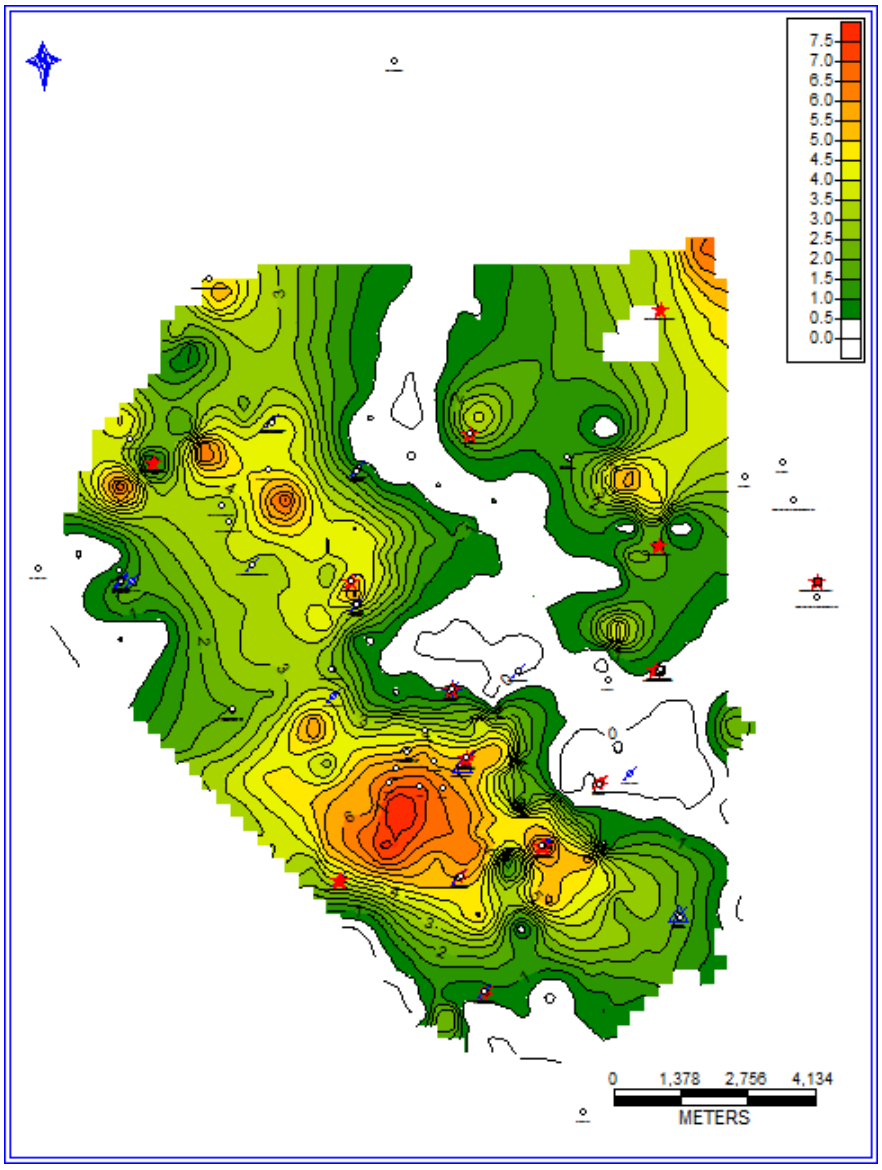

Figure 2.17 Isopach map of the marsh-grass supratidal deposits, now coal layers. Note the presence of an open estuary channel without coaly deposits

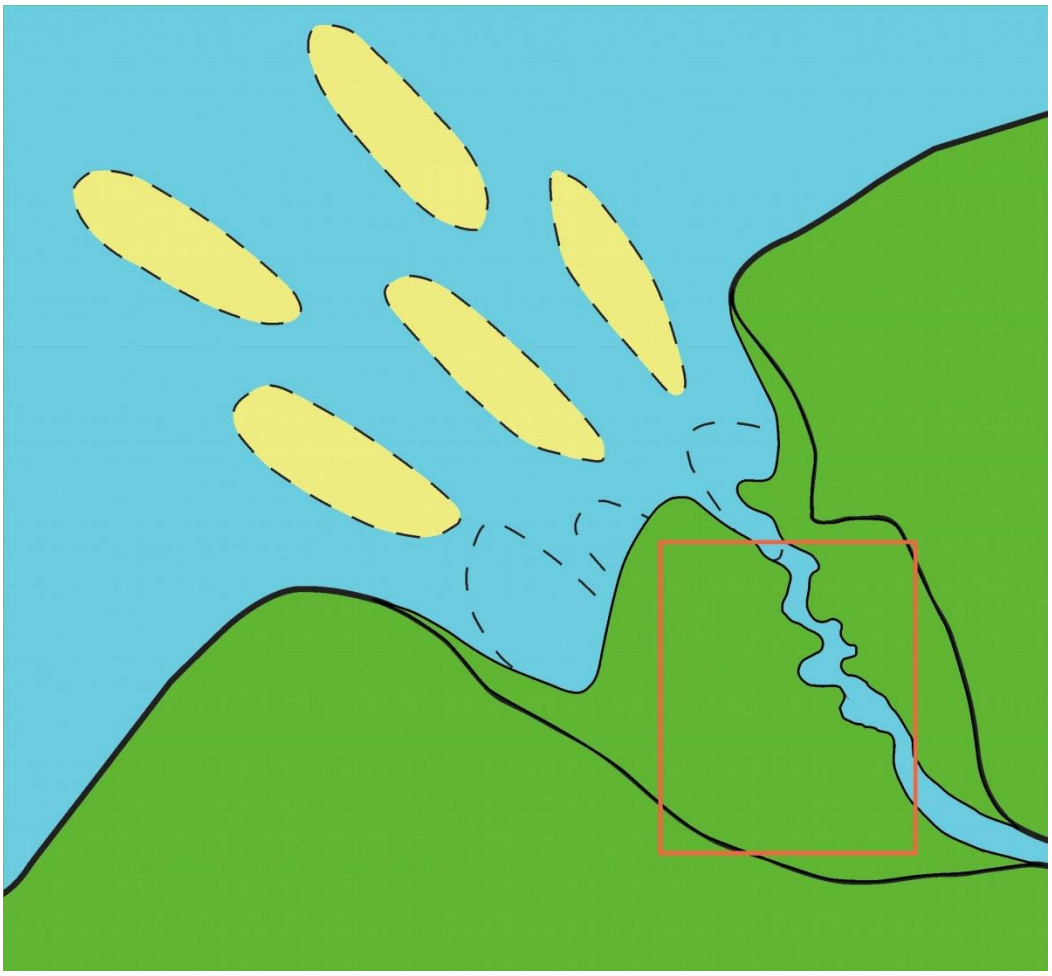

Figure 2.18 Reconstructed paleogeography during the deposition of muddy M1 sub-unit and coal layer.

2.3.3 Model for sediment bypass period after the deposition of tidal flat facies and salt marsh

As interpreted above, the tidal flat facies and salt marsh facies were deposited during regression. We interpret that regression continued after the deposition of the tidal flat facies and salt marsh facies, gradually infilling the estuary. During the continued regression, the shoreline was forced to prograde seaward. The study area became a non-marine environment and experienced sediment bypass. No sediment was deposited during

this time period due to sediment bypass through the continued active distributary channel. Figure 2.19 is the reconstructed paleogeography of this period. Figure 2.11C shows the three dimensional depositional model of this period.

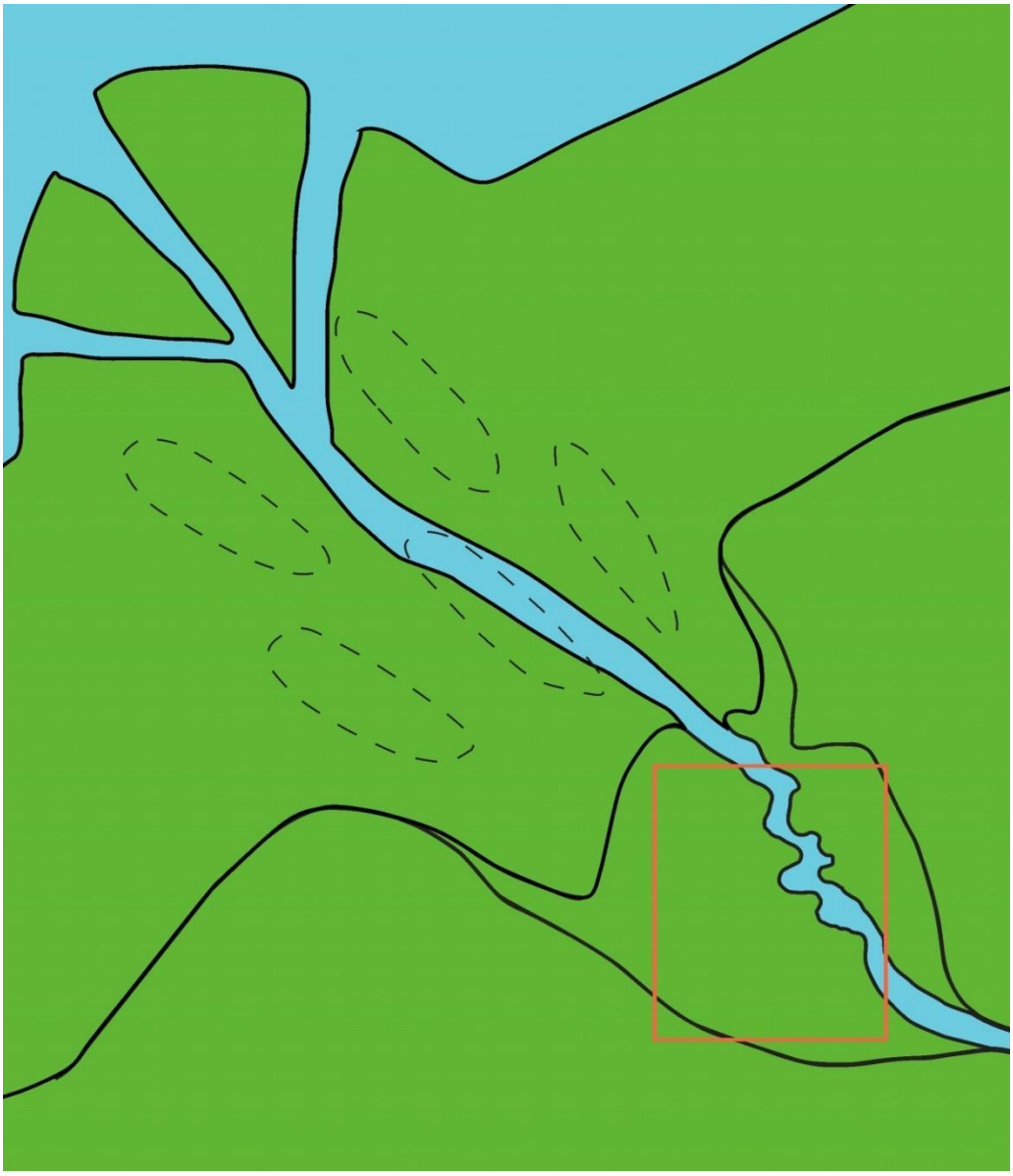

Figure 2.19 Reconstructed paleogeography during the period of sediment bypass.

2.3.4 Depositional model of upper M1 Sandstone

The fine to coarse grained sandstone near the top of M1 sandstone, also named "upper M1 Sandstone" by the oil field operator, is the secondary productive unit in M1 sandstone (Figure 1.3). Core study interpreted this sandstone to be tidal sand bar facies. This sandstone is underlain by tidal flat facies and salt marsh facies. On well logs, it is bounded by a sudden decrease of gamma ray reading (sharp contact) at bottom and bounded by the sudden increase of gamma ray (upward limit of sandstone) at top. The upper and lower boundaries are picked using gamma ray to map the thickness variation of this sandstone facies across the study area. The thickness of this sandstone is highly variable. Its thickness can be as much as 40% of total thickness of M1 sandstone but it can be thinner than 3 feet or even missing in many wells. As a result, this sandstone is amalgamated and shows a blocky gamma ray pattern in some of the wells but is only a thin layer of sand or not present in other wells. Two factors may be responsible for the thickness variation. First, the tidal sand bar was not well developed in some parts of the study area. Second, the top of M1 sandstone was subject to some subsequent erosion. The erosion may have removed part or total of this facies in some wells.

The distribution and orientation of tidal sand bars and tidal channels in upper M1 Sandstone are interpreted from the isopach map (Figure 2.20). A bank-attached bar and multiple smaller tidal sand bars are interpreted. The thickness distribution does not show multiple tidal channels. We interpreted a bank-attached tidal bar, multiple smaller tidal sand bars, a flood barb and a main ebb channel from the isopach map. Bank-attached tidal bars are the tidal bars attached to the bank in the tide-dominated estuaries. Bank-attached tidal bars build flood barbs on their side during flow of the subordinate flood tidal current moving landwards. A flood barb is a flood-dominated and headward-terminating channel confined by the bank and bank-attached tidal bar (Dalrymple and James, 2010). The

elongate direction of bank-attached tidal bar, flood barb, and other tidal sand bars are uniform. The flood barb terminates towards southeast, which indicates southeast is the landward. The reconstructed paleogeography indicated only two tidal channels are in the study area. We interpret that the study area is likely to be the upstream part of a tide-dominated estuary, and represents an entire estuary because the number of tidal channels in the modern estuaries tend to be few in the upstream and many in the downstream areas. Figure 2.21 is the reconstructed paleogeography of the entire Upper M1 tide-dominated estuary.

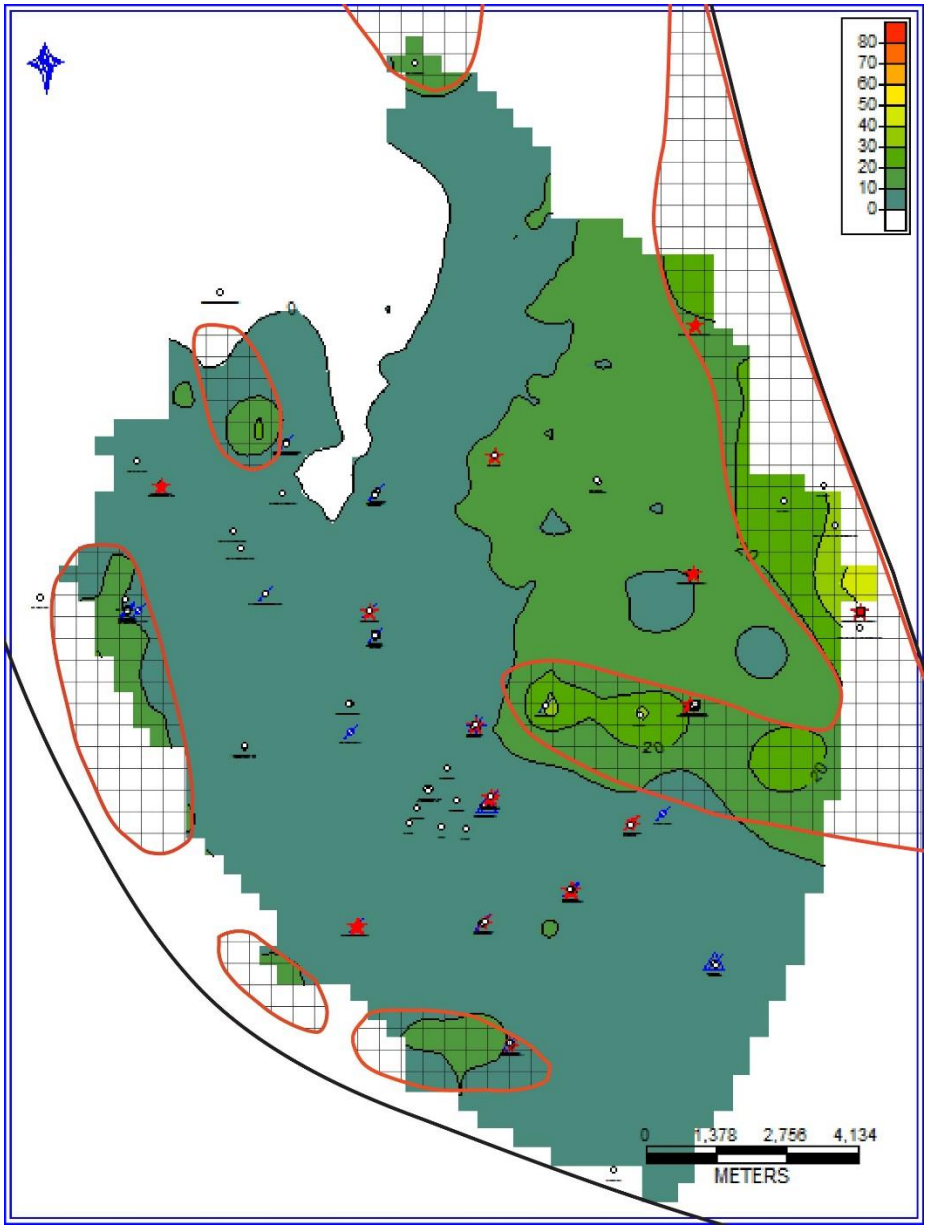

Figure 2.20 Isopach map of upper M1 Sandstone. Tidal sand bars are outlined with red boundaries.

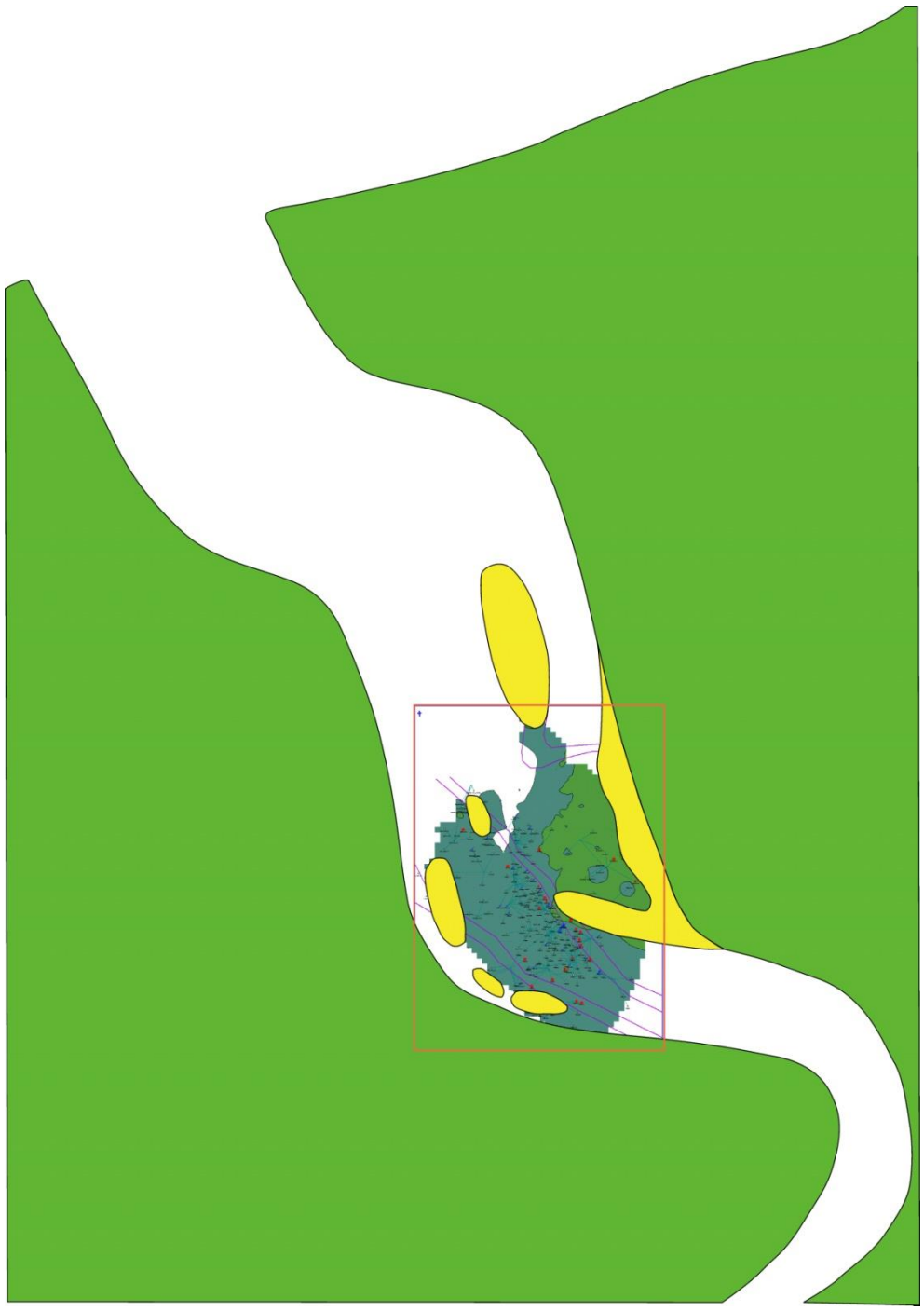

Figure 2.21 Reconstructed paleogeography during the deposition of upper M1 Sandstone.

Figure 2.11D shows the three dimensional depositional model of this tidal sand bar facies near the top of M1 sandstone. During the deposition of this facies, the relative sea level stopped falling and started rising. A new tide-dominated estuary was formed during this transgressive period and tidal sand bars were deposited inside the estuary.

2.4 SEQUENCE STRATIGRAPHY

Four depositional models have been built to explain the depositional processes and the relative sea level changes behind them. The sequence stratigraphy of M1 sandstone can be built by putting the four models in order of time. In the first depositional model, the tidal sand bar deposits at the bottom of the M1 sandstone were deposited in a tide-dominated estuary which was formed during the initial transgression. In the second depositional model, tidal sand flat, heterolithic tidal flat, tidal mud flat, and salt marsh deposits aggraded from the margin of tide-dominated estuary to the center of estuary; this process is caused by local regression. In the third depositional model, sediment bypass occurred in the study area as the regression which begun in the second depositional model continued. In the fourth depositional model, tidal sand bars near the top of the M1 sandstone were deposited in a tide-dominated estuary which was formed during the second transgression. The M1 sandstone went through the initial transgression, a subsequent regression, and a second transgression during the period which it was deposited.

2.5 SHALE BARRIERS

Three slightly sinuous, mud-rich “lineaments” up to 1 km wide have been mapped on seismic amplitude maps (Figure 2.8). They are named “shale barriers” by the oil field operator. Each of them is more than 15 km long and 20 – 30 meters thick. From the well logs near the “shale barriers”, it can be observed that: (1) they are dominated by mudstone and the thickness of tidal sand bar deposits (main M1 Sandstone) is significantly lower

than other wells (Figure 2.22); (2) mud thickens and sand thins toward the center of these shale barriers, with an overall decrease in total thickness of mud and sand (Figure 2.23). The "shale barriers" are important muddy architectures in the study area because they are believed to stop the oil migration. . The origin of the "shale barriers" has not been well explained. In this study, we investigated the origin of "shale barriers" from a depositional point of view.

The origin of "shale barriers" can be explained most simply in the context of the general evolution of the M1 depositional system. In the first depositional model of M1 sandstone, the "shale barriers" are interpreted as active tidal channels that never filled up with sand, because they have elongated, slight sinuous geometry and contain thinner sand, which is consistent with the character of abandoned tidal channels (Figure 2.11A). In the second depositional model of M1 sandstone, these tidal channels became inactive and were filled by muddy deposits (Figure 2.11B). This is because tidal flat and salt marsh aggraded from the margin to the center of the estuary and filled the tidal channels with muddy tidal flat deposits. . As a result, the outside geometry of "shale barriers" (i.e. the container) was formed during the initial transgression in the first depositional model, whereas the infill (i.e. the mud) was created by muddy tidal flat deposits during the subsequent regression in the second depositional model.

Another piece of evidence which support the hypothesis of "shale barriers" to be tidal channels is the depositional processes associated with tidal channels. As shown in Figure 2.24, tidal channels, like meandering channels, are erosive on one side (the cutbank) and depositional on the other side (the point bar side). On the erosive side, tidal channels keep eroding the adjacent tidal bars. The channel wall, the cut bank, is relatively steep due to erosion process. On the depositional side, the tidal bars keep building into tidal channels. The channel wall on the inside of the bend is relatively gentle. A well drilled in the center

of the tidal channel would have very thin sand and thick mud. However, as the well moves towards the depositional side of the tidal channel, the tidal sand bar deposits will appear at the bottom of the well. This is consistent with the core and well log data in the study area. Figure 2.22 shows the wells which penetrated shale barriers. It can be observed that most of these wells have thicker or thinner sand at the bottom of M1 sandstone. The sand found at the bottom of M1 sandstone in these wells could be the tidal sand bar deposits on the depositional side of the channel. Figure 2.25 shows the core log of M1 sandstone in well No. 3. This well was drilled at the margin of a "shale barrier". The thickness of mud in well No. 3 is obviously greater than wells far away from the "shale barriers", however, 30 feet of tidal sand bar deposits were found at the bottom of M1 sandstone. This confirms that the sand at the bottom of M1 sandstone in the above wells is tidal sand bar deposits, which proves the depositional processes associated with "shale barriers" are tidal channels. As a conclusion, the "shale barriers" are tidal channels filled with muddy deposits, sometimes tidal flat deposits.

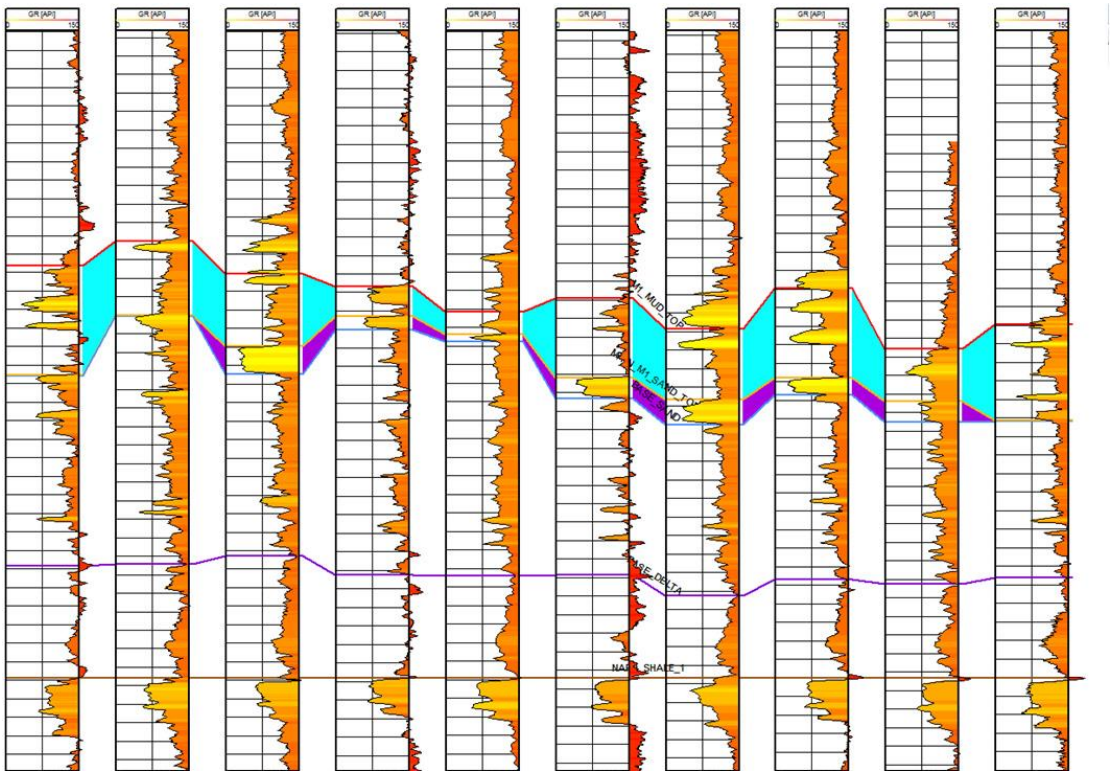

Figure 2.22 Well logs near the “shale barriers”. Mud-dominated intervals are marked by blue color; sandstone is marked by purple color.

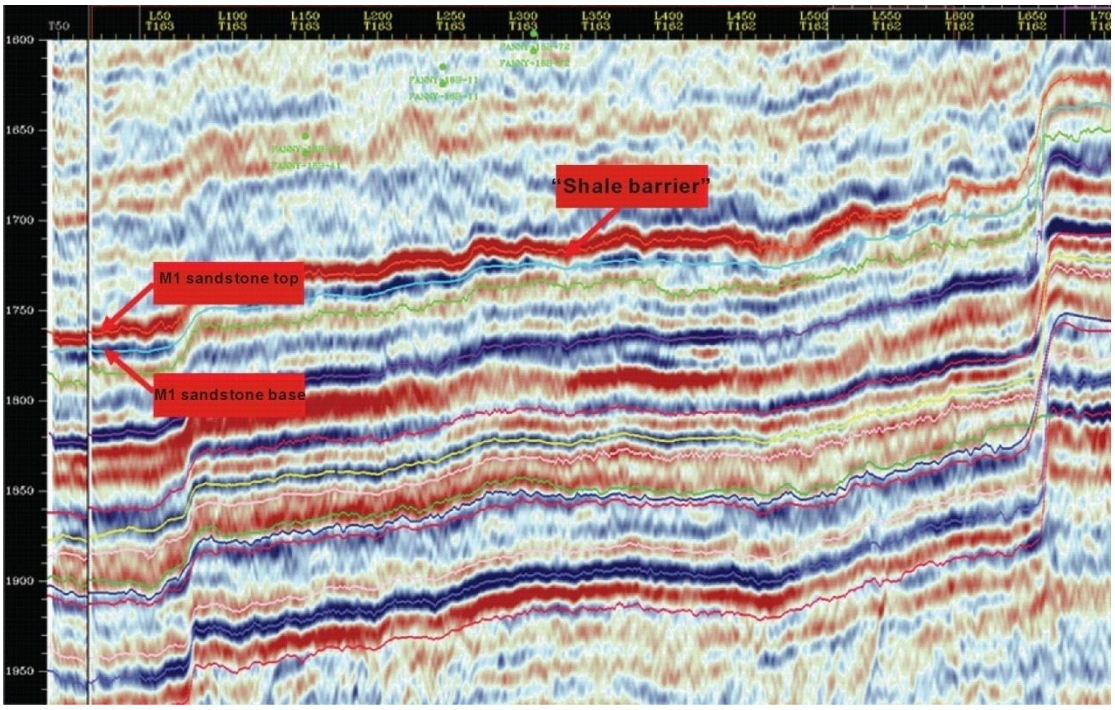

Figure 2.23 The geometry of "shale barrier" shown on seismic cross section. Sand (blue interval) thins towards the center of "shale barrier". The total thickness of mud and sand in M1 sandstone also decreases.

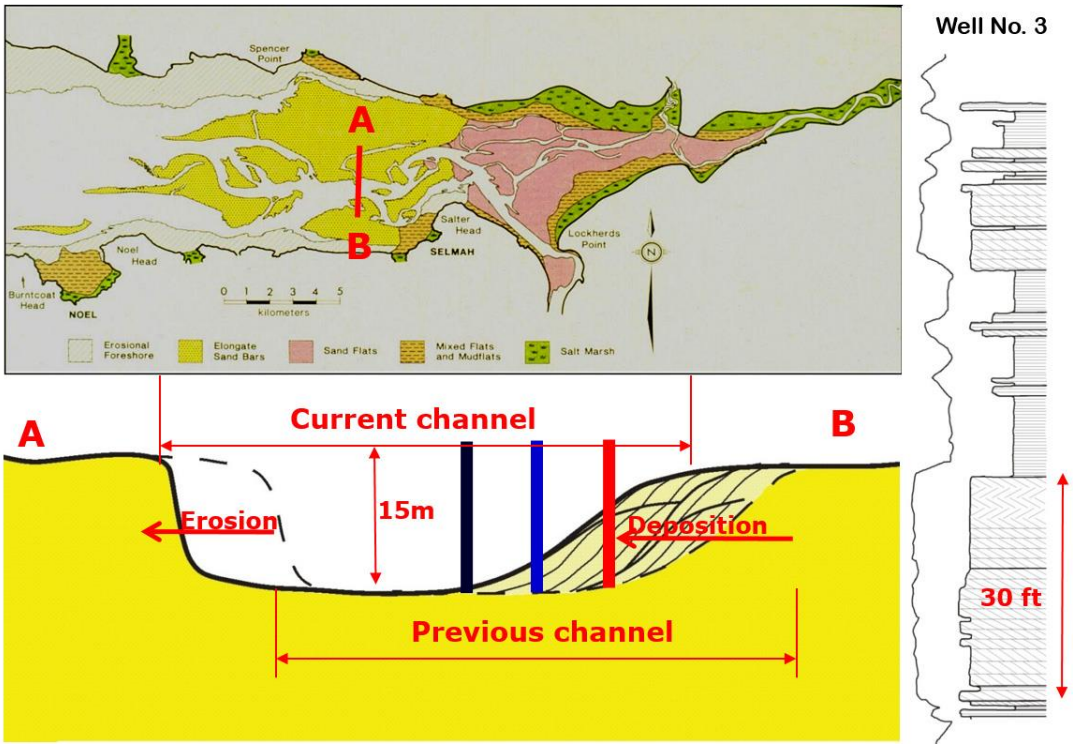

Figure 2.24 Schematic diagram showing the erosional and depositional processes associated with tidal channels. The core of well No. 3 is consistent with the depositional process of tidal channels.

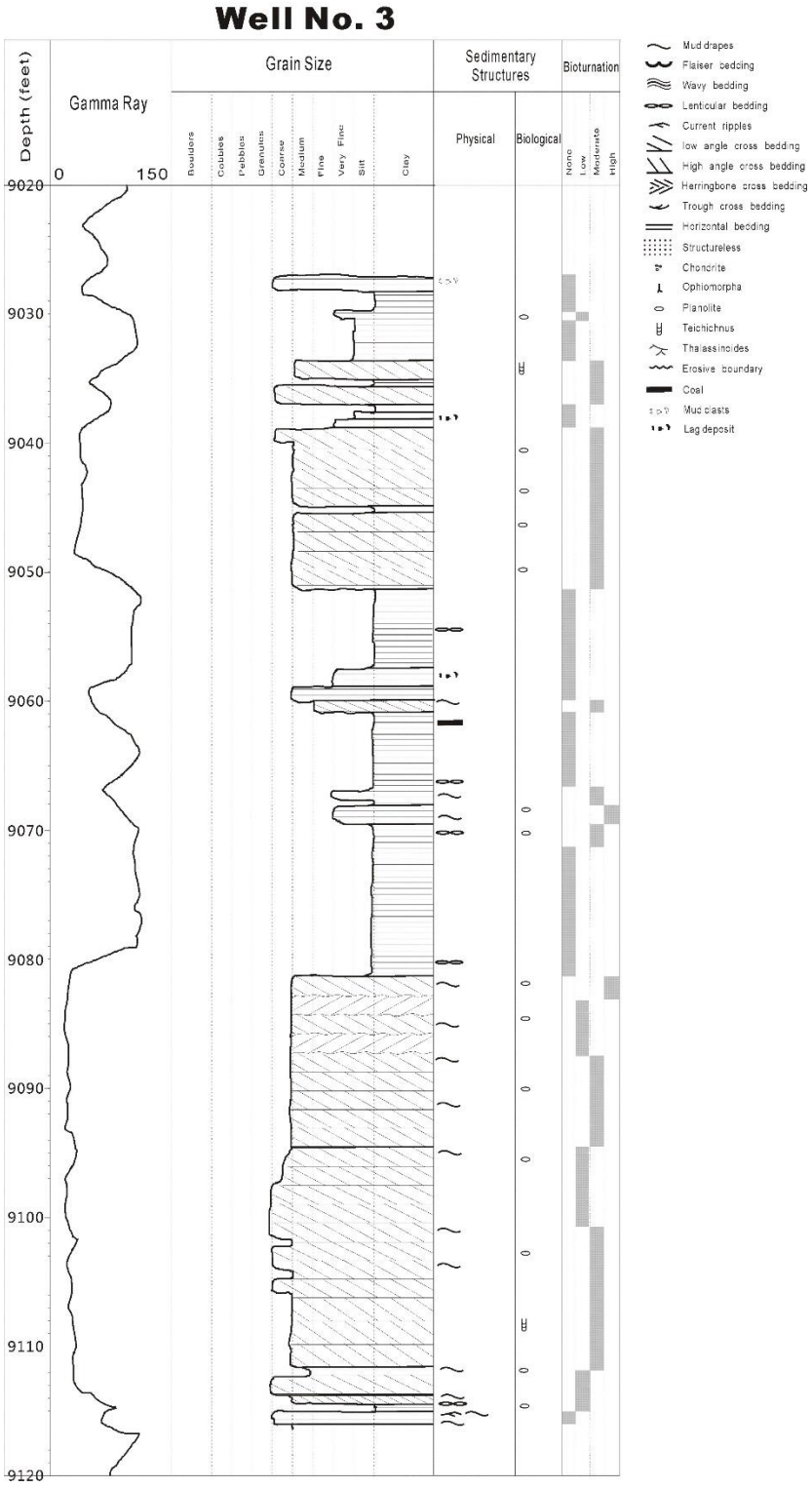

Figure 2.25 Core log of Well No. 3.

Chapter 3: Predictive Geological model of Tarapoa Northwest

3.1 Facies and depositional system interpretation of well No. 4 and Carabobo wells

The positions of well No. 4 and Carabobo wells are shown in Figure 3.1. The core of well No. 4 provides key facies information for the far northwestern area. Figure 3.2 is the core log of well No. 4. Four facies are interpreted from the core. They are, from bottom to top, delta front facies, tidal channel facies, tidal bar facies, and shelf sand ridge facies.

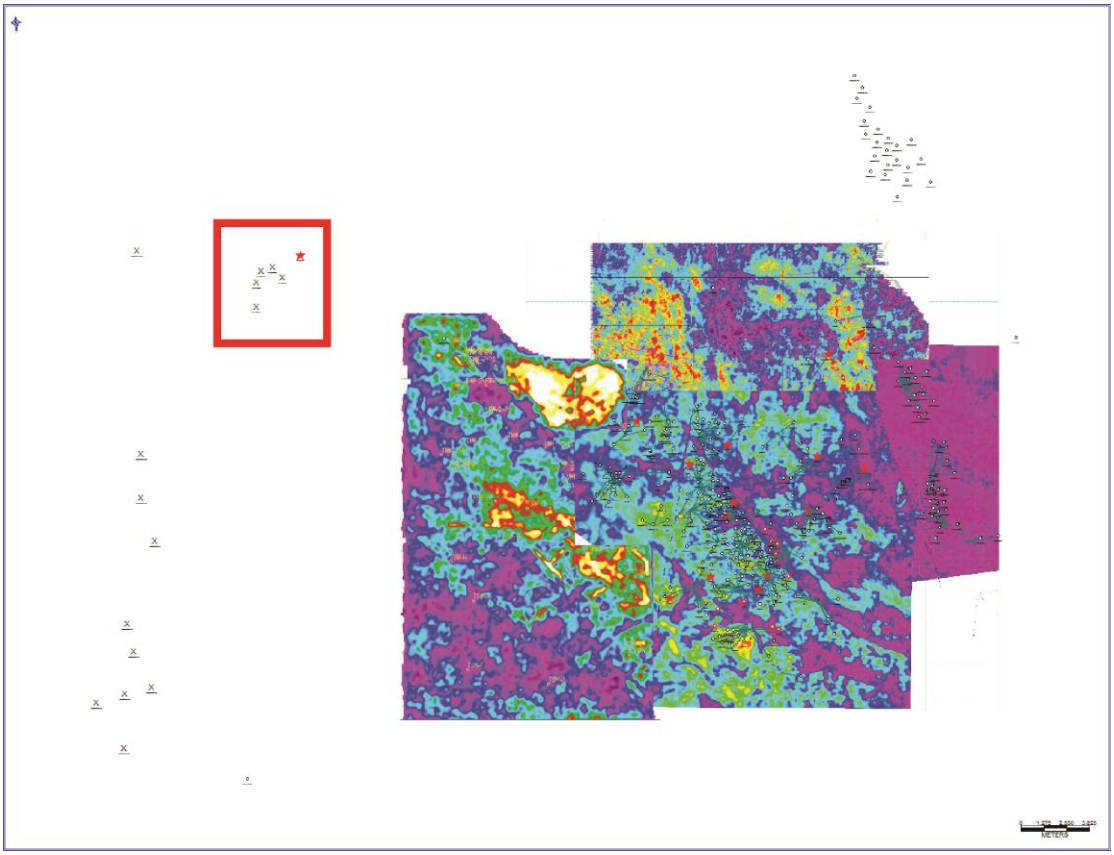

Figure 3.1 Position of well No. 4 and Carabobo wells (in red box) in relation to the other study area (area covered by seismic amplitude map).

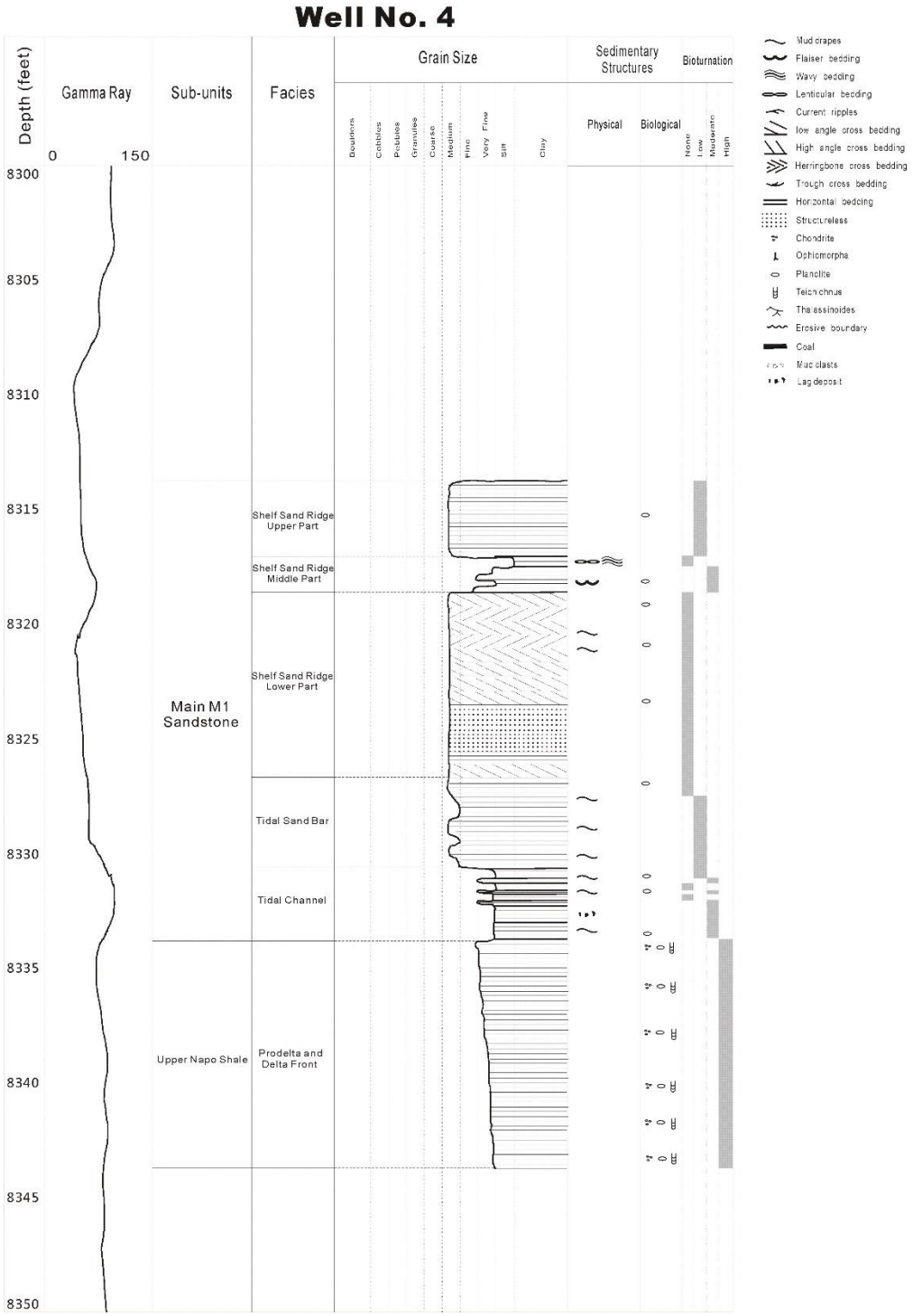

Figure 3.2 Corelog of well No. 4.

3.1.1 Facies and depositional system interpretation for Well No. 4 core

1. Heterolithic upward-coarsening deposits (prodelta to delta-front deposits)

The basal part of this core shows heterolithic deposits of siltstone and very fine grained sandstone with mud layers. It is white to grey colored, planar laminated, not oil stained, and intensely bioturbated (Figure 3.2). Above the heterolithic deposits, another heterolithic facies consists of fluid mud and lag deposits. A sharp contact is found between the two facies. This facies is 10 feet thick. The white to grey color is the result of varying grain size and content of mud in the heterolithic deposits. The grain size increases and content of mud decreases gradually from bottom to top. The lower part of this facies is dominated by siltstone; the content of mud is higher in this part (Figure 3.3A). The upper part of this facies is dominated by very fine grained sandstone; the content of mud is lower in this part (Figure 3.3B). Mud layers are interbedded with sandstone and siltstone in the lower part of this facies. Individual mud layer thickness is generally less than 3 mm. The thickness and abundance of mud layers decreases from lower to upper parts of this facies as the grain size increases. Oil stain is absent. Planar lamination is observed where the physical depositional structures are not completely destroyed by bioturbation (Figure 3.3C). Rhythmic alternation of siltstone and mud layers is observed in the lower part of this facies (Figure 3.3C); it is not observed in the upper part because of intense bioturbation. The abundance of bioturbation is high in this facies. Mud layers and planar lamination are destroyed where the facies is completely bioturbated. The types of bioturbation interpreted from this facies are *Planolites, Chondrites, and teichichnus*.

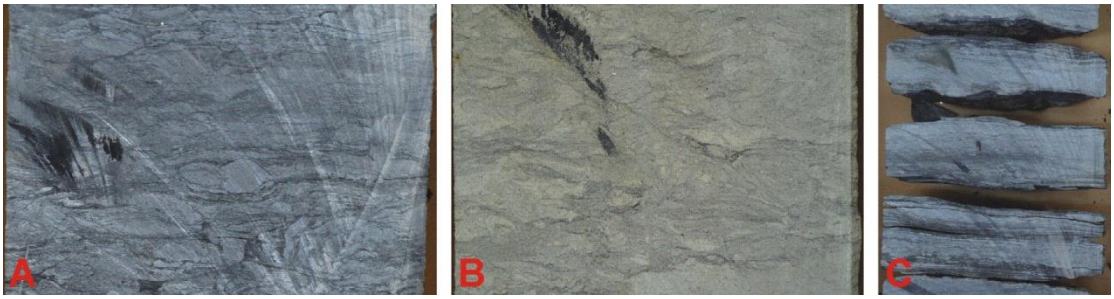

Figure 3.3: Core photos of prodelta to delta-front deposits. (A) Lower part of the prodelta-delta front facies. This part is dominated by siltstone. (B) Upper part of the prodelta-delta front facies. This part is dominated by sandstone. (C) Planar lamination and rhythmic alternation of siltstone and mud layers.

We interpret these heterolithic deposits as prodelta and delta-front facies. Coarsening upward of sediments strongly indicates this facies is deltaic. The presence of mud, small grain size, and planar lamination together suggest low current velocities. High abundance of bioturbation implies low sedimentation rate. The above evidence indicates a relatively distal part of delta. Rhythmic alteration of siltstone and mudstone may represent tidal influence, which implies tidally-influenced prodelta environment. Cores from Fly River Delta show that prodeltaic deposits are silty claystone with planar lamination (Harris et al, 1993), which is the same as we observe from the lower part of this facies. Therefore, we interpret that the lower part of this facies as prodeltaic. The upper part of this facies which is dominated by very fine-grained sand can be a more proximal part of the delta, i.e., the delta front. Although the small grain size, presence of mud, rhythmic alternation, and abundant bioturbation in this facies could alternatively favor a tidal flat interpretation, the coarsening upwards and lack of ripple bedforms makes this interpretation unlikely.

2. Heterolithic deposits with fine grained sandstone, fluid mud, and basal lag deposit (tidal-channel deposits)

These heterolithic deposits are dark grey colored, not oil stained, and partly bioturbated, and they lie close to the bottom of M1 sandstone in well No. 4 (Figure 3.2). Below the heterolithic deposits, there are prodelta facies consisting of grey colored, intensely bioturbated silt and sand. These two facies are juxtaposed across a sharp contact. Above the heterolithic deposits, there is an abrupt change to sand-dominated facies consisting of light brown colored, cross bedded sandstone with abundant mud drapes.

This facies is 3 feet in thickness. The dark grey color is the result of high mud content. Oil stain is absent. The deposits consist of three components. The sandstones are white to grey colored, not oil stained, fine grained with abundant mud drapes and a medium abundance of bioturbation (Figure 3.4A). Rhythmic alteration of sandstone and mud drapes is observed (Figure 3.4A). Mudstone occurs in multiple dark grey colored, non bioturbated, structureless, homogeneous thick layers (>1 cm) (Figure 3.4A). Sandstone and mudstone are interbedded. Basal lag deposit consists of grey and brown colored, poorly oriented, sub-rounded and sub-angular, pebble-sized mud clasts (Figure 3.4B). The physical sedimentary structure observed in this facies is planar lamination.

We interpret these heterolithic deposits as belonging to tidal channel facies. Rhythmic alteration of sandstone and mud drapes reflects a tidally-influenced environment. The sharp-based, basal lag deposit usually indicates a channel environment. This evidence loosely implies a tidal channel environment. Fluid mud is another piece of evidence consistent with a tidal channel environment. Fluid mud in the rock record occurs as layers which consist of non-bioturbated and structureless mudstone; the thickness of fluid mud is greater than 1 cm and greater than 0.5 cm if it is compacted (Dalrymple et al, 2003). In modern environments, fluid mud is defined as a body of fine grained sediment

which matches the following criteria: occurs near the bottom of water body; the suspended sediment concentration is greater than 10g/L; the suspended sediment is mainly composed of clay, silt, and organic matter (Kirby and Parker, 1983). In addition, fluid mud has no or very low degree of bioturbation. Fluid mud is typically deposited within hours, which makes it unlikely to have syndepositional bioturbation (horizontal burrows). Only post depositional bioturbation (vertical burrows) may exist in fluid mud (Ichaso and Dalrymple, 2009). The thickness of fluid mud is much greater than that of mud drapes. Due to the limitation of suspended sediment concentration, the mud drapes deposited during a slack-water period is not likely to be more than 1-2 mm in thickness (McCave, 1971; Ichaso and Dalrymple, 2009), whereas the thickness of compacted fluid mud is generally greater than 5 mm (Ichaso and Dalrymple, 2009). Fluid mud is very commonly found in areas beneath the turbidity maximum in tide-influenced estuaries and deltas (Ichaso and Dalrymple, 2009; Kirby and Parker, 1983; Kineke et al, 1996). It is also occurring in wave-influenced delta front and continental shelves (Gabioux et al, 2005; Dalrymple et al, 2003; Hill et al, 2007). Floods and storms can also generate fluid mud in some cases (Ichaso and Dalrymple, 2009). Even though fluid mud can be found in multiple environments and can be produced by several processes, it is most common in tidal channel environments. As conclusion, these heterolithic deposits belong to a tidal channel facies.

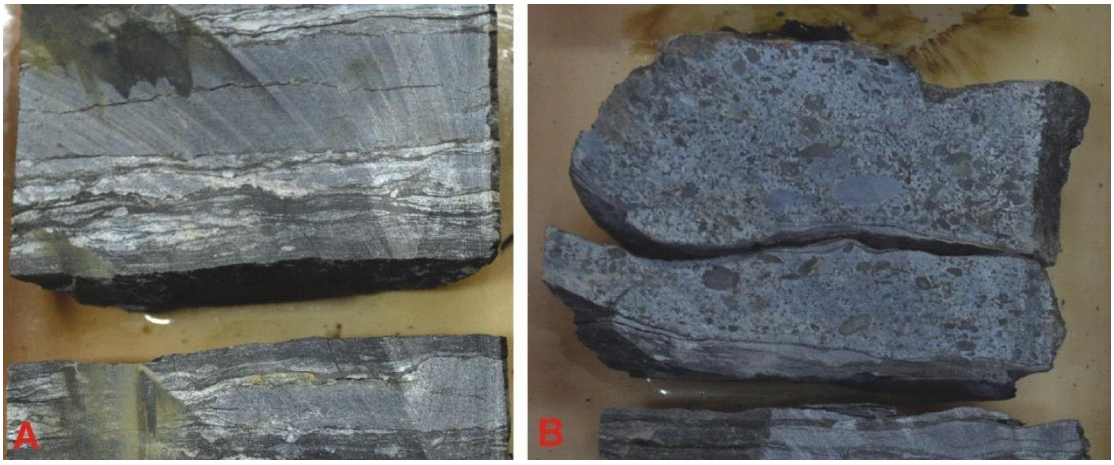

Figure 3.4: Core photos of tidal-channel deposits. (A) Fluid mud (dark grey) and fine grained sandstone. (B) Lag deposits near the base of the tidal channel facies.

3. Planar laminated sandstone with mud drapes (tidal sand bars).

This sandstone facies consists of two different types of sandstone. Brown colored sandstone is fine to medium-grained, planar laminated, not bioturbated, and oil stained with a low abundance of mud drapes. White colored sandstone is fine grained, planar laminated, bioturbated, and not oil stained with abundant mud drapes. Below this sandstone, the prodelta and delta-front facies consists of fine-grained sandstone, fluid mud, and basal lag deposit. The prodelta and delta-front facies changed abruptly into this sandstone facies, however, the contact surface is missing in the core. Above this sandstone, another sandstone facies consists of darker colored, cross bedded sandstone. This sandstone passes gradually to the cross bedded sandstone above it (Figure 3.2).

This facies is 4 feet in thickness. The brown color of fine to medium grained sandstone is the result of medium degree of oil stain (Figure 3.5A). The brown colored sandstone is planar laminated; individual bed or set thickness ranges from 0.2 to 0.3 feet. This sandstone has no bioturbation. It has a moderate abundance of mud drapes. The brown

colored sandstone is interbedded with the white colored fine grained sandstone (Figure 3.5B). The white colored sandstone is planar laminated; individual bed thickness is smaller than 0.2 feet. It has a low degree of bioturbation. The mud drapes in the white colored sandstone are more abundant than in the brown colored sandstone. Crinkle mud drapes and double mud drapes are found in this white colored sandstone (Figure 3.5C, Figure 3.5B).

We interpret this sandstone as tidal sand bar facies. Double mud drapes are considered as a good indication of tidal processes (Dalrymple, 2012). The presence of crinkle mud drapes also suggests tidal processes (Shanmugam et al, 2000). Therefore, the environment of this facies is tidally-influenced. The brown colored sandstone is fine to medium grained, not bioturbated, and has moderately abundant mud drapes; these characteristics are most common in the bottomsets of tidal sand dunes (which are building blocks of tidal bars). The white colored sandstone is fine grained and it has abundant mud drapes; these are the characteristics of reactivation surfaces. The interbedding of these two types of sandstone compose the tidal sand bar deposits. However, cross bedding, which is prominent in tidal sand bars is missing in this sandstone, adding uncertainty to our interpretation. This could be associated with the bottomsets of tidal sand dunes. As this facies passes gradually to the cross bedded sandstone above, the individual bed thickness of brown colored sandstone increases and cross bedding starts to appear (Figure 3.5D). This could imply that the apparent absence of cross bedding in this facies is associated with the limitation of bed thickness (<0.3 feet).

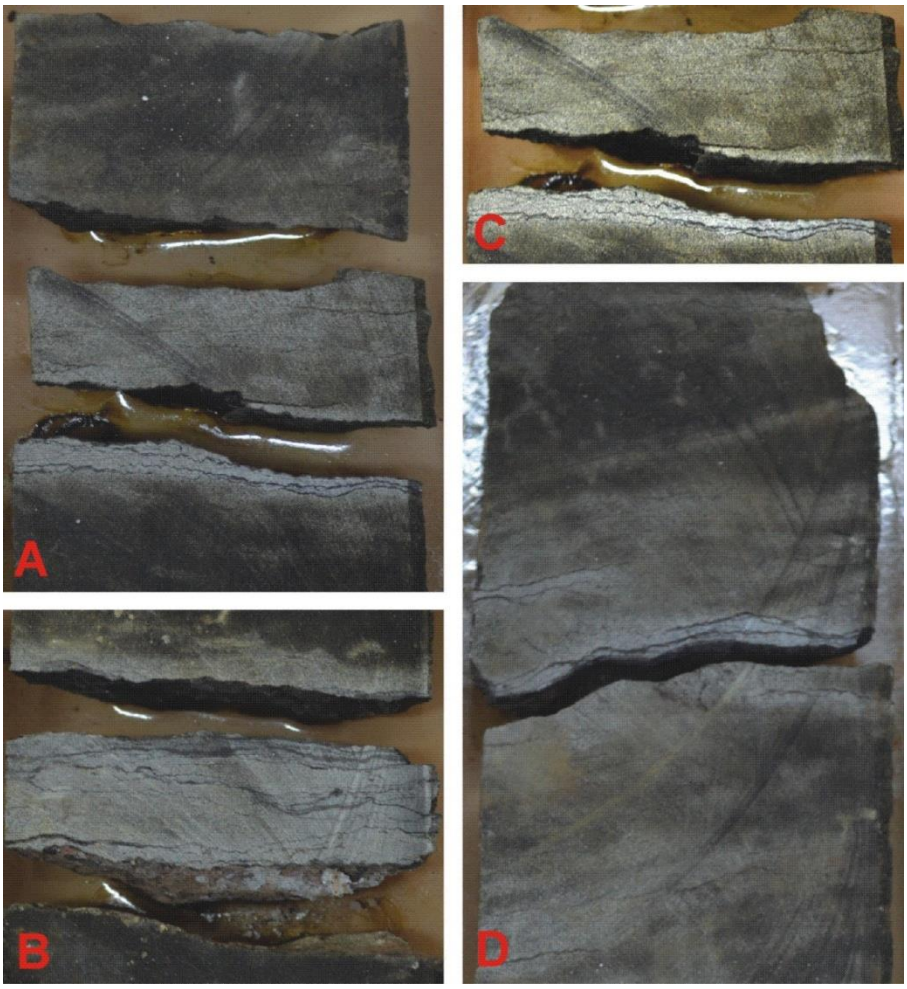

Figure 3.5: Core photos of tidal sand bars. (A) Brown colored, planar laminated sandstone in tidal sand bar facies. (B) Reactivation surface in tidal sand bar facies. (C) Crinkle mud drapes and double mud drapes. (D) Cross bedding in the transition zone between tidal sand bar facies and shelf sand ridge facies.

4. Cross bedded sandstone overlain by with fine-upward deposits and planar laminated sandstone (tidal sand ridge deposits)

This facies is the uppermost facies in the core of well No. 4 (Figure 3.2). It consists of three parts. The sandstone in the lower part is black colored, fine to medium grained,

cross-bedded, oil stained, and not bioturbated. The deposits in the middle part are grey colored, planar laminated, not oil stained, and bioturbated. The sandstone in the upper part is dark brown colored, fine to medium grained, planar laminated, oil stained, and not bioturbated. Below his sandstone, the tidal sand bar facies consists of cross-bedded and planar laminated sandstone. The tidal sand bar facies passes gradually upward to this facies.

This facies is 13 feet thick. In the lower part, the black color of fine to medium grained sandstone is caused by high degree of oil stain. Cross-bedding is prominent and bidirectional (herringbone) cross-bedding is present in this sandstone (Figure 3.6A). Individual bed thickness ranges from 0.3 to 2 feet. This sandstone contains no bioturbation. It has very few mud drapes; the abundance of mud drapes is much lower than in the tidal sand bar facies in main and upper M1 sandstone in Tarapoa oil field. This sandstone also lacks reactivation surfaces which are common in tidal sand bar facies in Main and upper M1 Sandstone in Tarapoa oil field. The black colored, cross bedded sandstone in the lower part fines quickly upward to sediment in the middle part. Although the transition between the two parts is short, no sharp contact is presents between them. This fining-upward sediment consists of very fine to medium grained sandstone, siltstone, and mudstone (Figure 3.6B). It is 1 ft thick. The overall color of this sediment is grey. Moderate bioturbation is observed. Oil stain is absent in this sediment. This sediment changes abruptly upwards to the dark brown colored, planar laminated sandstone in the upper part. The contact surface between the two parts is missing in the core. The planar laminated sandstone consists of fine to medium grained sandstone (Figure 3.6C). It is 4 feet thick. The dark brown color of this sandstone is caused by a high degree of oil stain. Planar lamination is the only physical sedimentary structure. This sandstone has a low degree of bioturbation at its base and almost no bioturbation in other parts. It has low abundance of mud drapes.

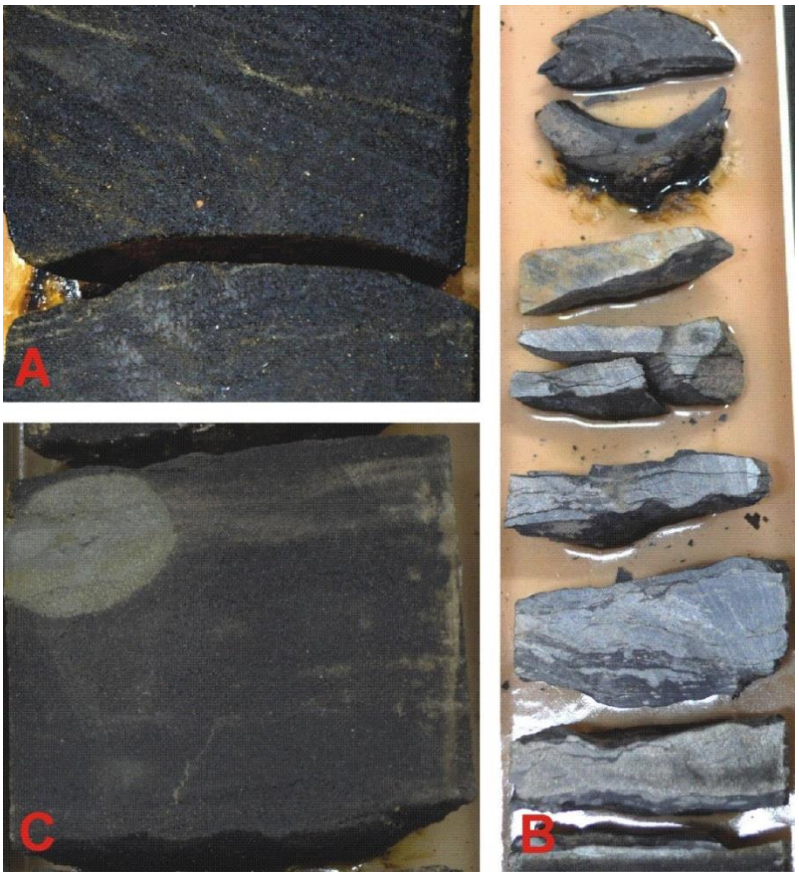

Figure 3.6: Core photos of tidal sand ridge deposits. (A) Bidirectional (herringbone) cross bedding in the lower part of shelf ridge facies. (B) Fining-upward sediment of the lower part of shelf ridge facies. (C) Planar laminated sandstone in the upper part of shelf sand ridge facies.

We interpret the cross bedded sandstones and planar laminated sandstone as shelf sand ridge facies. The cross bedded sandstone in the lower part of this facies is similar to the tidal sand bar facies in main and upper M1 sandstone in Tarapoa oil field. Some characteristics are common in both of them: unidirectional and bidirectional (herringbone) cross bedding which are widely used as indicators of tidal deposition (Dalrymple, 2012); fine to medium grain sizes which imply high current speed; low abundance or absent bioturbation suggests high sedimentation rate. These similarities makes people think that

they are both tidal sand bar facies. However, important differences exist between them. First, reactivation surfaces are absent in this sandstone. Second, the abundance of mud drapes is lower in this sandstone, which implies the suspended sediment concentration associated with this environment is lower than tidal sand bars. Figure 3.7 shows the suspended sediment concentration decreases seaward in tide-dominated estuaries. This suggests that this facies is deposited in a tidally-influenced environment which is seaward of tidal sand bars. This environment is likely to have been a tidally-influenced shelf. Tidal currents induce the deposition of shelf sand ridges on shelves and tidal sand bars in tide-dominated estuaries. Therefore, shelf sand ridges have similar depositional processes with tidal sand bars. This makes their facies similar in many aspects but the key differences indicate this sandstone is an open shelf sand ridge facies and is not occurring within an estuary.

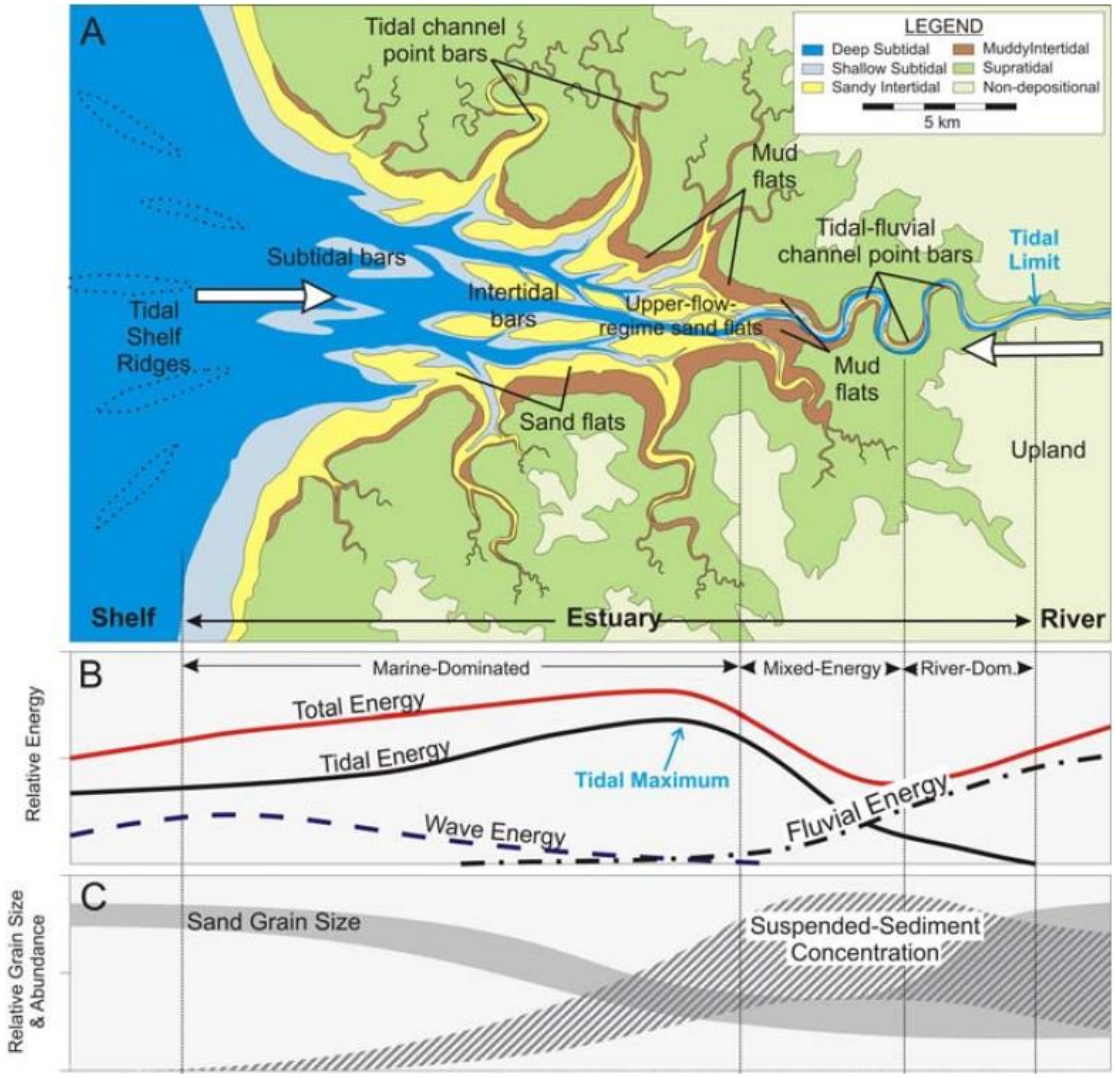

Figure 3.7: Variation of suspended sediment concentration in tide-dominated estuaries (from Dalrymple et al, 2012)

The fining -upward sediment in the middle part of the body does not have distinct characteristics to identify its depositional environment. Nonetheless, we can explain it with current knowledge of shelf sand ridges. It is commonly assumed that shelf sand ridges consist of tidal dunes, which result in sediment coarsening upward (Dalrymple et al, 2012). However, when the energy of tidal currents decreases gradually, an interval of fining -

upward deposits can therefore be formed on top of the shelf sand ridges. This can happen as the shelf sand ridge grows large enough and the ridge crest enters the zone of weaker currents (Dalrymple et al, 2012). The fining-upward sediment found in the middle part could be the product of such process.

The planar laminated, fine to medium grained sandstone in the upper part of this facies is interpreted to be associated with shelf sand ridges. Presence of mud, planar lamination, and fine to medium grain sizes together indicate low current speed which is insufficient to produce cross bedding. Mud drapes indicates slack water period; low abundance of mud drapes indicates low suspended sediment concentration which is typically found in distal environments such as on the shelf. Low degree of bioturbation indicates that the rate of sedimentation can be relatively high. We interpret this sandstone to have been deposited on top of shelf sand ridges during a period which the tidal current speed was low and supply of sediment was limited. As conclusion, we interpret the cross-bedded sandstones overlain by fining -upward deposits and planar laminated sandstone as belonging to shelf sand ridge facies.

3.1.2 Facies and depositional system interpretation based on thickness profile of M1 sandstone in the Pichincha-Carabobo area

Another important piece of evidence which supports the shelf sand ridge interpretation is the thickness profile of M1 sandstone in the Pichincha-Carabobo area. The well No. 4 and Carabobo wells are closely spaced in the Pichincha-Carabobo area. In the core of well No. 4, M1 sandstone is the combination of tidal bar facies and shelf sand ridge facies. On the well logs, M1 sandstone is bounded at the bottom by a sudden decrease of gamma ray reading compared to the underlying upper Napo shale; M1 sandstone is bounded at its top by low gamma ray readings. Figure 3.8 is the well log cross section which shows the thickness of M1 sandstone in well No. 4 and Carabobo wells. The

thickness profile of M1 sandstone shows a dome shaped sand body. Modern shelf sand ridges are also dome shaped sand bodies. Figure 3.9 shows the longitudinal and transverse cross section of modern shelf sand ridges found in the Celtic sea. Comparing two figures, it is clear that the shape of sand bodies in the Pichincha-Carabobo area resemble shelf sand ridges. This supports our interpretation that M1 sandstone in the Pichincha-Carabobo area is shelf sand ridge facies.

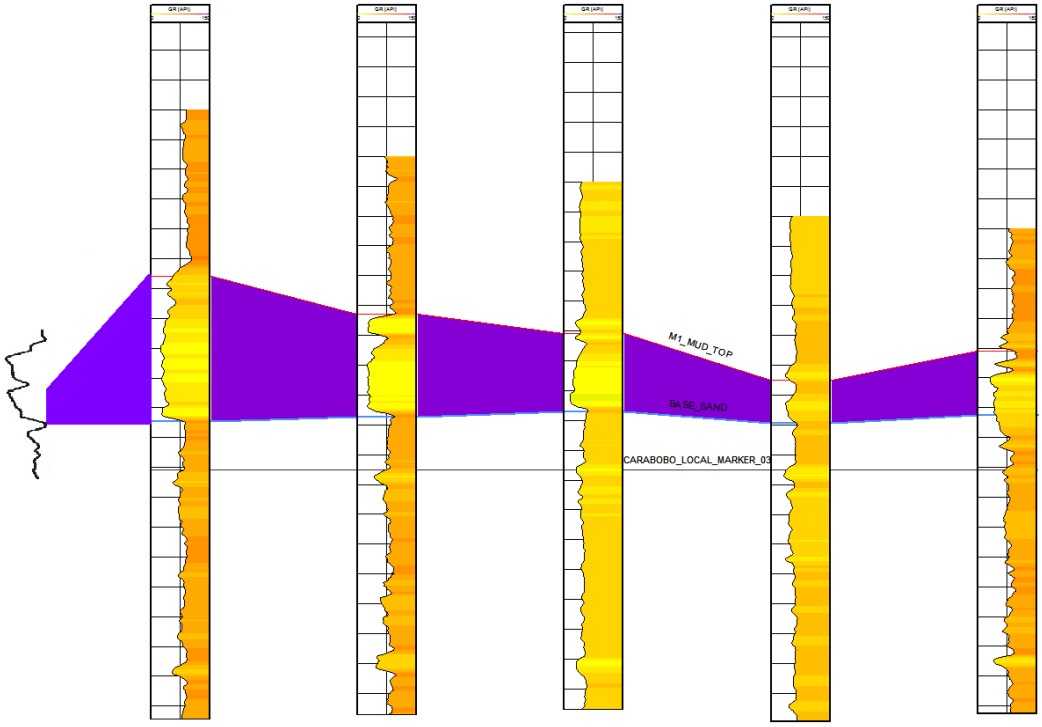

Figure 3.8: Well logs of well No. 4 and Carabobo wells. M1 sandstone is marked by purple color. The thickness profile of M1 sandstone shows shape of dome, consistent with the shelf tidal sand ridge interpretation

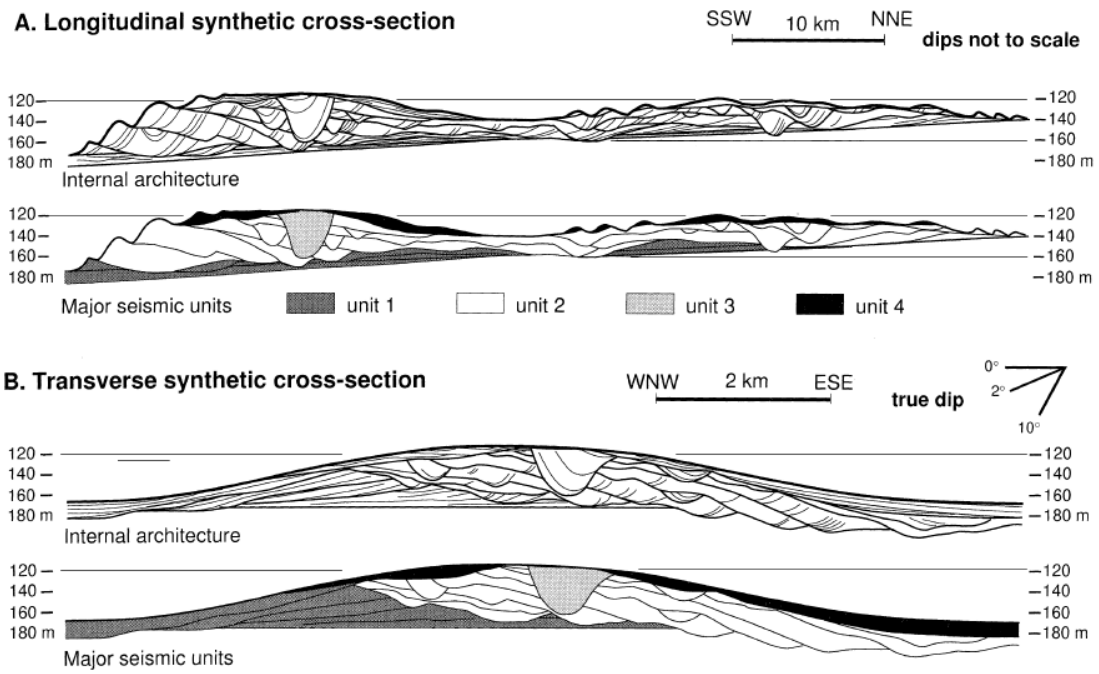

Figure 3.9: Longitudinal and transverse sections through a shelf sand ridge in Celtic Sea (from Renaud et al, 1999)

3.2 PREDICTION OF FACIES, DEPOSITIONAL SYSTEMS, SANDBODIES, AND HETEROGENEITY IN THE TARAPOA NORTHWEST AREA

3.2.1 Facies and depositional system in the Tarapoa northwest area

In the Tarapoa oil field, the depositional system of M1 sandstone is a tide-dominated estuary. The cross bedded sandstone at the bottom of M1 sandstone (i.e. "main M1 sandstone") belongs to the tidal sand bar facies; the mud-rich part of M1 sandstone (i.e. "muddy M1") belongs to tidal flat facies; the organic-rich and coaly part of M1 sandstone belongs to salt marsh facies; the cross bedded sandstone near the top of M1 sandstone (i.e. "upper M1 sandstone") belongs to tidal sand bar facies.

In the Pichincha-Carabobo area, the depositional systems of M1 sandstone are (1) tide-dominated estuary and (2) tide-influenced open shelf. The heterolithic facies with

cross bedded sandstone and mud drapes at the bottom of M1 sandstone belongs to tidal sand bar facies; the cross bedded sandstone that fines-upward into planar laminated sandstone belongs to shelf sand ridge facies.

The facies at the bottom of M1 sandstone in Tarapoa oil field and in the Pichincha-Carabobo area are the same, i.e., tidal sand bar facies. In Pichincha-Carabobo area, tidal sand bar facies gradually changed upwards into shelf sand ridge facies. This change is not observed in M1 sandstone in Tarapoa oil field. This indicates that while the tidal sand bars were being deposited in the Tarapoa oil field, shelf sand ridges were developing in the Pichincha-Carabobo area. The distribution of depositional systems is shown in the reconstructed paleogeography of M1 Sandstone (Figure 2.9). The paleogeography shows that the Tarapoa oil field lies inside the tide-dominated estuary; the Pichincha-Carabobo area is on the open shelf, outside the tide-dominated estuary; the Tarapoa northwest area is estimated to lie near the entrance of the tide-dominated estuary. The facies of sandstone changes from tidal sand bars facies in the Tarapoa oil field to the shelf sand ridge facies in the Pichincha-Carabobo area. Because the Tarapoa northwest area lies between the Tarapoa oil field and Pichincha-Carabobo area, the facies of main M1 sandstone in the the Tarapoa northwest area is likely to be a transitional facies between tidal sand bar facies and shelf sand ridge facies.

M1 sandstone in the Pichincha-Carabobo area entirely lacks any mud-rich part and coaly part of M1 sandstone. This indicates that the far northwestern area was not part of the tide-dominated estuary when the tide-dominated estuary in Tarapoa oil field was being filled and covered by tidal flats and salt marsh deposits. This is shown in the reconstructed paleogeography of tidal sand bar facies (Figure 2.18). The paleogeography of tidal flat facies and salt marsh facies shows that the Tarapoa oil field inside the tide-dominated estuary is covered by tidal flat and salt marsh deposits; the Pichincha-Carabobo area

outside the tide-dominated estuary is not covered by tidal flat and salt marsh deposits. The Tarapoa northwest area which is close to the entrance of the tide-dominated estuary could be partially covered by tidal flat and salt marsh deposits. As a result, the tidal flat facies and salt marsh facies may exist in the Tarapoa northwest area, but thinner than the tidal flat facies and salt marsh facies in the Tarapoa oil field.

Also, "upper M1 Sandstone" is not found in the far northwestern area. This may because far northwestern area was not part of the new tide-dominated estuary which deposited the "upper M1 Sandstone" in Tarapoa oil field.

As conclusion, we suggest that the facies M1 sandstone in the Tarapoa northwest area is likely to be transitional facies between facies in Pichincha-Carabobo area and Tarapoa oil field.

3.2.2 Prediction of sandstone bodies and heterogeneity in the Tarapoa northwest area

We have interpreted that the facies of the main M1 Sandstone in the Tarapoa northwest area was a transisional facies between tidal sand bar facies and shelf sand ridge facies. The sandbodies and heterogeneity in the Tarapoa northwest area are determined by facies of "main M1 Sandstone". Therefore, the geometry of sandbodies in the Tarapoa northwest area is likely to be a transition between geometries of tidal sand bars and shelf sand ridges; the heterogeneity (i.e. geometry of "shale barriers") in the Tarapoa northwest area is also likely to be a transition between the "shale barriers" in the Tarapoa oil field and Pichincha-Carabobo area. The sandstone bodies and heterogeneity in all areas are described below:

Sandstone bodies and heterogeneity in the Tarapoa oil field

In the Tarapoa oil field, main M1 sandstone belongs to the estuarine tidal sand bar facies and "shale barriers" are mud-filled tidal channels. Tidal sand bars in the tide-dominated estuaries generally are sheet-like sand bodies. The lateral geometry of tidal bars is elongated; the length of tidal bars is usually 1-15 km and the width usually ranges from a few hundred meters to nearly 4 km (Dalrymple et al, 2010). The thickness of tidal bars (i.e. relief from the bottom of adjacent tidal channel to the crest of bar), however, can be poor because it is restricted by the water depth in the tide-dominated estuaries. The thickness of tidal bars usually ranges from a few meters to 20 meters (Dalrymple et al, 2010). The bar crest can be narrow and sharp or broad and flat (Dalrymple et al, 2010). Tidal bars with narrow and sharp crest are usually found in places where the space is not totally filled by tidal bars; this is relatively common in the seaward end of tide-dominated estuaries (Harris, 1988; Dalrymple et al, 1990; Ryan et al, 2007). Tidal bars with broad and flat crests are usually found in places where the tidal bars filled up all the available space; this is relatively common in the inner part of tide-dominated estuaries (Harris, 1988; Dalrymple et al, 1990; Ryan et al, 2007). In this case, we assume the tidal bars in the study area have relatively broad and flat tops.

The geometry of "shale barriers" is affected by depth, width, and channel walls of tidal channels. The relief from the bottom of adjacent tidal channel to the crest of bar usually range from a few meters to 20 meters (Dalrymple et al, 2010); this is the thickness of "shale barriers". As mentioned in the previous chapters, a tidal channel in the tide-dominated estuary is erosive on one side and depositional on the other side. The slope of channel wall on the erosive side is relatively steep due to erosive processes on the cutbank; the slope of the channel wall on the depositional side is relatively gentle due to bar depositional processes. The relatively steep channel wall on the erosive side may limit the

width of tidal channels. In addition, the tidal bars usually have considerable width (range from a few hundred meters to nearly 4 km) (Dalrymple et al, 2010). As shown in Figure 2.25, the broad and flat bar crest can considerably limit the width of tidal channels. The above factors make the "shale barriers" in the Tarapoa oil field to have relatively steep channel walls and limited width.

Sandstone bodies and heterogeneity in the Pichincha-Carabobo area

In the Pichincha-Carabobo area, most of the M1 sandstone belongs to shelf sand ridge facies. The shelf sand ridges can be 7.5-40 meters high, 10-120 km long, 10 km wide, and have 1-30 km of space between each other (Houbolt, 1968; Stride et al, 1982; Wood, 2003; Renaud and Dalrymple, 2010). The documented size of shelf sand ridges is much greater than tidal sand bars. Because of this, we assume that the shelf sand ridges in the Pichincha-Carabobo area are larger than tidal sand bars in the Tarapoa oil field. The shelf sand ridges are dome shaped sand bodies. Unlike tidal sand bars which can be flat-topped in the relatively inner part of the estuary, shelf sand ridges always have narrow and sharp crest.

The "shale barriers" in the Tarapoa oil field are identified by seismic maps and isopach maps. However, no seismic data is available in the Pichincha-Carabobo area and the density of wells is not sufficient to generate an isopach map which can show the existence of "shale barriers". In this area, "shale barriers" are identified on the well log cross section (Figure 3.8). We interpret that the "shale barriers" in the Pichincha-Carabobo area are the mud-filled channels between the shelf sand bars. Because the shelf tidal bars have the shape of a dome and sharp crest, the width of channel can be considered to be from the crest of a shelf sand ridge to another. This makes the "shale barriers" extremely

wide in the Pichincha-Carabobo area. The great channel width also results in very gentle channel walls.

Sandstone bodies and heterogeneity in the Tarapoa northwest area

As conclusion, the shape of sand bodies in the Tarapoa northwest area is likely to be transitional between “sheet-like” sand bodies with broad and flat top and “dome-like” sand bodies with narrow and sharp top. The size of sand bodies in the Tarapoa northwest area is larger than the tidal sand bars in the Tarapoa oil field and smaller than the shelf sand ridges in the Pichincha-Carabobo area. The width of “shale barriers” in the Tarapoa northwest area is greater than that in the Tarapoa oil field and smaller than the shelf sand ridges in the Pichincha-Carabobo area. The channel walls of shale barriers” in the Tarapoa northwest area is gentler than that in the Tarapoa oil field and steeper than the shelf sand ridges in the Pichincha-Carabobo area.

Chapter 4: Discussion

Although most evidence suggests that the main M1 sandstone and "shale barriers" are originated within a tide-dominated estuary, there is also another reasonable alternative hypothesis that can possibly explain the origin of the main M1 Sandstone and its "shale barriers" in the Tarapoa Field.

An important reason for suggesting that the main M1 Sandstone was deposited in a tide-dominated estuary but not a tide-dominated delta is the sharp contact between the main M1 sandstone and the underlying Napo shale. The upward coarsening developed within the upper Napo shale is interpreted as deposits of a Napo prograding delta. These coarsening upward deltaic deposits do not gradually change into "main M1 sandstone", instead, a sharp contact exists between the coarsening upward delta deposits and "main M1 sandstone". The sharp contact is interpreted as a product of transgressive ravinement. However, an alternative hypothesis suggests that this sharp contact was actually produced during a strong regression. This hypothesis is supported by the study on the Fly River Delta. The Fly River Delta is a typical tide-dominated delta on the coast of Gulf of Papua. A study of sedimentation in the Fly River Delta analyzed three large subaqueous distributary channels in the delta. One of the distributary channels has a much longer range of salt water intrusion than the others; only 10% of the river outflow is discharged through this distributary channel (Wolanski et al, 1997). Evidence of bedload transport indicates this distributary channel experiences greater tidal influence than other distributary channels (Harris et al, 2004). The bathymetry map of the Fly River Delta reveals that a 10-meter deep submarine channel developed into this distributary channel (Figure 4.1) (Harris et al, 1993). The facies distribution map (Figure 4.2) and percentage mud content map (Figure 4.3) show that the submarine channel cuts the delta front deposits and exposes the pro-delta

deposits. If tidal sand bars are deposited into this distributary channel, there will be a sharp contact between the muddy pro-delta deposits and sandy tidal sand bar deposits.

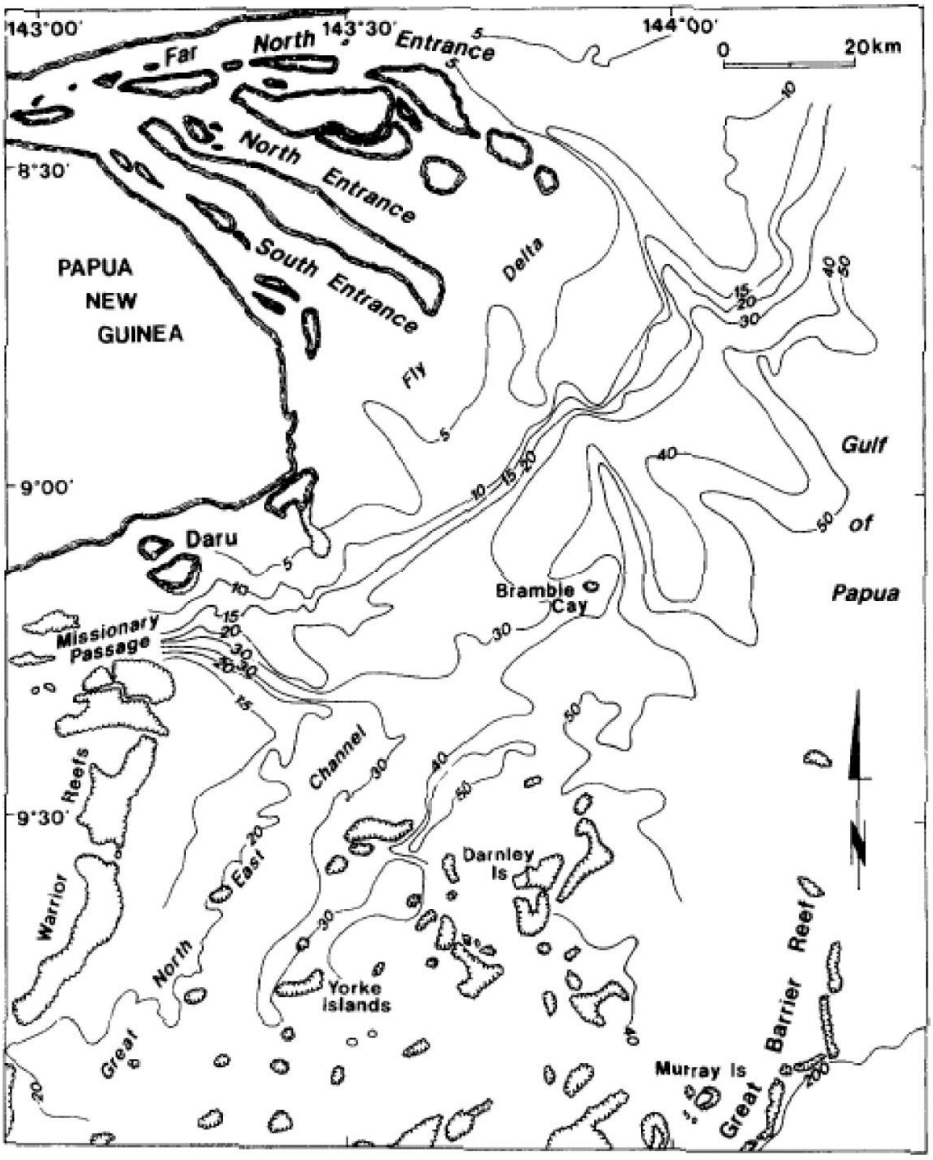

Figure 4.1: Bathymetry map of Fly River Delta and adjacent area (from Harris et al, 1993). Note the 3 large subaqueous distributary channels filled by tidal bars that cut down into the delta front and make a possible Delta analog alternative for the MI Main Sandstone

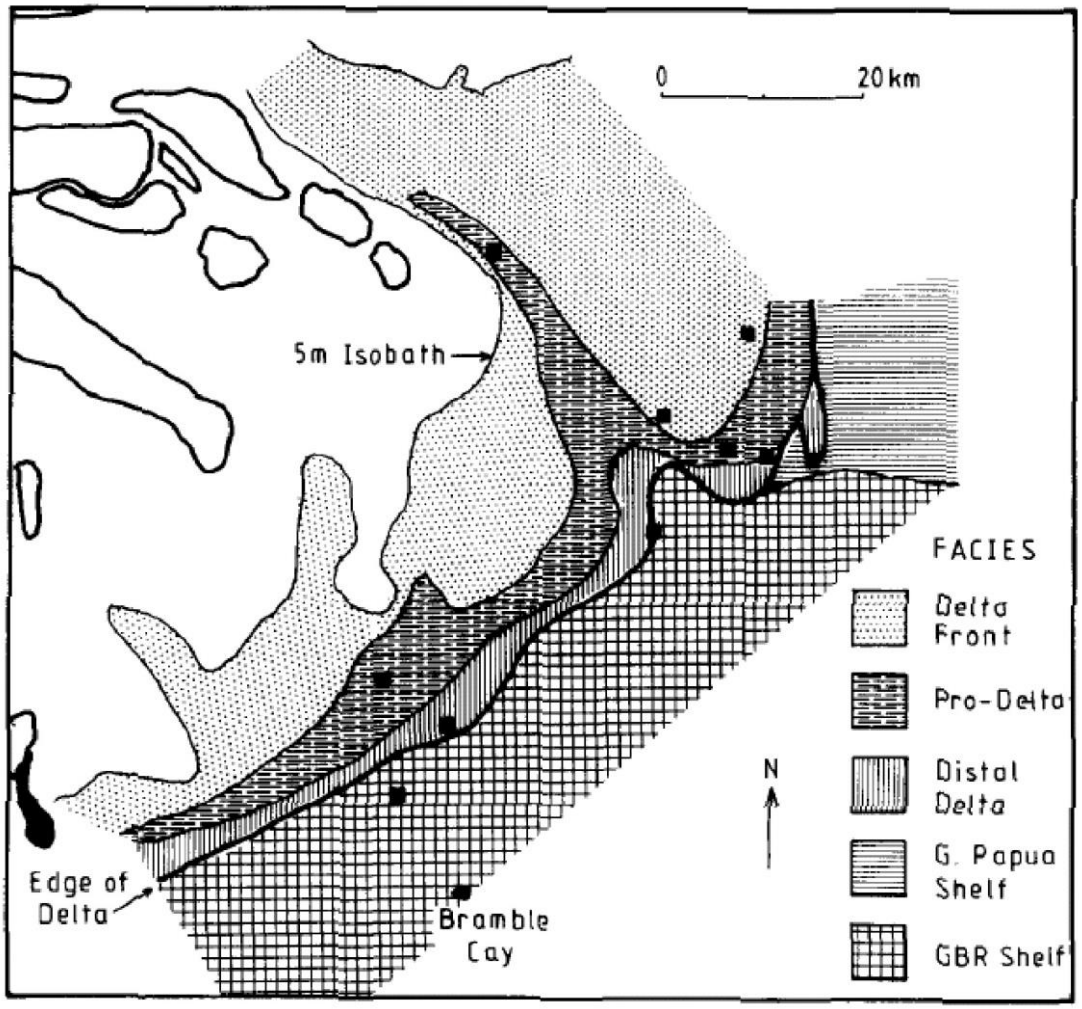

Figure 4.2: Facies distribution map of Fly River Delta (from Harris et al, 1993)

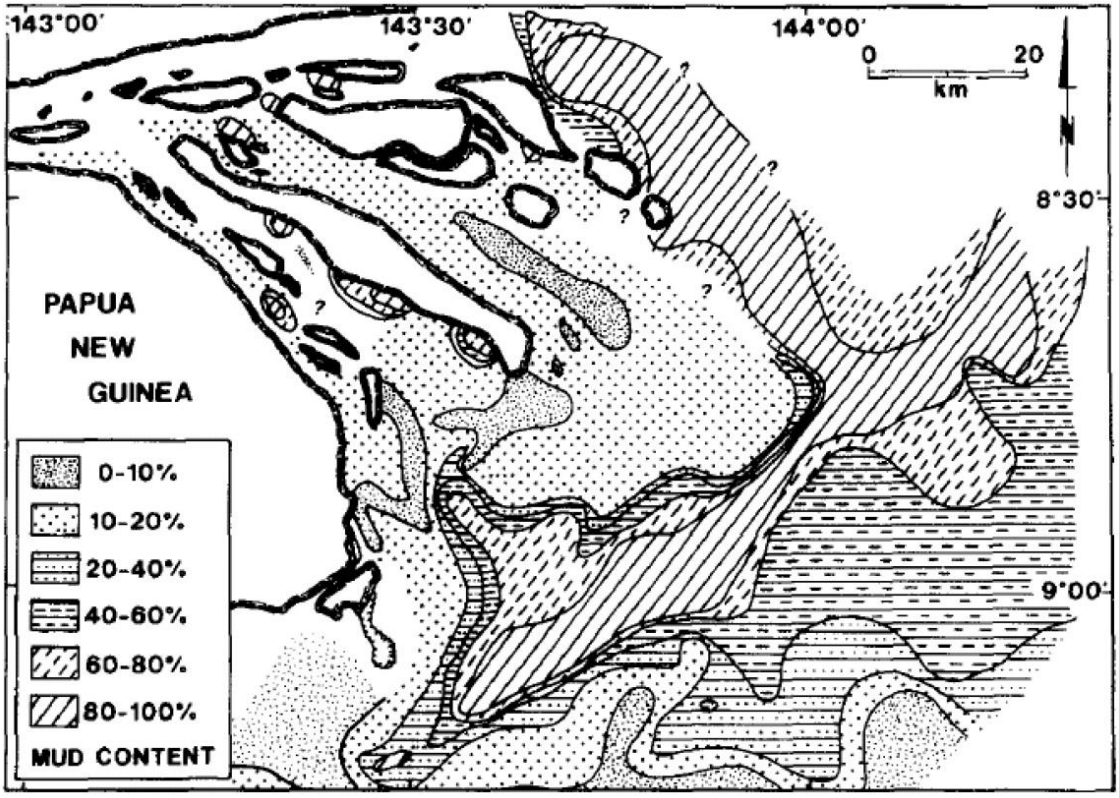

Figure 4.3: Mud content of surface sediment in the Fly River Delta (from Harris et al, 1993)

This scenario can widely occur in large tide-dominated deltas with very low fluvial discharges. As illustrated by the distributary channels of Fly River Delta, very low fluvial discharge allows greater tidal influence. Consequently, tidal erosion removed delta-front deposits and exposed pro-delta deposits. In a tide-dominated delta with very low fluvial discharges, this process can occur in all the distributary channels. As a result, a sharp contact can widely exist between the muddy pro-delta deposits and overlying tidal sand bar deposits in this type of tide-dominated delta (Figure 4.4A and Figure 4.4B). This process has the potential to create exactly the lithofacies relationships seen in the Tarapoa area M1

sandstone: the upward coarsening deltaic deposits (Napo), tidal bar deposits (M1), and the sharp contact between them.

The stacking pattern of M1 Sandstone can be explained in full by the evolution of depositional system. The first three stages are progradation of tide-dominated delta; the last stage is the formation of a tide-dominated estuary. In the first stage, the study area was located in the pro-delta and delta-front area; upward-coarsening pro-delta and delta-front sediments were deposited in the study area (Figure 4.4A). In the second stage, the delta-front sediments were removed by tidal erosion; pro-delta deposits were exposed. Then subtidal sand bars (main M1 Sandstone) were deposited on top of finer-grained pro-delta deposits, forming a sharp contact between them (Figure 4.4B). In the third stage, the delta continued to prograde. In the study area, subtidal sand bars became intertidal; tidal flats deposits (muddy M1) were laid down on top of the subtidal sand bars. Then the study area became supratidal and subtidal sand bars became vegetated islands; vegetation deposited organic-rich materials (which became coal) on the tidal flats deposits. Ultimately, as regression continued, the islands merged into the margin of delta. The tidal channels along the margin of delta were progressively abandoned and filled with muddy tidal flat deposits, forming “shale barriers” (Figure 4.4C). The last stage is exactly the same with the previous hypothesis. A transgression occurred; a tide-dominated estuary was formed over the study area; tidal sand bars were deposited in the estuary, which become upper M1 Sandstone (Figure 4.4D).

In conclusion, the main M1 Sandstone, shale barriers, and the overlying stacking pattern of tidal flat and salt marsh facies may be explained by the progradation of tide-dominated deltas as an alternative to the tide-dominated estuary hypothesis. The concept of M1 tide-dominated deltas leads to a new version of sequence stratigraphy of M1 sandstone. In this hypothesis, “main M1 sandstone”, “shale barriers”, tidal flat facies, and

salt marsh facies are all deposited during a single large-scale regression (i.e. progradation of delta). However it should be noted that this regressive hypothesis does not fit well with the interpretation of the tidal shelf sand ridges in the Carabobo region, because sand ridges are always developed during transgressive conditions.

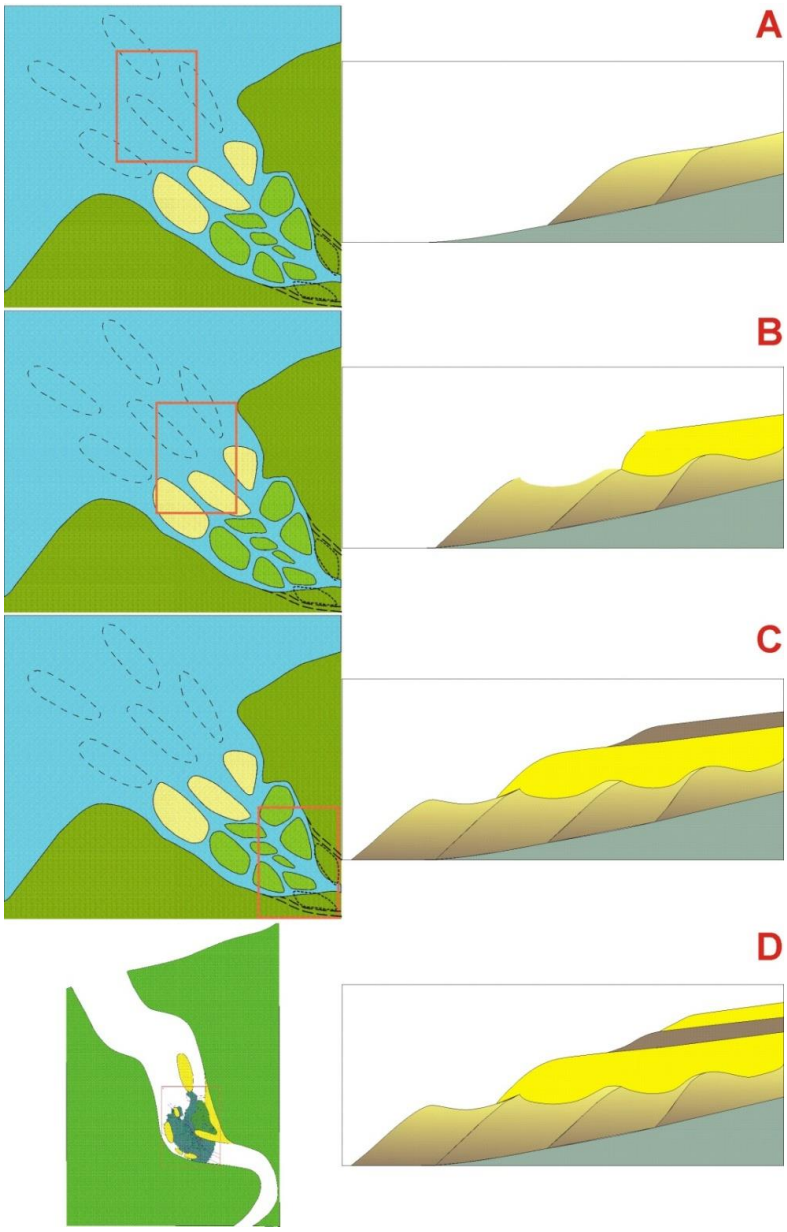

Figure 4.4: An alternative model for M1 Sandstone: (A) The first stage of depositional system evolution; deposition of pro-delta and delta-front. (B) The second stage of depositional system evolution; erosion of delta-front and deposition of main M1 Sandstone. (C) The third stage of depositional system evolution; deposition of muddy M1 and coal. (D) The last stage of depositional system evolution; deposition of upper M1 Sandstone.

Chapter 5: Conclusions

M1 sandstone is one of the major hydrocarbon-producing sandstone units in the Tarapoa oil field; it is also a potential major hydrocarbon-producing sandstone unit in the new area northwest to the Tarapoa oil field. This sedimentological study had two objectives. The first objective was to improve the geological understanding of M1 sandstone by giving detailed description and explanation of facies, depositional systems, sequence stratigraphy, and "shale barriers". Five depositional facies are observed from the 12 cores in the Tarapoa oil field, namely tidal sand bar facies, tidal sand flat facies, heterolithic tidal flat facies, tidal mud flat facies, and salt marsh facies. Based on the facies observed from the cores, we interpret the depositional system of M1 sandstone as a tide-dominated estuary. Isopach maps of facies and facies association were made based on the surfaces picked on more than 300 Well logs. Four Paleogeography maps and depositional models were built based on these isopach maps. The depositional models indicate four stages of deposition. In the first stage, an initial transgression on top of the Napo delta created an erosively-based tide-dominated estuary. Tidal sand bars were widely deposited and tidal channels were created in this tide-dominated estuary during the time of transgression. In the second stage, a regression occurred. The falling relative sea level forced tidal flats and salt marshes to prograde out from the margin of estuary to the center of the gradually infilling estuary. In this process, tidal channels were filled with muddy tidal flat deposits, forming "shale barriers". Tidal bars were covered first by tidal flat deposits, then by salt marsh deposits. In the third stage, the regression continued, pushing the shoreline further seaward and making sediment bypass in the study area. In the fourth stage, a new transgression occurred. A new tide-dominated estuary was created over the study area and tidal sand bars were deposited in the new estuary.

The second objective of this study was to help improve geological understanding of M1 sandstone in the Tarapoa northwest area by making a new predictive geological model involving the facies, depositional systems, and "shale barriers". We interpret that the facies, depositional systems, sand bodies, and "shale barriers" in the Tarapoa northwest area are transitions between the Tarapoa oil field and Pichincha-Carabobo area which is further northwest of the Tarapoa northwest area. Four facies are observed from the core of well No. 4 in the Pichincha-Carabobo area, namely delta front facies, tidal channel facies, tidal sand bar facies, and shelf sand ridge facies. Based on the facies observed from the core, we interpret the depositional system of M1 sandstone as a tidal-influenced open shelf. The characters of the facies, depositional systems, sand bodies, and "shale barriers" in this area are interpreted based on the facies and depositional system. As a result, we interpret that the facies of main M1 sandstone in the Tarapoa northwest area is transitional between tidal sand bar and shelf sand ridge; the area was located near the entrance of the tide-dominated estuary; the sand bodies were larger and sharp-crested compared to the sand bodies in the Tarapoa oil field; the "shale barriers" are relatively wider and the channel walls are gentler than the "shale barriers" in the Tarapoa oil field.

Finally, an alternative hypothesis is also offered for the main M1 Sandstone in Tarapoa Oilfield. Instead of being a sand-rich estuary, it is also possible that Main M1 could be tide-dominated delta distributary channels developed during regression. The facies would be similar in both models, though the alternative, the regressive model fits less well with the predicted shelf sand ridge interpretation of the northwesterly exploration area beyond Tarapoa field.

Appendix

The cores described in this study are listed here. All the cores contribute to the conclusion of this thesis but some of the cores are not mentioned in the discussion in this thesis.

Well No. 1

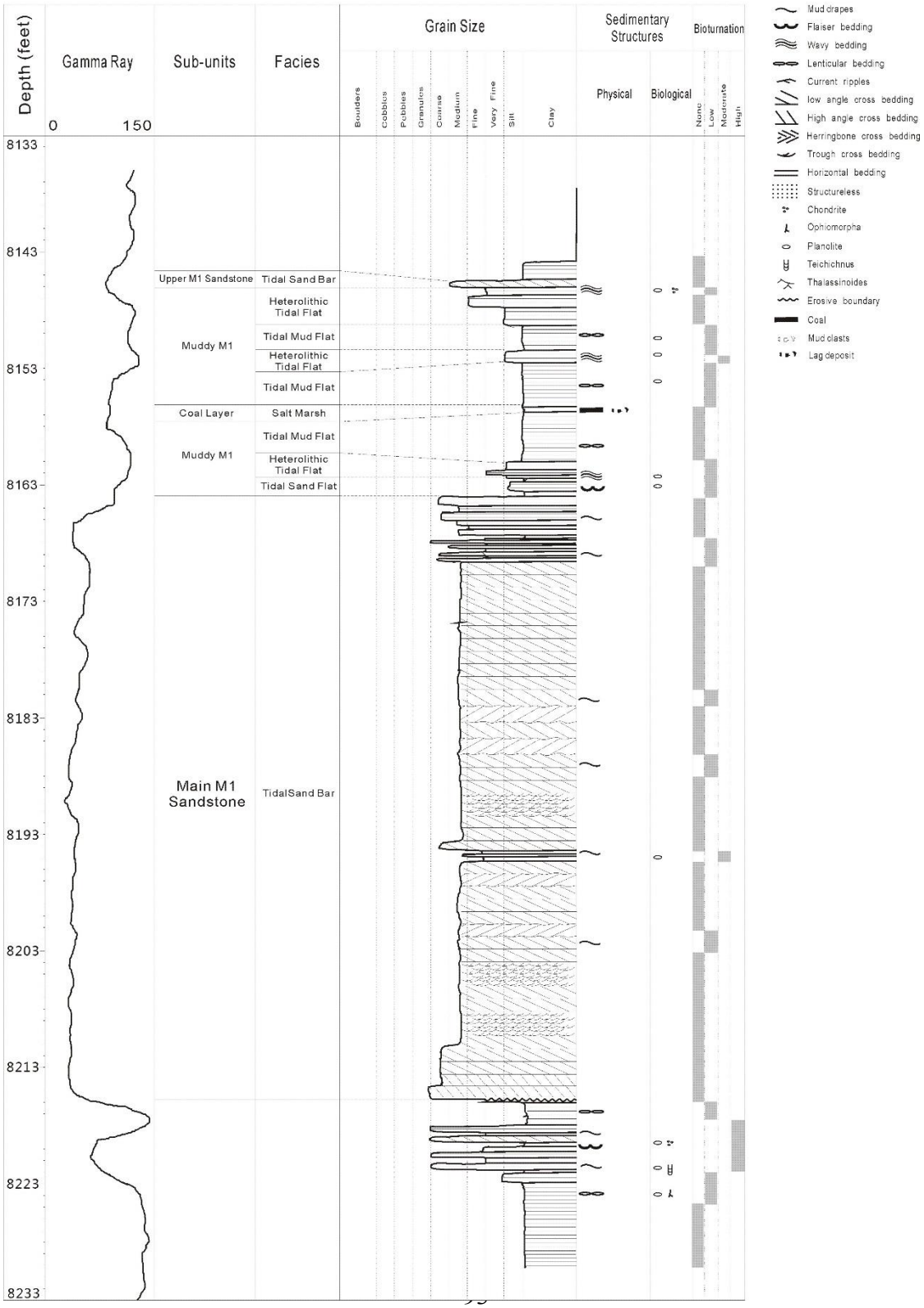
Depth (feet)
Gamma Ray
0
150
Sub-units
Facies
Grain Size
Boulders
Cobbles
Pebbles
Granules
Coarse
Medium
Fine
Very Fine
Silt
Clay
Sedimentary Structures
Physical
Biological
Bioturnation
None
Low
Moderate
High
8133
8143
8153
8163
8173
8183
8193
8203
8213
8223
8233
Upper M1 Sandstone
Tidal Sand Bar
Heterolithic Tidal Flat
Muddy M1
Tidal Mud Flat
Heterolithic Tidal Flat
Tidal Mud Flat
Coal Layer
Salt Marsh
Muddy M1
Tidal Mud Flat
Heterolithic Tidal Flat
Tidal Sand Flat
Main M1 Sandstone
TidalSand Bar
Mud drapes
Flaiser bedding
Wavy bedding
Lenticular bedding
Current ripples
low angle cross bedding
High angle cross bedding
Herringbone cross bedding
Trough cross bedding
Horizontal bedding
Structureless
Chondrite
Ophiomorpha
Planolite
Teichichnus
Thalassinoides
Erosive boundary
Coal
Mud clasts
Lag deposit

Well No. 2

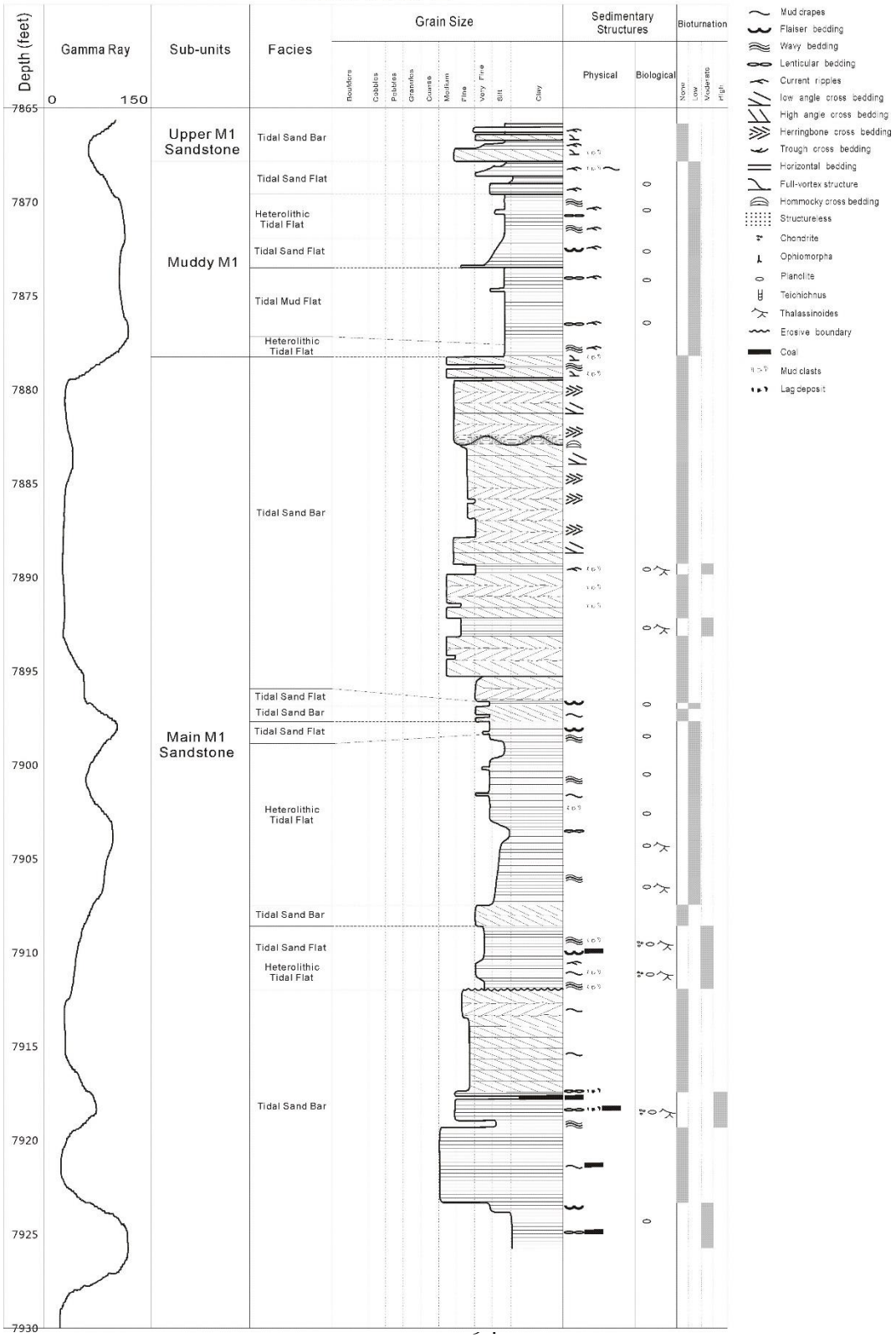
Depth (feet)
Gamma Ray
0
150
Sub-units
Facies
Grain Size
Boulders
Cobbles
Pebbles
Granules
Coarse
Medium
Fine
Very Fine
Silt
Clay
Sedimentary Structures
Physical
Biological
Bioturnation
None
Low
Moderate
High
7865
7870
7875
7880
7885
7890
7895
7900
7905
7910
7915
7920
7925
7930
Upper M1 Sandstone
Muddy M1
Main M1 Sandstone
Tidal Sand Bar
Tidal Sand Flat
Heterolithic Tidal Flat
Tidal Mud Flat
Mud drapes
Flaiser bedding
Wavy bedding
Lenticular bedding
Current ripples
low angle cross bedding
High angle cross bedding
Herringbone cross bedding
Trough cross bedding
Horizontal bedding
Full-vortex structure
Hommocky cross bedding
Structureless
Chondrite
Ophiomorpha
Planolite
Teichichnus
Thalassinoides
Erosive boundary
Coal
Mud clasts
Lag deposit

Well No. 3

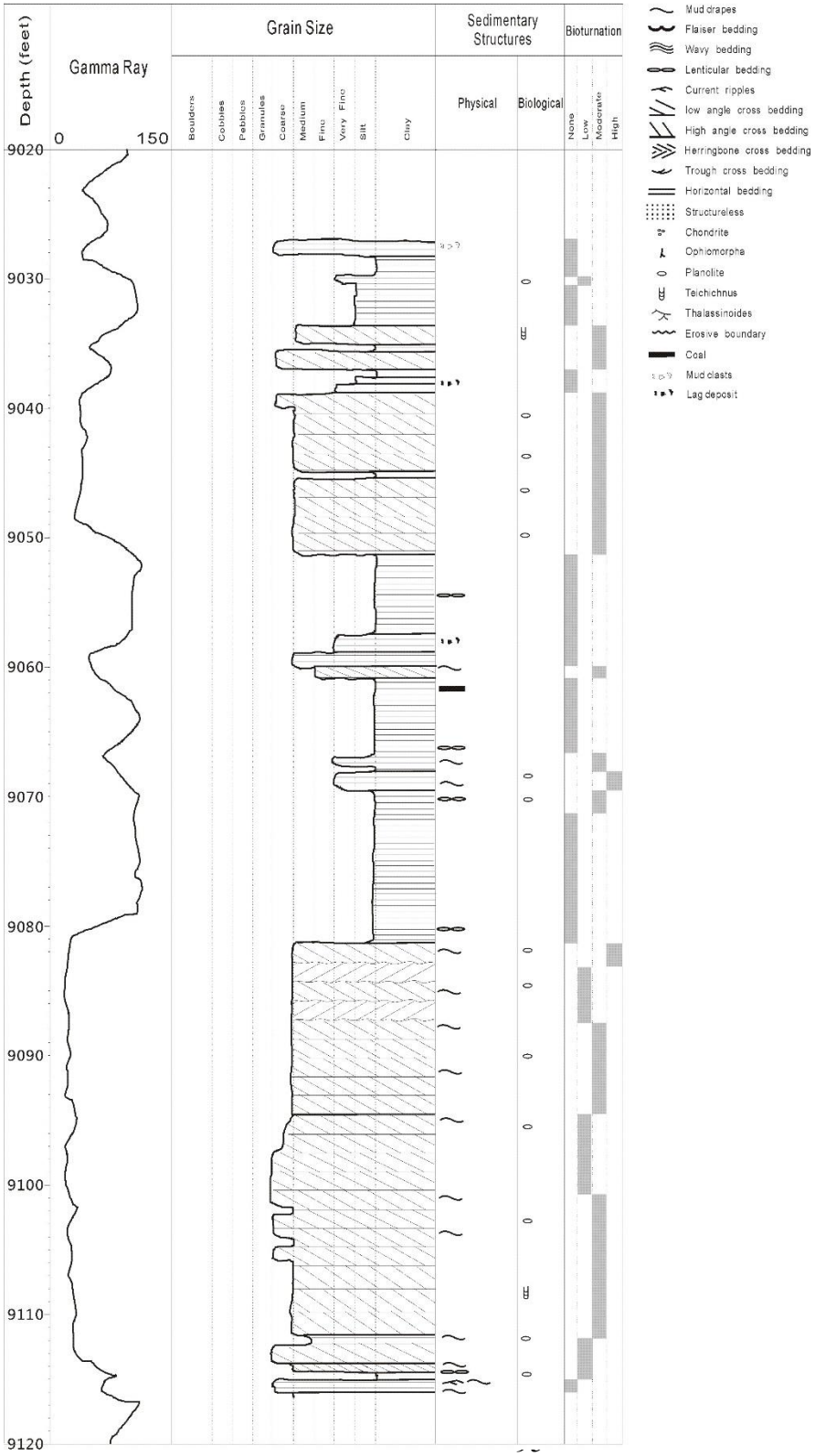
Depth (feet)
Gamma Ray
0
150
Grain Size
Boulders
Cobbles
Pebbles
Granules
Coarse
Medium
Fine
Very Fine
Silt
Clay
Sedimentary Structures
Physical
Biological
Bioturnation
None
Low
Moderate
High
9020
9030
9040
9050
9060
9070
9080
9090
9100
9110
9120
Mud drapes
Flaiser bedding
Wavy bedding
Lenticular bedding
Current ripples
low angle cross bedding
High angle cross bedding
Herringbone cross bedding
Trough cross bedding
Horizontal bedding
Structureless
Chondrite
Ophiomorpha
Planolite
Teichichnus
Thalassinoides
Erosive boundary
Coal
Mud clasts
Lag deposit

Well No. 4

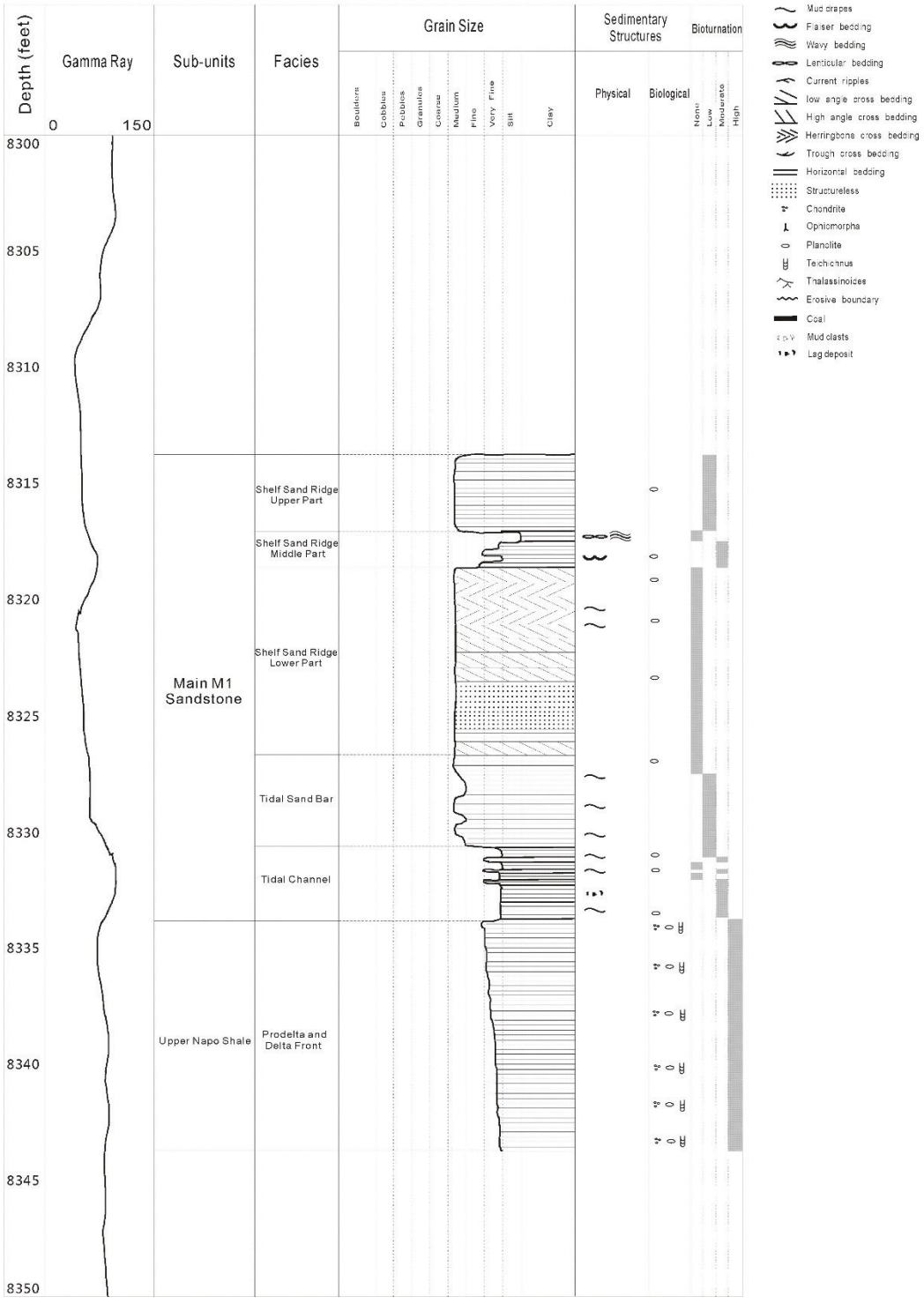
Depth (feet)
Gamma Ray
0
150
Sub-units
Facies
Grain Size
Boulders
Cobbles
Pebbles
Granules
Coarse
Medium
Fine
Very Fine
Silt
Clay
Sedimentary Structures
Physical
Biological
Bioturnation
None
Low
Moderate
High
8300
8305
8310
8315
8320
8325
8330
8335
8340
8345
8350
Main M1 Sandstone
Upper Napo Shale
Shelf Sand Ridge Upper Part
Shelf Sand Ridge Middle Part
Shelf Sand Ridge Lower Part
Tidal Sand Bar
Tidal Channel
Prodelta and Delta Front
Mud drapes
Flaser bedding
Wavy bedding
Lenticular bedding
Current ripples
low angle cross bedding
High angle cross bedding
Herringbone cross bedding
Trough cross bedding
Horizontal bedding
Structureless
Chondrite
Ophiomorpha
Planolite
Teichichnus
Thalassinoides
Erosive boundary
Coal
Mud clasts
Lag deposit

Well No. 5

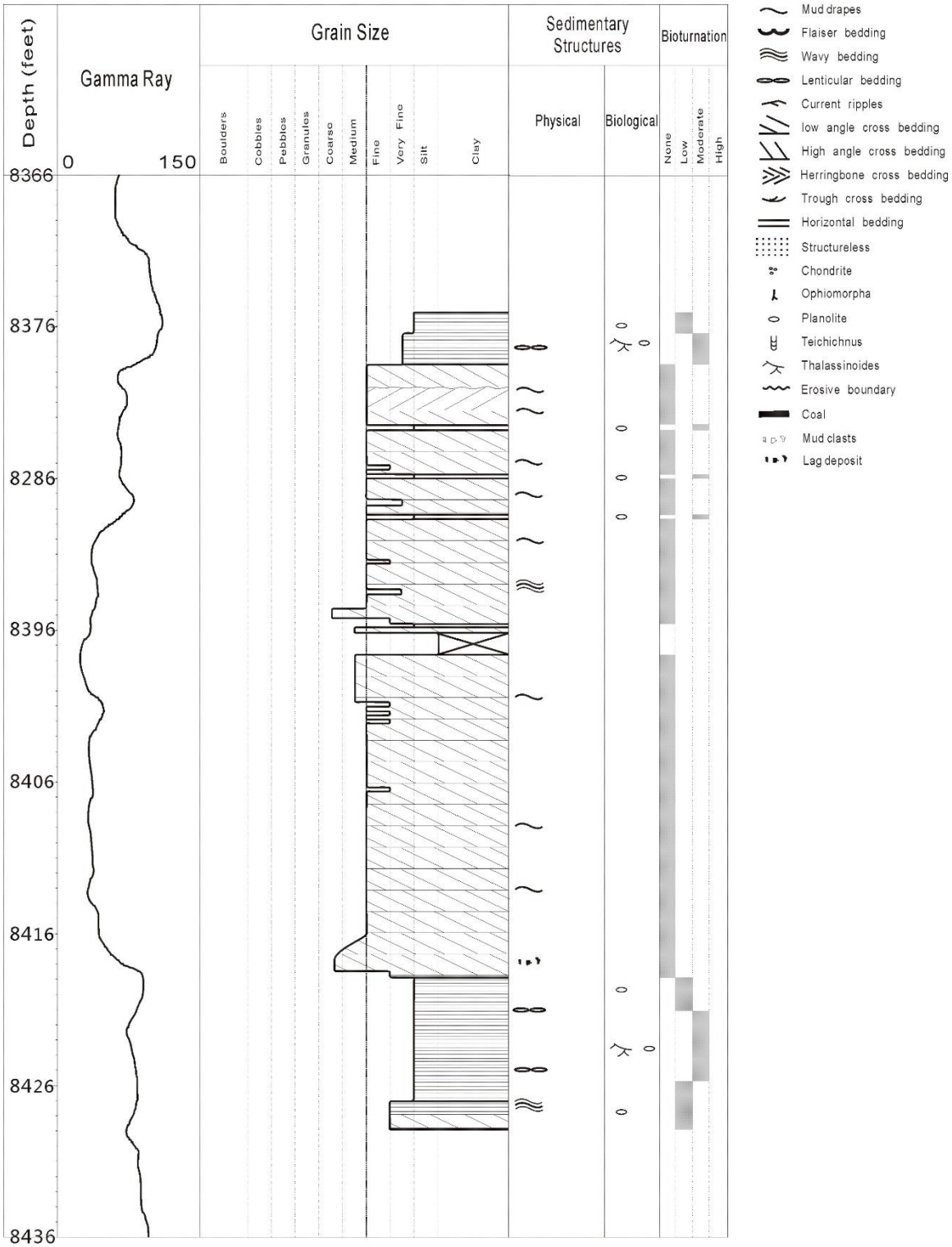
Depth (feet)
Gamma Ray
0
150
Grain Size
Boulders
Cobbles
Pebbles
Granules
Coarse
Medium
Fine
Very Fine
Silt
Clay
Sedimentary Structures
Physical
Biological
Bioturnation
None
Low
Moderate
High
8366
8376
8286
8396
8406
8416
8426
8436
Mud drapes
Flaiser bedding
Wavy bedding
Lenticular bedding
Current ripples
low angle cross bedding
High angle cross bedding
Herringbone cross bedding
Trough cross bedding
Horizontal bedding
Structureless
Chondrite
Ophiomorpha
Planolite
Teichichnus
Thalassinoides
Erosive boundary
Coal
Mud clasts
Lag deposit

Well No. 6

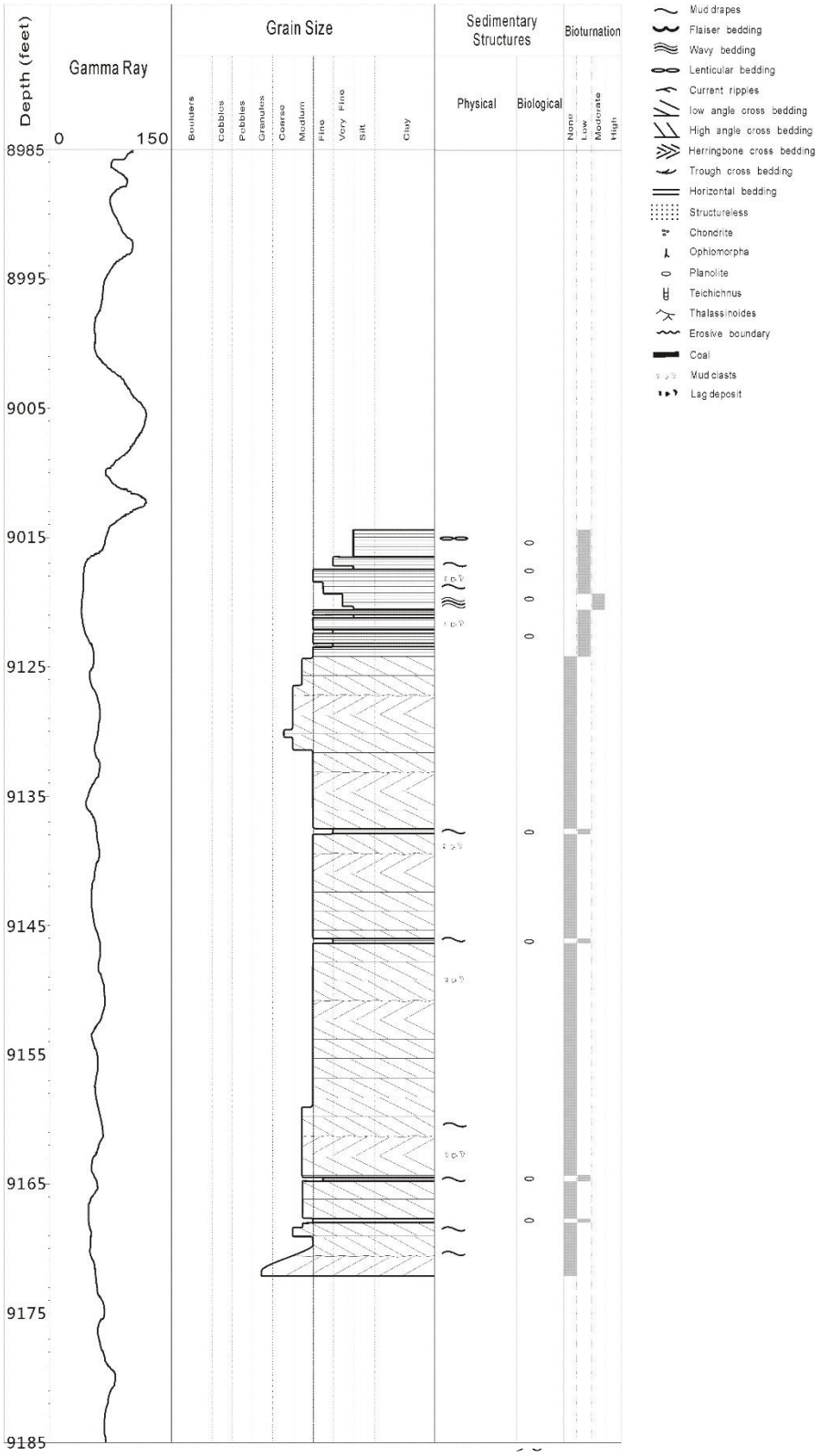
Depth (feet)
Gamma Ray
0
150
8985
8995
9005
9015
9125
9135
9145
9155
9165
9175
9185
Grain Size
Boulders
Cobbles
Pebbles
Granules
Coarse
Medium
Fine
Very Fine
Silt
Clay
Sedimentary Structures
Physical
Biological
Bioturnation
None
Low
Moderate
High
Mud drapes
Flaiser bedding
Wavy bedding
Lenticular bedding
Current ripples
low angle cross bedding
High angle cross bedding
Herringbone cross bedding
Trough cross bedding
Horizontal bedding
Structureless
Chondrite
Ophiomorpha
Planolite
Teichichnus
Thalassinoides
Erosive boundary
Coal
Mud clasts
Lag deposit

Well No. 7

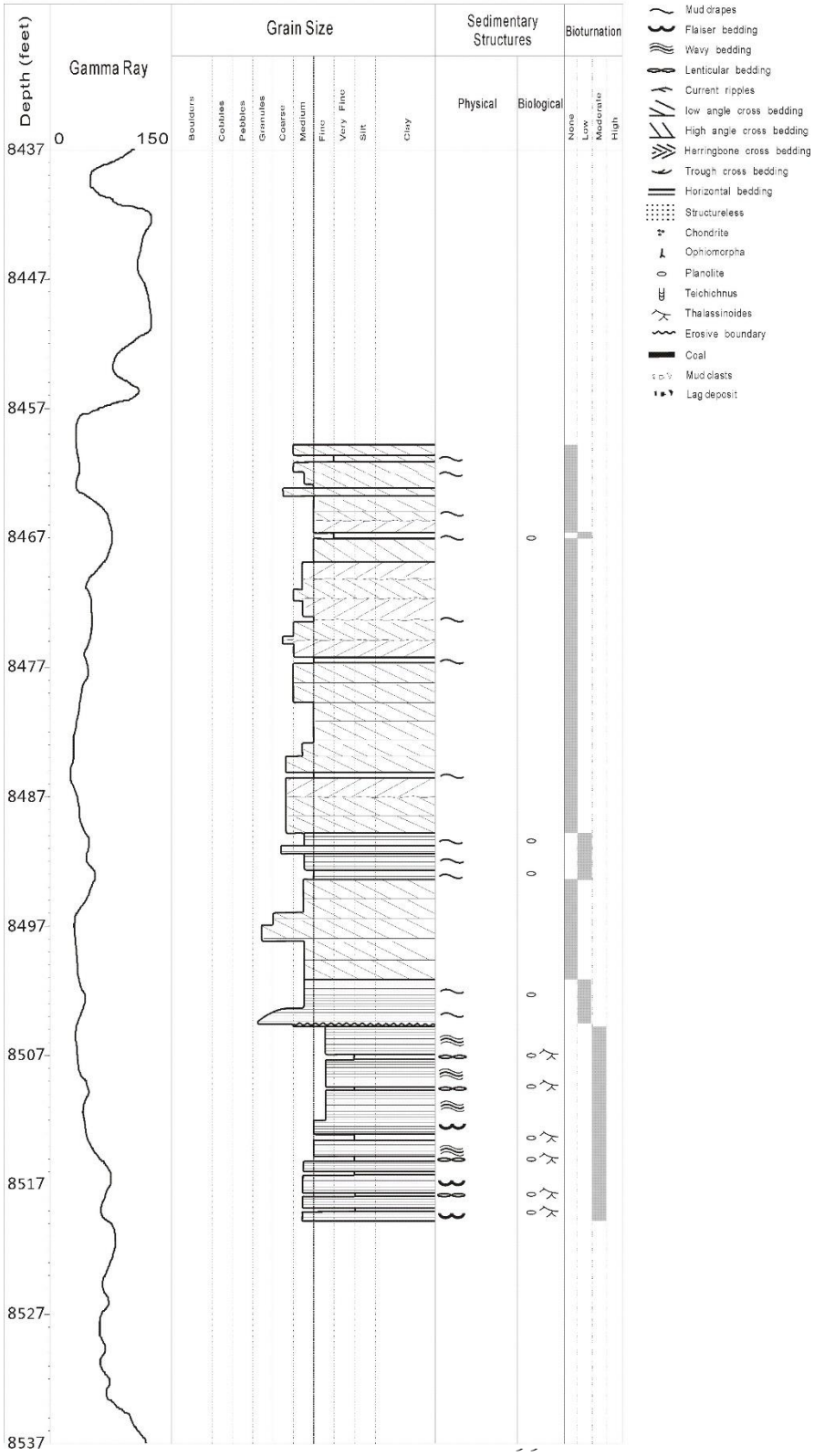
Depth (feet)
Gamma Ray
0
150
8437
8447
8457
8467
8477
8487
8497
8507
8517
8527
8537
Grain Size
Boulders
Cobbles
Pebbles
Granules
Coarse
Medium
Fine
Very Fine
Silt
Clay
Sedimentary Structures
Physical
Biological
Bioturnation
None
Low
Moderate
High
Mud drapes
Flaiser bedding
Wavy bedding
Lenticular bedding
Current ripples
low angle cross bedding
High angle cross bedding
Herringbone cross bedding
Trough cross bedding
Horizontal bedding
Structureless
Chondrite
Ophiomorpha
Planolite
Teichichnus
Thalassinoides
Erosive boundary
Coal
Mud clasts
Lag deposit

Well No. 8

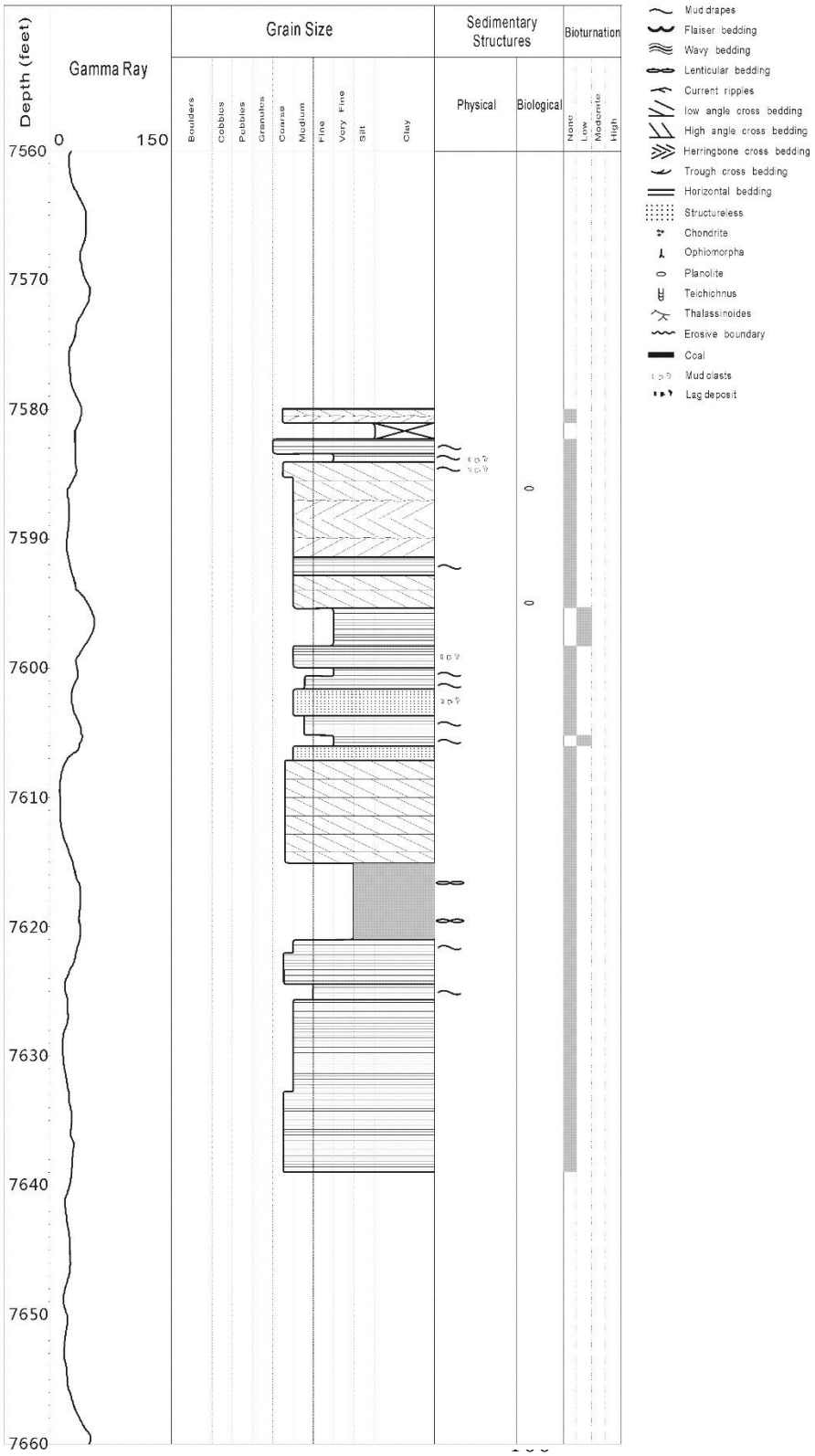
Depth (feet)
Gamma Ray
0
150
7560
7570
7580
7590
7600
7610
7620
7630
7640
7650
7660
Grain Size
Boulders
Cobbles
Pebbles
Granules
Coarse
Medium
Fine
Very Fine
Silt
Clay
Sedimentary Structures
Physical
Biological
Bioturnation
None
Low
Moderate
High
Mud drapes
Flaiser bedding
Wavy bedding
Lenticular bedding
Current rippies
low angle cross bedding
High angle cross bedding
Herringbone cross bedding
Trough cross bedding
Horizontal bedding
Structureless
Chondrite
Ophiomorpha
Planolite
Teichichnus
Thalassinoides
Erosive boundary
Coal
Mud clasts
Lag deposit

Bibliography

Baby, P., Rivadeneira, M., Barragán, R., & Christophoul, F. (2013). Thick-skinned tectonics in the Oriente foreland basin of Ecuador. *Geological Society, London, Special Publications, 377*(1), 59-76.

Barwis, J. H. (1977). Sedimentology of some South Carolina tidal-creek point bars, and a comparison with their fluvial counterparts, in Miall, A. D., ed., Fluvial Sedimentology. *Canadian Society of Petroleum Geologists, 5,* 129-160.

Christophoul, F., Baby, P., & Dávila, C. (2002). Stratigraphic responses to a major tectonic event in a foreland basin: the Ecuadorian Oriente Basin from Eocene to Oligocene times. *Tectonophysics, 345*(1), 281-298.

Dalrymple, R. W. (2012). Tidal depositional systems, in Davis Jr, R. A., & Dalrymple, R. W., eds., *Principles of Tidal Sedimentology.* (pp. 201-231). Springer Netherlands.

Dalrymple, R. W. W., Mackay, D.A., Ichaso, A.A., & Choi, K.S. (2012). Processes, Morphodynamics, and Facies of Tide-dominated Estuaries, in Davis Jr, R. A., & Dalrymple, R. W., eds., *Principles of Tidal Sedimentology.* (pp. 201-231). Springer Netherlands.

Dalrymple, R. W., Zaitlin, B. A., & Boyd, R. (1992). Estuarine facies models: conceptual basis and stratigraphic implications: perspective. *Journal of Sedimentary Research, 62*(6), 1130-1146

Dalrymple, R. W., Baker, E. K., Harris, P. T., & Hughes, M. G. (2003). Sedimentology and stratigraphy of a tide-dominated, foreland-basin delta (Fly River, Papua New Guinea). *Society for Sedimentary Geology Special Publication, 76*, 147-173.

Dashwood, M. F., & Abbotts, I. L. (1990). Aspects of the petroleum geology of the Oriente Basin, Ecuador. *Geological Society, London, Special Publications*, *50*(1), 89-117.

Estupiñan, J., Marfil, R., Scherer, M., & Permanyer, A. (2010). Reservoir sandstones of the Cretaceous Napo Formation U and T members in the Oriente basin, Ecuador: Links between diagenesis and sequence stratigraphy. *Journal of Petroleum Geology*, *33*(3), 221-245.

Gabioux, M., Vinzon, S. B., & Paiva, A. M. (2005). Tidal propagation over fluid mud layers on the Amazon shelf. *Continental Shelf Research, 25*(1), 113-125.

Harris, P. T., Baker, E. K., Cole, A. R., & Short, S. A. (1993). A preliminary study of sedimentation in the tidally dominated Fly River Delta, Gulf of Papua. *Continental Shelf Research, 13*(4), 441-472.

Harris, P. T., Hughes, M. G., Baker, E. K., Dalrymple, R. W., & Keene, J. B. (2004). Sediment transport in distributary channels and its export to the pro-deltaic environment in a tidally dominated delta: Fly River, Papua New Guinea. *Continental Shelf Research, 24*(19), 2431-2454.

Higgs, R., Shanmugam, G., & Poffenberger, M. (2002). Tide-dominated estuarine facies in the Hollin and Napo (T and U) formations (Cretaceous), Sacha field, Oriente Basin, Ecuador: Discussion. *AAPG Bulletin, 86*(2), 329-334.

Higley, D. K. (2001). *The Putumayo-Oriente-Maranon Province of Columbia, Ecuador, and Peru, Mesozoic-Cenozoic and Paleozoic Petroleum Systems*. US Department of the Interior, US Geological Survey.

Hill, P.L., Fox, J.M., Crockett, J.S., Curran, K.J., Friedrichs, C.L., Geyers, W.R., Milligan, T.G., Ogston, A.S., Puig, P., Scully, M.E., Traykovski, P.A., & Wheatcroft, R.A., 2007, Sediment delivery to the seabed on continental margins. in Nittrouer, C.C., Austin, J.A., Field, M.E., Kravitz, J.H., Syvitski, J.P.M., & Wiberg, P.L., eds., Continental Margin Sedimentation: From Sediment Transport to Sequence Stratigraphy. *IAS special publication, 37*, 49–99.

Houbolt, J.J.H.C. (1968). Recent sediments in the southern bight of the North Sea. *Geologie en Mijnbouw, 47*, 245- 273.

Ichaso, A. A., & Dalrymple, R. W. (2009). Tide-and wave-generated fluid mud deposits in the Tilje Formation (Jurassic), offshore Norway. *Geology, 37*(6), 539-542.

Jaillard, E., Bengtson, P., & Dhondt, A. V. (2005). Late Cretaceous marine transgressions in Ecuador and northern Peru: a refined stratigraphic framework. *Journal of South American Earth Sciences, 19*(3), 307-323.

Kineke, G. C., Sternberg, R. W., Trowbridge, J. H., & Geyer, W. R. (1996). Fluid-mud processes on the Amazon continental shelf. *Continental Shelf Research*, *16*(5), 667-696.

Kirby, R., & Parker, W. R. (1983). Distribution and behavior of fine sediment in the Severn Estuary and Inner Bristol Channel, UK. *Canadian Journal of Fisheries and Aquatic Sciences*, *40*(S1), 83-95.

McCave, I. N. (1971). Wave effectiveness at the sea bed and its relationship to bed-forms and deposition of mud. *Journal of Sedimentary Research*, *41*(1), 89-96

Reineck, H. E., & Wunderlich, F. (1968). Classification and origin of flaser and lenticular bedding. *Sedimentology*, *11*(1-2), 99-104.

Reynaud, J. Y., Tessier, B., Proust, J. N., Dalrymple, R., Marsset, T., De Batist, M., ... & Lericolais, G. (1999). Eustatic and hydrodynamic controls on the architecture of a deep shelf sand bank (Celtic Sea). *Sedimentology*, *46*(4), 703-721.

Robinson, A. H. W. (1960). Ebb-flood channel systems in sandy bays and estuaries. *Geography*, *45*, 183-199.

Shanmugam, G., Poffenberger, M., & Alava, J. T. (2000). Tide-Dominated Estuarine Facies in the Hollin and Napo ("T" and "U") Formations (Cretaceous), Sacha Field, Oriente Basin, Ecuador. *AAPG bulletin*, *84*(5), 652-682.

Smith, D. G. (1987). Meandering river point bar lithofacies models: modern and ancient examples compared, in Ethington, F. G., Flores, R. M., & Harvey, M. D., eds., Recent Develpments in Fluvial Sedimentology. *SEPM Special Publication, 39*, 83-91.

Spikings, R. A., Seward, D., Winkler, W., & Ruiz, G. M. (2000). Low-temperature thermochronology of the northern Cordillera Real, Ecuador: Tectonic insights from zircon and apatite fission track analysis. *Tectonics*, *19*(4), 649-668.

Stride, A.H., Belderson, R.H., Kenyon, N.H., & Johnson, M.A. (1982). Offshore tidal deposits: sand sheet and sand bank facies, in Stride, A.H., ed., *Offshore Tidal Sands: Processes and Deposits*. New York, Chapman and Hall, 95-125.

Terwindt, J. H. J. (2009). Origin and sequences of sedimentary structures in inshore mesotidal deposits of the North Sea. *Holocene marine sedimentation in the North Sea Basin, 5*, 4-26.

Wolanski, E., & King, B., Galloway, D. (1997). Salinity intrusion in the Fly River estuary, Papua New Guinea. *Journal of Coastal Research 13 (4)*, 983–994.

Wood, L.J. (2003). Predicting tidal sand reservoir architecture using data from modern and ancient depositional systems, in Grammer, G.M., Harris, P.M., & Eberli, G.P., eds., Integration of Outcrop and Modern Analogs in Reservoir Modeling. *American Association of Petroleum Geologists Memoir, 80*, 1- 22.